

ASSESSMENT OF VARIABLE SOURCE AREA HYDROLOGICAL MODELS IN THE UPPER CAUVERY BASIN, KARNATAKA, INDIA

Thesis

**Submitted in partial fulfillment of the requirements for the degree of
DOCTOR OF PHILOSOPHY**

By

KUMAR RAJU B. C.



**DEPARTMENT OF APPLIED MECHANICS AND HYDRAULICS
NATIONAL INSTITUTE OF TECHNOLOGY KARNATAKA,
SURATHKAL, MANGALORE – 575 025**

FEBRUARY 2016

ASSESSMENT OF VARIABLE SOURCE AREA HYDROLOGICAL MODELS IN THE UPPER CAUVERY BASIN, KARNATAKA, INDIA

Thesis

**Submitted in partial fulfillment of the requirements for the degree of
DOCTOR OF PHILOSOPHY**

By

KUMAR RAJU B. C.

Under the guidance of

Dr. LAKSHMAN NANDAGIRI

Professor

Dept. of Applied Mechanics & Hydraulics
NITK, Surathkal



**DEPARTMENT OF APPLIED MECHANICS AND HYDRAULICS
NATIONAL INSTITUTE OF TECHNOLOGY KARNATAKA,
SURATHKAL, MANGALORE – 575 025**

FEBRUARY 2016

D E C L A R A T I O N

By the Ph.D. Research Scholar

I hereby *declare* that the Research Thesis entitled **Assessment of Variable Source Area Hydrological Models in the Upper Cauvery Basin, Karnataka, India**, Which is being submitted to the **National Institute of Technology Karnataka, Surathkal** in partial fulfilment of the requirements for the award of the Degree of **Doctor of Philosophy in Applied Mechanics and Hydraulics Department** is a *bonafide report of the research work* carried out by me. The material contained in this Research Thesis has not been submitted to any University or Institution for the award of any degree.

AM11F03, KUMAR RAJU B. C.

(Register Number, Name & Signature of the Research Scholar)

Department of Applied Mechanics and Hydraulics

Place: NITK-Surathkal

Date:

C E R T I F I C A T E

This is to *certify* that the Research Thesis entitled **Assessment of Variable Source Area Hydrological Models in the Upper Cauvery Basin, Karnataka, India**, submitted by KUMAR RAJU B. C. (Register Number: AM11F03) as the record of the research work carried out by him, is *accepted as the Research Thesis submission* in partial fulfilment of the requirements for the award of degree of **Doctor of Philosophy**.

Dr. Lakshman Nandagiri

Professor

Research Guide

(Name and Signature with Date and Seal)

Chairman - DRPC

(Signature with Date and Seal)

ACKNOWLEDGEMENTS

With deep sense of gratitude, I express my heartfelt thanks to the eminent Professor from the Department of Applied Mechanics and Hydraulics, NITK, Surathkal, Dr. Lakshman Nandagiri, for doing a marvelous job at supervising my research work. His logical and tactical suggestions have been very valuable and encouraging during the development of this research.

I am grateful to Research Progress Committee members, Prof. Kandaswamy and Dr. Paresch Chandra Deka, for their critical evaluation and useful suggestions during the progress of the work.

I am greatly indebted to Prof. M. K. Nagaraj and Prof. Subba Rao, the former Head of the Department of Applied Mechanics and Hydraulics, NITK, Surathkal, and Prof. Dwarakish G.S., the present Head of the Department, for financial assistance and granting me the permission to use the departmental computing facilities available for necessary research work to the maximum extent, which was very vital for the completion of the computational aspects relevant to this research.

I thank the Director of the NITK, Surathkal, Prof. Sawapan Bhattacharya, for granting me the permission to use the institutional infrastructure facilities, without which this research work would have been impossible.

I sincerely acknowledge the help and support rendered by all the Faculties, staffs and Research scholars of Department of Applied Mechanics & Hydraulics.

I also express my deep sense gratitude to my friend Dr. Prashanth J for his valuable suggestion in report writing.

I express heartfelt gratitude to authors of all those research publications which have been referred in this thesis and also like to thank all the Government Departments and Organizations for providing required data.

Finally, I wish to express gratitude, love and affection to my beloved family members for their encouragement and moral support on the road to the completion of my research.

Kumar Raju B. C.

ABSTRACT

With increased availability of spatial data-sets of catchment characteristics and hydrometeorological variables, distributed hydrological models are being applied to solve a variety of problems related to catchment hydrology and water resources management. However, experimental results obtained in recent decades have shown the possibility of existence of runoff generation mechanisms other than the conventional infiltration-excess (Hortonian) mechanism. In particular, it has been shown that Variable Source Area (VSA) mechanism of runoff generation may prevail in humid steeply sloping and well vegetated watersheds. Accordingly, efforts have been made by previous researchers to incorporate this mechanism into distributed hydrological models and their performances have been evaluated in mostly humid temperate regions and not so much in humid tropical regions.

The primary objective of the present study was to compare the performances of hydrological models which incorporate the Variable Source Area (VSA) mechanism of runoff generation with that of the Soil and Water Assessment Tool (SWAT) which employs the conventional infiltration-excess mechanism of runoff generation. One of the VSA based model used, SWAT-VSA, has been proposed by earlier researchers as a re-conceptualization of the SWAT model and uses a topography-based wetness index to identify source areas and simulates runoff in a manner consistent with VSA hydrology. In the present study, the topography-based wetness index was replaced with a Modified Normalized Difference Water Index (MNDWI) derived from satellite imagery resulting in a new VSA model version, SWAT-MNDWI. Performance evaluation of the models was carried out through their application in two humid tropical watersheds (Hemavathi – 2974 km²; Harangi – 538.8 km²) located in the Upper Cauvery River Basin (36,682 km²), India wherein previous studies have shown the existence of VSA hydrology.

The other aspects addressed in this study include: assessment of significance and magnitude of trends in historical records of observed hydrometeorological variables in the Upper Cauvery Basin, evaluation of uncertainties associated with streamflow

predictions of the 3 hydrological models and simulation of the hydrologic impacts of hypothetical land use/land cover (LU/LC) changes in the Hemavathi and Harangi watersheds.

The present study examined the significance and magnitude of trends in the monthly rainfall (33 rain gauges), maximum and minimum temperature (6 climate stations) and streamflow at 4 gauge sites in the Upper Cauvery Basin for the historical 30 year period 1981-2010. The statistical parameters - Coefficient of Variation (CV) and percentage departure were calculated for average monthly values separately for 3 decades. The Seasonal-Kendall and Sen's slope estimator were used to calculate significance and magnitude of trends in rainfall, temperature and streamflow data. Detrended Fluctuation Analysis (DFA) method was used to detect long-term persistence in the time series data. As expected, the CV of rainfall shows a large variation in the month December to March, while the percentage departure also varies during these months for different decades. But there was no significant trend found for all rain gauge stations and sub basins except for the Arkavathi sub basin. For maximum temperature there was not much variation except in the months of May and June at the Hassan climate station. Statistically significant trend was observed in maximum temperature for Chikmagalur and Hassan stations. The CV of minimum temperature shows a large variability from November to March for all climate stations and also a significant increasing trend for Hassan and Bangalore stations, while for Madikeri a decreasing trend was observed with a variation of $-0.16^{\circ}\text{C}/\text{year}$. There was not much variation found for streamflow except in K M Vadi gauge site and T.Narasipur gauge site which showed a significant decreasing trend of $-0.778 \text{ m}^3/\text{s}/\text{year}$. Long range dependence analysis revealed a weak persistence for both rainfall and streamflow of the basin.

Using relevant data inputs pertaining to rainfall, climate, elevation, Land use/Land Cover (LU/LC) and soils, the SWAT, SWAT-VSA and SWAT-MNDWI models were applied separately to both watersheds using a daily time step. Models were calibrated for the historical period 2000-2003 and validated for the period 2004-2006 using observed daily streamflow records at the watershed outlets. The comparative assessment focused specifically on the following aspects for the six cases considered

(3 models applied to 2 watersheds): 1) sensitivity of model parameters 2) accuracy of daily streamflow predictions at the watershed outlets 3) predictions of spatially and temporally averaged annual water balance components 4) differences in spatial patterns of source areas of surface runoff. Sensitivity analysis indicated that for the SWAT model, Curve Number (CN) was the most important parameter while for the VSA based models, parameters related to the unsaturated zone and shallow groundwater were important, a result consistent with the runoff mechanism incorporated in the models. The accuracies of streamflow prediction as determined from scatter plots and model performance statistics were more or less similar both in calibration and validation for all the three models with the models performing better in the forested Harangi watershed. Overall, the SWAT-MNDWI model proved to be the best one in simulating daily streamflow with Nash-Sutcliffe efficiency (E_{NS}) of 0.85, coefficient of determination (R^2) of 0.88, percentage bias (PBIAS) of 13.2% and root mean square error (RMSE) of 37.48 m³/s for the Hemavathi watershed and corresponding values of 0.88, 0.88, 1.09% and 16.67 m³/s for the Harangi watershed. All three models simulated spatially and temporally averaged major water balance components in a consistent manner resulting in a residual error of <5% of annual rainfall in the annual water balance. However, evapotranspiration loss as a percentage of rainfall appeared unreasonable (27% - 32%) for the wet Harangi watershed probably on account of it being predominantly forested. The spatial patterns of surface runoff generation were somewhat similar for the SWAT-VSA and SWAT-MNDWI models, but completely different for the SWAT model, again a result consistent with the runoff generation mechanism adopted. Overall results of this study have demonstrated that models incorporating VSA hydrology, and in particular the SWAT-MNDWI model proposed in this study, provide accurate and convenient tools for distributed hydrologic modelling in humid tropical watersheds.

This study also focuses on assessing uncertainties associated with SWAT-MNDWI, SWAT-VSA and SWAT models using SWAT-CUP (Calibration and Uncertainty Programs) tool. Two multi-objective uncertainty techniques (Generalized Likelihood Uncertainty Equation (GLUE) and Sequential Uncertainty Fitting algorithm (SUFI-2)) were tested for the Hemavathi and Harangi watersheds. The goodness-of-fit and efficiency of the models have been tested using E_{NS} as the objective function. GLUE

and SUFI-2 techniques yielded good results in minimizing the differences between observed and simulated streamflows at the outlets of the Hemavathi and Harangi watersheds. The results show that GLUE performance was slightly better than the SUFI-2 technique for all models for both the watersheds during calibration and validation periods. The 95PPU estimated by the GLUE and SUFI-2 techniques are very close to each other and larger than 45% (P-factor) for all models for both the watersheds during calibration and validation periods. For GLUE, R-factor values during the validation phase for the Hemavathi watershed were 0.35, 0.38 and 0.34 for the SWAT-MNDWI, SWAT-VSA and SWAT models respectively with corresponding values for the Harangi watershed being 0.41, 0.39 and 0.40. It should be noted that both GLUE and SUFI-2 cannot accurately quantify the prediction uncertainty of SWAT-MNDWI, SWAT-VSA and SWAT models. Overall results indicated that the GLUE technique applied on the SWAT-MNDWI model performed best in quantifying the prediction uncertainty of streamflow at the outlets of both watersheds.

In order to simulate the hydrologic impacts of LU/LC changes in the study area, two hypothetical LU/LC change scenarios were formulated for Hemavathi and Harangi watersheds. The SWAT-MNDWI, SWAT-VSA and SWAT models were used to simulate the hydrologic responses under these scenarios. Values of average annual water balance components and their percentage change with respect to reference results were calculated for both watersheds using the three models. Additionally, an effort was also made to construct the Flow Duration Curves (FDCs) using daily streamflow values generated under each scenario. Differences in optimal parameters of an empirical model for the FDC, magnitudes of flow quantiles, high flow index and low flow index were computed for each scenario. For the Hemavathi watershed, with increase in agricultural land there is increase in water yield predicted by all three models. With increase in forest cover there is decrease in water yield predicted by SWAT-VSA and SWAT models while for SWAT-MNDWI an increase in water yield was found. For Harangi watershed, with increase in agricultural land or forested area there is decrease in water yield for all three models except SWAT-VSA model in scenario I. Both the scenarios appeared to have significant impacts on the runoff

regime as indicated by significant changes in FDC model parameters, flow quantiles and flow indices.

Overall results of this study provide useful inputs with regard the magnitude and direction of likely future changes in important hydrometeorological variables which can be used to prepare plans for mitigation and adaptation to climate change in the Upper Cauvery Basin.

The present study has demonstrated an overall methodology for application, performance evaluation and uncertainty analysis of distributed hydrological models using a variety of ground-based inputs and satellite data within a GIS framework. Since previous studies in similar watersheds in the Western Ghats region have identified VSA as a dominant mechanism of runoff generation, the spatial patterns obtained with the SWAT-VSA and SWAT-MNDWI models provide information which will prove to be extremely useful in soil and water conservation measures and in identifying source areas of non-point pollution.

The SWAT-MNDWI model proposed in this study is particularly attractive since it employs satellite imagery to accurately identify areas of different wetnesses within the watershed and integrates this information into a distributed hydrological model. As the results of this study have demonstrated, such a modelling approach using VSA hydrology provides an accurate and convenient tool for distributed hydrologic modelling and impact assessment of LU/LC changes in humid tropical watersheds.

Key words: Hydrological Modeling, SWAT, wetness index, Variable Source Area, Surface Water Hydrology, Remote Sensing, GIS, Hydrometeorological Analysis, Uncertainty Analysis, LU/LC changes, Hydrological impacts, Upper Cauvery Basin.

CONTENTS

ABSTRACT.....	i
CONTENTS.....	vi
LIST OF FIGURES.....	ix
LIST OF TABLES.....	xiii
LIST OF ABBREVIATIONS.....	xvii
CHAPTER 1 INTRODUCTION	1
1.1 General	1
1.2 Runoff Generation Mechanisms.....	2
1.3 Justification for the present study	5
1.4 Model Uncertainty Analysis.....	7
1.5 Trend analysis of historical hydroclimatic data	9
1.6 Hydrological impacts of LU/LC changes	10
1.7 Study Objectives	11
1.8 Overview of Research Methodology	11
1.9 Organization of Thesis	12
CHAPTER 2 REVIEW OF LITERATURE	15
2.1 General	15
2.2 Analysis of Hydrometeorological Variables	15
2.3 Soil and Water Assessment Tool (SWAT)	21
2.3.1 Hydrological Water Balance Studies Using SWAT	21
2.3.2 Uncertainty Analysis Studies Using SWAT	30
2.3.3 LU/LC Change Studies Using SWAT	34
2.3.4 VSA Modeling Using SWAT	37
2.4 Summary	40
CHAPTER 3 STUDY AREA AND DATA	43
3.1 Description of the Study Area.....	43
3.2 Climate	45
3.3 Land Use/Land Cover	47

3.4 Soils.....	50
3.5 Hydrometeorological Data	52
3.6 Topographic Data.....	54
3.7 Satellite Imagery	54
CHAPTER 4 ANALYSIS OF HYDROMETEOROLOGICAL DATA	57
4.1 General	57
4.2 Seasonal-Kendall Test.....	58
4.3 Sen’s Slope Estimator	59
4.4 Detrended Fluctuation Analysis	59
4.5 Methodology	60
4.6 Results and Discussion.....	61
4.6.1 Statistical Analysis of Hydrometeorological Variables	61
4.7 Trend analysis of hydrometeorological time series.....	75
4.8 Long–Term Persistence in Hydrometeorological Time Series	77
4.9 Summary and Conclusions.....	78
CHAPTER 5 HYDROLOGICAL MODELING.....	81
5.1 General	81
5.2 Description of Models Used.....	81
5.2.1 SWAT	81
5.2.2 SWAT-VSA	82
5.2.3 SWAT-MNDWI.....	84
5.3 Description of Watersheds	85
5.3.1 Hemavathi Watershed	85
5.3.2 Harangi Watershed.....	85
5.4 Methodology	93
5.4.1 Input Data.....	93
5.4.2 HRU Definitions	93
5.4.3 Sensitivity Analysis.....	94
5.4.4 Model Calibration and Validation.....	95
5.4.5 Model Performance Evaluation.....	96
5.5 Results and Discussion.....	97

5.5.1 Sensitivity Analysis.....	97
5.5.2 Model Calibration Results	99
5.5.3 Accuracy of Streamflow Predictions	101
5.5.4 Water Balance Components.....	105
5.5.5 Spatial Patterns of Surface Runoff.....	108
5.6 Summary and Conclusions.....	110
CHAPTER 6 UNCERTAINTY ANALYSIS	113
6.1 General	113
6.2 SWAT-CUP TOOL.....	113
6.2.1 Generalized Likelihood Uncertainty Equation.....	114
6.2.2 Sequential Uncertainty Fitting algorithm.....	115
6.3 Results and Discussion.....	116
6.3.1 Sensitivity Analysis Using GLUE and SUFI-2.....	116
6.3.2 Uncertainty Analysis Using GLUE and SUFI-2.....	123
6.4 Summary and Conclusions.....	129
CHAPTER 7 HYDROLOGIC RESPONSES TO LAND COVER CHANGES	131
7.1 General	131
7.2 LU/LC Change Scenarios	131
7.3 Flow Duration Curves	132
7.4 Results and Discussion.....	136
7.4.1 Effects of LU/LC Change on Hydrologic Responses	136
7.4.2 Effects of LU/LC Change on Streamflow Regime	139
7.5 Summary and Conclusions.....	142
CHAPTER 8 CONCLUSIONS.....	143
8.1 General	143
8.2 Hydro meteorological Data Analysis	143
8.3 Hydrological Modeling	144
8.4 Uncertainty Analysis	146
8.5 Hydrologic Responses to Land Cover Changes	146
8.6 Limitations of the study	147
8.7 Scope for Future Studies	148

LIST OF FIGURES

Fig. 1.1 Representation of the runoff generation mechanism	3
Fig. 1.2 Dominant processes of hill slope response to rainfall (Beven, 2001)	3
Fig. 1.3 The mechanism and the effects of piping (Kirkby, 1978).....	6
Fig. 3.1 Map of Upper Cauvery Basin showing locations of rainfall, temperature and streamflow gauging stations	44
Fig. 3.2 Monthly mean minimum and maximum daily temperature for climate stations in the Upper Cauvery Basin	46
Fig. 3.3 Monthly mean rainfall (mm) for sub basins in the Upper Cauvery Basin	47
Fig. 3.4 LU/LC map of the Upper Cauvery Basin (KSRSAC).....	49
Fig. 3.5 Soil map of the Upper Cauvery Basin (NBSS and LUP)	50
Fig. 3.6 Topography map of the Upper Cauvery Basin.....	55
Fig. 4.1 Percentage departure of monthly maximum temperature of different decades from 30 years normal value.....	67
Fig. 4.2 Percentage departure of monthly minimum temperature of different decades from 30 years normal value.....	68
Fig. 4.3 Percentage departure of monthly rainfall of different decades from 30 years normal value for sub basins.....	69
Fig. 4.4 Percentage departure of monthly rainfall of different decades from 30 years normal value for different rainfall stations.....	73
Fig. 4.5 Percentage departure of monthly streamflow of different decades from 30 years normal value.....	74

Fig. 5.1 Location Maps of (a) Hemavathi and (b) Harangi watersheds showing elevations, stream network and location of dams, rain gauges and climate stations.....	87
Fig. 5.2 LU/LC of the Hemavathi watershed.....	88
Fig. 5.3 Soil map of the Hemavathi watershed.....	89
Fig. 5.4 LU/LC of the Harangi watershed.....	90
Fig. 5.5 Soil map of the Harangi watershed.....	91
Fig. 5.6 Spatial distribution of wetness classes derived from (a) MNDWI and (b) STI for Hemavathi and Harangi watersheds.....	92
Fig. 5.7 Flowchart for creating HRUs and defining CN for SWAT-MNDWI, SWAT-VSA and SWAT models.....	94
Fig. 5.8 Sensitivity ranks for hydrological parameters of SWAT-MNDWI, SWAT-VSA and SWAT models for (a) Hemavathi (b) Harangi watersheds.....	98
Fig. 5.9 Relation between effective precipitation and observed stream flow for (a) Hemavathi and (b) Harangi watersheds.....	100
Fig. 5.10 Time Series and scatter plots of observed and simulated daily stream flow inflow in the Hemavathi watershed using SWAT-MNDWI (a), SWAT-VSA (b) and SWAT (c) at the Hemavathi dam gauge site.....	103
Fig. 5.11 Time series and scatter plots of observed and simulated daily stream flow inflow in the Harangi watershed using SWAT-MNDWI (a), SWAT-VSA (b) and SWAT (c) at the Harangi dam gauge site.....	104
Fig. 5.12 Spatial distribution of surface runoff (mm) modeled by (a) SWAT-MNDWI, (b) SWAT-VSA and (c) SWAT for specific rainfall events over the sub watersheds of Hemavathi and Harangi watersheds.....	109

Fig. 6.1 Scatter plots of E_{NS} efficiency (y-axis) against each aggregate SWAT parameter (x-axis) conditioning with GLUE for Hemavathi watershed	119
Fig. 6.2 Scatter plots of E_{NS} efficiency (y-axis) against each aggregate SWAT parameter (x-axis) conditioning with SUFI-2 for Hemavathi watershed.....	120
Fig. 6.3 Scatter plots of E_{NS} efficiency (y-axis) against each aggregate SWAT parameter (x-axis) conditioning with GLUE for Harangi watershed.....	121
Fig. 6.4 Scatter plots of E_{NS} efficiency (y-axis) against each aggregate SWAT parameter (x-axis) conditioning with SUFI-2 for Harangi watershed	122
Fig. 6.5 95PPU (shaded area) derived by GLUE during calibration and validation period. The black dash line corresponds to the observed discharge at the outlet, while the black solid line represents the best simulation obtained for Hemavathi watershed	125
Fig. 6.6 95PPU (shaded area) derived by SUFI-2 during calibration and validation period. The black dash line corresponds to the observed discharge at the outlet, while the black solid line represents the best simulation obtained for Hemavathi watershed	126
Fig. 6.7 95PPU (shaded area) derived by GLUE during calibration and validation period. The black dash line corresponds to the observed discharge at the outlet, while the black solid line represents the best simulation obtained for Harangi watershed.....	127
Fig. 6.8 95PPU (shaded area) derived by SUFI-2 during calibration and validation period. The black dash line corresponds to the observed discharge at the outlet, while the black solid line represents the best simulation obtained for Harangi watershed.....	128
Fig. 7.1 Hypothetical LU/LC change scenario I and II for Hemavathi watershed	134
Fig. 7.2 Hypothetical LU/LC change scenario I and II for Harangi watershed.....	135

LIST OF TABLES

Table 3.1 Tributaries of the Upper Cauvery Basin	45
Table 3.2 Characteristics of LU/LC in the Upper Cauvery Basin	48
Table 3.3 Characteristics of soil in the Upper Cauvery Basin	51
Table 3.4 Rain gauge stations in the Upper Cauvery Basin	52
Table 3.5 Climatic Station in the Upper Cauvery Basin.....	53
Table 3.6 Major Dams in the Upper Cauvery Basin.....	54
Table 3.7 Stream gauge Sites in the Upper Cauvery Basin	54
Table 4.1 Coefficients of variation for rainfall (a), maximum temperature (b), minimum temperature (c) and streamflow (d)	63
Table 4.2 Sen's slopes, significant of trend using the Seasonal-Kendall method, DFA exponent and coefficients of variation for rainfall stations	65
Table 4.3 Sen's slopes and significant of trend using the Seasonal-Kendall method for a) rainfall, b) temperature and c) streamflow	76
Table 4.4 DFA exponent for monthly (a) rainfall and (b) streamflow time series	77
Table 5.1 Characteristics of LU/LC in the Hemavathi watershed	86
Table 5.2 Characteristics of LU/LC in the Harangi watershed.....	91
Table 5.3 Parameter and their ranges considered in the sensitivity analysis	95
Table 5.4 Adjusted parameters for SWAT-MNDWI, SWAT-VSA and SWAT models for Hemavathi and Harangi watersheds	101
Table 5.5 Performance evaluation criteria for the three models during calibration and validation for Hemavathi and Harangi Watersheds	105

Table 5.6 Average annual water balance components for the Hemavathi watershed derived using SWAT-MNDWI, SWAT-VSA and SWAT models (all values are in mm of water)	107
Table 5.7 Average annual water balance components for the Harangi watershed derived using SWAT-MNDWI, SWAT-VSA and SWAT models (all values are in mm of water)	107
Table 6.1 Parameter sensitivities for Hemavathi Watershed	118
Table 6.2 Parameter sensitivities for Harangi Watershed.....	118
Table 6.3 Performance evaluation criteria for the three models during calibration and validation for Hemavathi Watershed.....	124
Table 6.4 Performance evaluation criteria for the three models during calibration and validation for Harangi Watershed	124
Table 7.1 Hypothetical scenarios for impact assessment of LU/LC changes on hydrologic responses for Hemavathi and Harangi watersheds	132
Table 7.2 Distribution of water balance components over the period of 2000-2003 for the Hemavathi watershed using SWAT-MNDWI, SWAT-VSA and SWAT for scenario I.....	137
Table 7.3 Distribution of water balance components over the period of 2000-2003 for the Hemavathi watershed using SWAT-MNDWI, SWAT-VSA and SWAT for scenario II	137
Table 7.4 Distribution of water balance components over the period of 2000-2003 for the Harangi watershed using SWAT-MNDWI, SWAT-VSA and SWAT for scenario I	138
Table 7.5 Distribution of water balance components over the period of 2000-2003 for the Harangi watershed using SWAT-MNDWI, SWAT-VSA and SWAT for scenario II.....	138

Table 7.6 Changes in streamflow regime of Hemavathi watershed for different scenarios using SWAT-MNDWI, SWAT-VSA and SWAT Models..... 140

Table 7.7 Changes in streamflow regime of Harangi watershed for different scenarios using SWAT-MNDWI, SWAT-VSA and SWAT Models 141

LIST OF ABBREVIATIONS

Abbreviation	Description
ANN	Artificial Neural Network
ASTER	Advanced Spaceborne Thermal Emission and Reflection Radiometer
AVHRR	Advanced Very High Resolution Radiometer
BaRE	Bayesian Recursive Estimation
BMA	Bayesian Model Averaging
CN	Curve Number
CV	Coefficient of Variation
CWC	Central Water Commission
DCV	Dynamic Contributing Volume
DEM	Digital Elevation Model
DFA	Detrended Fluctuation Analysis
EnKF	Ensemble Kalman Filter
ETM+	Enhanced Thematic Mapper Plus
GCMs	General Circulation Models
GIS	Geographic Information System
GLUE	Generalized Likelihood Uncertainty Estimation
HRUs	Hydrological Response Units
IRS	Indian Remote Sensing
KSRSAC	Karnataka State Remote Sensing Application Center
LAI	Leaf Area Index
LH	Latin Hypercube
LU/LC	Land Use / Land Cover
MCMC	Markov Chain Monte Carlo
MIR	Middle Infrared
MNDWI	Modified Normalized Differential Water Index
MODIS	Moderate Resolution Imaging Spectrometer
NBSS &LUP	National Bureau of Soil Survey and Land Use Planning
NDVI	Normalized Differential Vegetation Index
NIR	Near Infrared

NS	Nash Sutcliffe
OAT	One-factor-At-a-Time
PAN	Panchromatic
ParaSol	Parameter solutions
PBAIS	Percent BIAS
R ²	Coefficient of determination
RCMs	Regional Climate Models
RMSE	Root Mean Square Error
RS	Remote Sensing
SCS	Soil Conservation Service
SRTM	Shuttle Radar Topography Mission
STI	Soil Topographic Index
SUFI-2	Sequential Uncertainty Fitting
SWAT	Soil and Water Assessment Tool
TEMPMIN	Minimum Temperature
TEMPMX	Maximum Temperature
VSA	Variable Source Area
WRDO	Water Resources Development Organization

CHAPTER 1

INTRODUCTION

1.1 GENERAL

Assessment and management of available water resources, evaluation of hydrological impacts induced by changes in land cover and/or climate and other such analyses are critically dependent on accurate characterization of hydrological processes at catchment-scale. Hydrological processes exhibit significant spatial variations, especially in catchments possessing heterogeneity in climate, Land Use/Land Cover (LU/LC), topography and soils. These processes also exhibit large temporal variations in catchments located in the humid tropics on account of pronounced changes in rainfall and temperature regimes during a year. Therefore, characterization of such spatial and temporal variations in the hydrological cycle can be a challenging task in heterogeneous catchments located in the humid tropics. Given the fact that in these regions, water resources are being over-exploited to cater to the needs of a growing population, there is an urgent need to develop appropriate hydrological tools for mapping spatial and temporal patterns of hydrologic variables with the highest possible accuracy.

A large number of hydrological models have been developed over the past several decades to simulate catchment-scale processes and thereby serve as tools for water resources planning and management. Models differ in the manner in which key hydrological processes are represented and parameterized. Despite large differences in input data requirements, model parameterizations and resulting model complexities, it has been found that the ability of models to simulate quantity and quality of runoff at the catchment outlet does not differ much (e.g., Refsgaard and Knudsen, 1996). In other words, complex models appear to be only marginally better than simpler models in simulating catchment-scale hydrologic responses. This raises the question as to whether most models provide the right answers for the wrong reasons. As pointed out by Kirchner (2006), while such models may be good enough for operational purposes,

for advancement of the science of hydrology, it is imperative that models provide the right answers for the right reasons. Furthermore, water managers today seek accurate, location-specific estimates of hydrological variables within the catchment so that conservation measures can be implemented in a more focused manner. It is for these reasons that the recent past has been witness to sustained efforts being initiated by hydrologic modellers to incorporate more physically realistic representations of processes into spatially distributed models. These efforts have focused on utilizing knowledge on hydrologic fluxes and pathways gained from innumerable field experiments carried out in different hydro-climatic settings of the world.

1.2 RUNOFF GENERATION MECHANISMS

This approach is best exemplified by the manner in which a few recently developed hydrologic models represent runoff generation using mechanisms other than the conventional infiltration excess (Hortonian) mechanism. According to Dunne (1978), the principal runoff generation mechanisms can be classified into three types:

- (i) Infiltration excess overland flow (Hortonian overland flow): Storm runoff generated when rainfall intensity is greater than the infiltration capacity of the soil (Fig1.1a) (Horton, 1933).
- (ii) Saturation excess overland flow (source area runoff): Storm runoff generated when subsurface flow saturates the soil near the bottom of a slope and overland flow then occurs as rain falls on this saturated soil (Fig1.1b) (Dunne and Black, 1970).
- (iii) Subsurface storm flow (interflow): This is the horizontal subsurface flow caused by rapid movement of water in the near-surface soil, through macro pores and naturally formed pipes.

Beven (2001) provides an overview indicating which of the above mechanisms might be dominant in different hydrogeoclimatic environments (Fig 1.2).

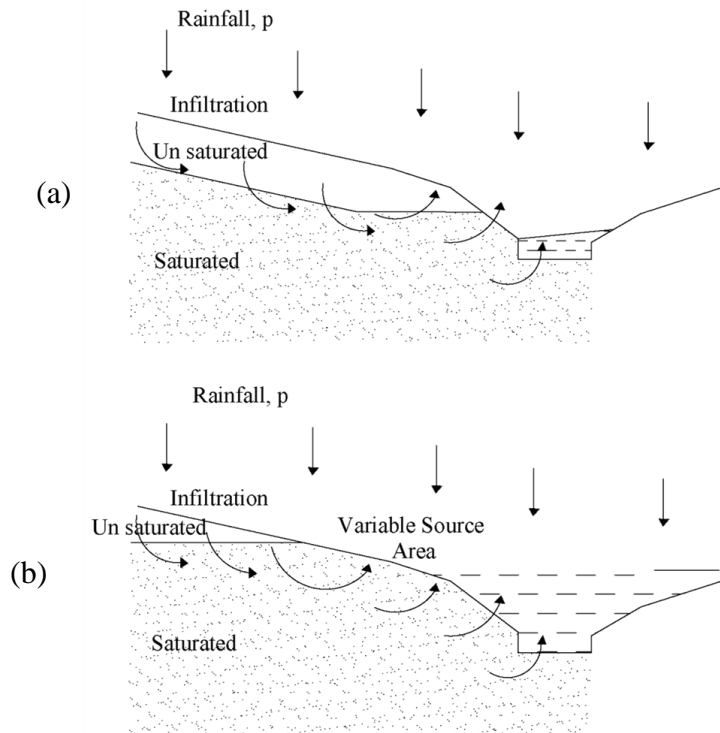


Fig. 1.1 Representation of the runoff generation mechanism

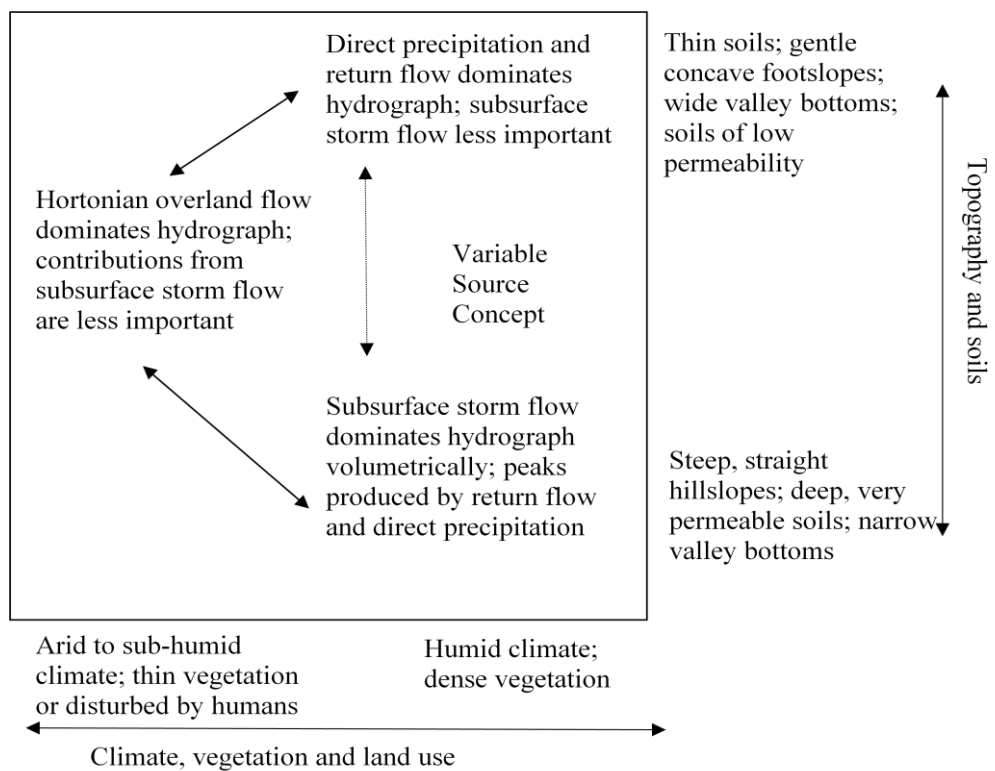


Fig. 1.2 Dominant processes of hill slope response to rainfall (Beven, 2001)

Storm runoff generation mechanisms in forested and hilly humid areas are different from those in plain temperate areas. Hewlett and Hibbert (1967) proved through experiments that infiltration excess overland runoff does not occur in hilly and forested areas of humid regions. A review by Dunne (1978) on hill slope hydrology presented further refinements to the saturation excess overland flow concept by emphasizing the development of Variable Source Areas (VSAs). Occurrence of rainfall over a permeable soil profile underlain by less permeable restricting layers results in convergence of lateral flow which subsequently leads to saturated conditions at the base of the hillslope (Fig. 1.1). With continuing rainfall such saturated areas tend to expand in areal extent and contribute runoff to the stream and have been termed Variable Source Areas (VSA). These typically occur in riparian areas and generate runoff by return flow and direct precipitation. In contrast to the infiltration excess mechanism which assumes runoff generation to take place from the entire catchment, VSA hydrology assumes that the majority of runoff is contributed from a relatively small portion of the catchment. VSAs alongside the channel expand and shrink according to rainfall characteristics and antecedent conditions.

Jones (Jones, 1971, 1979) introduced the concept of Dynamic Contributing Volume (DCV), which extended the model of Hewlett and Hibbert (1967) by including the flow in pipes. According to Jones (1979) the naturally formed pipe networks in many forested and mountainous watersheds drain a volume of soil, which varies with antecedent moisture balance and storm intensity and duration. In the presence of such pipe spaces, surface saturation is not required to generate flow. The pipes may either provide a direct route to the stream channel, in which case pipe flow may contribute to streamflow independent of any extension in the dynamic contributing areas, or they may issue on to the lower slopes and contribute to the expansion of the dynamic contributing areas.

Several studies have been carried out to assess the hydrologic response of forested and hilly humid areas (Edwards and Blackie, 1981; Golding, 1980; Hewlett and Hibbert, 1967; Hopkins, 1960). These studies indicate that a small region of the watershed will have dramatic effect on the local hydrologic cycle and little or no effect on the catchment cycle.

1.3 JUSTIFICATION FOR THE PRESENT STUDY

Most of the studies related to VSA hydrology have focused on humid watersheds located in temperate regions. Fewer studies have been reported from humid tropical regions. For instance, in India it is likely that VSA hydrology may be prevalent in thickly vegetated, steep sloping upland catchments of the humid tropical Western Ghats (also known as Sahayadri mountain ranges) located in the southern part of the country. Experimental evidence of a combination of Hortonian overland flow, saturated area runoff and pipe overland flow contributing to streamflow in this region has been provided by Putty and Prasad (2000). Application of a lumped CN-based model to five catchments in the Western Ghats region by Putty (2009) indicated that although delayed runoff contributed a large portion of streamflow, significant contributions were also derived from VSA and pipeflow mechanisms. Venkatesh (2011) measured saturated hydraulic conductivities of surface soils in three watersheds located in the Western Ghats, compared these with rainfall intensities and deduced that VSA mechanism of runoff generation was prevalent in these well vegetated permeable hill slopes. Based on the results of these studies runoff generation mechanisms in the Western Ghats regions can be explained through a schematic representation as depicted in Fig. 1.3.

Characterizing runoff generation mechanisms in the Western Ghats region is critical since all the major rivers of Peninsular India originate here. The Cauvery is one of the major rivers which originate in the Western Ghats (Fig. 3.1). The basin is flanked on the west by the Western Ghats and a large part of the river flow is derived from runoff generated on thickly forested mountain slopes. The Cauvery River basin extends over four south Indian States of Kerala, Karnataka, Tamil Nadu and Pondicherry. It is considered to be one of the most important river basins of peninsular India and caters to water needs of millions of people in the region. Extensive development of water resources – both surface and groundwater has taken place in this river basin for several decades.

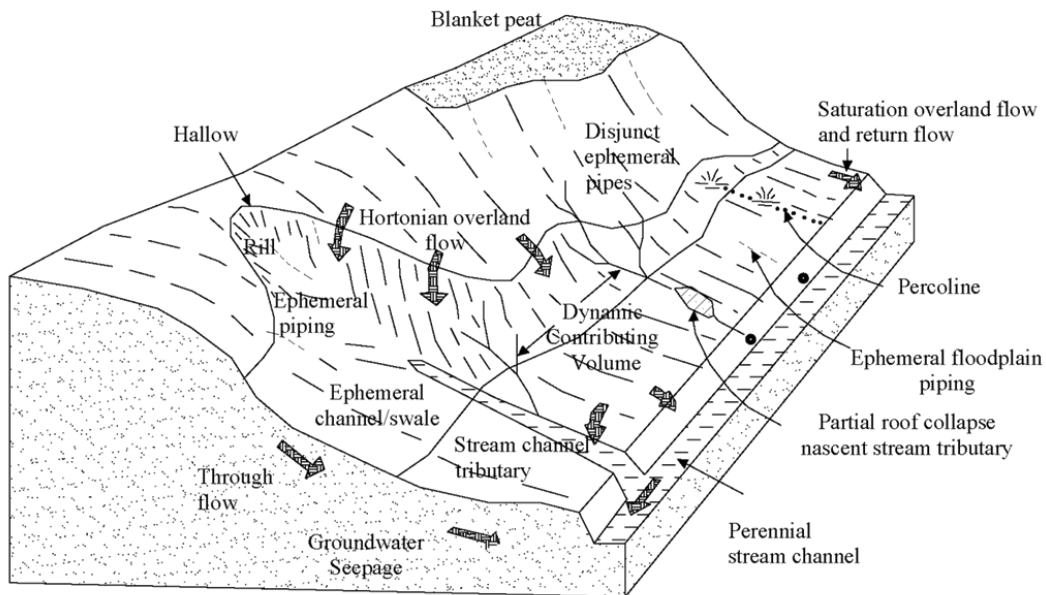


Fig. 1.3 The mechanism and the effects of piping (Kirkby, 1978)

Being one of the basins with the highest percentage of water resources utilization in the country, it is not surprising that there is a long standing dispute on water sharing between the riparian States. The Upper Cauvery basin which forms a part of the larger Cauvery basin encompasses the State of Karnataka. The Upper Cauvery Basin supports more than 20 million people. Agriculture in this basin provides livelihood to a large population and contributes significantly to the food production of Karnataka State. More than 70, 000 ha of land is irrigated from canals, groundwater wells and tanks. Water is also used for domestic, hydropower, tourism and industrial purposes. Due to rapid urbanization and industrial growth, the demand for water has increased significantly in the past two decades, which is likely to further increase the pressure on water availability from the surface as well as ground water sources within the basin. The increased development of the upstream command areas, compounded by the frequent failure of monsoons, has resulted in over-exploitation of ground water for irrigation, domestic and industrial uses. Also, changes in rainfall and climate patterns in the upstream area have led to frequent shortages of water for irrigation.

Therefore, there is an urgent need to develop an appropriate hydrological modeling tool which incorporates the prevalent runoff generation mechanisms and permits more

accurate simulation of hydrological processes and provides realistic estimates of the temporal and spatial distribution of available water resources. Identification of the source areas of runoff will aid in better conservation practices related to water quantity and quality. The main focus of the present study was to model temporal and spatial variability of runoff in watersheds of the Upper Cauvery basin which are located in the humid tropical Western Ghats region. The objective was to investigate whether adoption of VSA hydrology would yield more realistic estimates of runoff patterns in comparison to using the conventional infiltration-excess mechanism. Accordingly, the conventional (infiltration-excess) version of SWAT and also the SWAT-VSA version (Easton et al., 2008) models were applied to two watersheds. While the land cover in one of the watersheds was dominated by forest, the other watershed possessed a large proportion of agricultural land use. Therefore, comparison of results between the two watersheds provided an opportunity to evaluate the effect of LU/LC on temporal and spatial patterns of runoff produced by both runoff mechanisms adopted. Also, an attempt was made in this study to replace the topography-based wetness index used in SWAT-VSA with a satellite-based wetness index called Modified Normalized Differential Water Index (MNDWI). Accordingly, a new version of the model, SWAT-MNDWI was also included in the comparison. Subsequently, the three models were applied to the Hemavathi and Harangi watershed of the Upper Cauvery Basin.

1.4 MODEL UNCERTAINTY ANALYSIS

In recent times, it is widely accepted that all hydrological modeling exercises must provide a detailed report of the associated uncertainty in predictions. Proper consideration of uncertainty in hydrological modeling is essential for assessment of water balance components and optimal planning and management of water and land resources (Wagener and Gupta, 2005). Uncertainty analysis is a process of identifying and quantifying uncertainties associated with model structure, input data and parameters of a hydrological model (Beven and Binley, 1992; Muleta and Nicklow, 2005). The uncertainty associated with model structure and its parameters and input data effects the efficiency of the predictions of hydrological models. The various sources of error and uncertainty in hydrological modeling have been analysed by

various researchers (Beven and Freer, 2001; Ewen et al., 2006; Schaepli et al., 2007). Ewen et al. (2006) gave a comprehensive description (Table 1.1) of the error sources in hydrological modeling, which were categorized into three groups: 1) model structure error 2) model parameter error and 3) run time error. These three components contribute to the “integrated” model output error, but the individual contribution of each error cannot be isolated because it is difficult to assess such individual hydrologic responses.

Table 1.1 Error components of hydrological modeling (Ewen et al., 2006)

Model structure error	<ul style="list-style-type: none"> • It is a philosophical question whether any model can exactly represent the truth, so even the best possible model might give “integrated” error. • From conceptual and mathematical simplification • From using approximate numerical solutions, finite time steps, etc. • From conceptual, mathematical and programming mistakes made by the modeler
Parameter error	<ul style="list-style-type: none"> • From incomplete or erroneous calibration data (i.e. forcing and response data used in calibration) • From the calibration process, to compensate for the model structure error • By not using the optimal parameter values • From the mistakes made by the modeler in setting parameter values
Run time error	<ul style="list-style-type: none"> • From incomplete and erroneous forcing data • From mistakes in forcing data made by the modeler and from mistakes in the way the model is used and the results interpreted

Many uncertainty analysis methods have been introduced in hydrological modeling, which include Generalized Likelihood Uncertainty Estimation (GLUE) (Beven and Binley, 1992), Importance sampling (Kuczera and Parent, 1998), Markov Chain Monte Carlo (MCMC) (Kuczera and Parent, 1998; Vrugt et al., 2003), Sequential Uncertainty Fitting (SUFI-2) (Abbaspour et al., 2004), Parameter solutions (ParaSol)

(Van Griensven et al., 2006), Ensemble Kalman Filter (EnKF) (Vrugt et al., 2005), Bayesian Recursive Estimation (BaRE) (Thiemann et al., 2001), and Bayesian Model Averaging (BMA) (Ajami et al., 2007; Duan et al., 2007; Vrugt and Robinson, 2007). Among the many uncertainty analysis methods that have been introduced in hydrological modeling, GLUE and SUFI-2 use the flexible likelihood function to assign different levels of confidence to different parameter sets or models.

Since the present study is concerned with application of hydrological models, detailed uncertainty analysis of model predictions was carried out.

1.5 TREND ANALYSIS OF HISTORICAL HYDROCLIMATIC DATA

Climate change impacts on water resources are likely to be most critical in river basins such as the Upper Cauvery which are located in the humid tropics. Therefore, characterization of the impacts of climate changes on the temporal and spatial distribution of available water resources is critical to ensuring sustainable development of water, land and other related natural resources. As a first step towards achieving this, it is necessary to create scenarios of possible future climatic conditions.

An important approach to characterizing and predicting future climatic conditions is through analysis of historical records of hydro-climatic variables such as air temperature, precipitation and streamflow. Various types of sophisticated statistical techniques/tools have been developed to identify the direction and magnitude of trends exhibited in long time-series of historical observations of hydro-climatic variables. Over the past few decades, several world-wide trend detection studies have been carried out by previous researchers at different temporal and spatial scales (Bartzokas et al., 2003; Chen et al., 2007; George, 2007; Shao and Li, 2011; Zhang et al., 2011). Several studies have been taken up in various regions of India to assess trends in hydro-climatic variables (Gadgil et al., 2002; Gosain et al., 2006; Munot and Kumar, 2007; Pai and Rajeevan, 2006). Jain et al. (2013) provide a comprehensive review of studies taken up in India to analyse trends in temperature and rainfall in different hydro-climatic regimes. A few studies have also been taken up to evaluate

trends in hydro-climatic variables in the Upper Cauvery Basin (Francis and Gadgil, 2009; Kumar et al., 2010; Parthasarathy et al., 1993).

Since the present study utilized a reasonably large database of ground-based historical measurements of various hydroclimatic variables pertaining to the Upper Cauvery basin, an attempt was made to characterize trends in these variables. Climate changes are likely to significantly effect the temporal and spatial distribution of water resources and thereby effect the sustainability of agriculture in the region. Therefore, there is an urgent need to characterize historical and recent trends in hydro-climatic variables so that further studies aimed at assessing agro-hydrological impacts and formulating mitigation measures for climate change will be benefitted.

1.6 HYDROLOGICAL IMPACTS OF LU/LC CHANGES

Over the past few decades, significant changes in the LU/LC of Western Ghats region has taken place through deforestation and simultaneous afforestation of degraded lands and grass lands by planting exotic species such as Acacia (Jha et al., 2000). Large scale plantation of exotic species in parts of Western Ghats may have detrimental impacts on the hydrology of the region (Vandana and Bandyopadhyay, 1983) and specifically on soil moisture regime (Venkatesh et al., 2011) and subsurface water (Calder et al., 1992).

Impact assessment of LU/LC changes on spatial distribution of water availability is critically dependent on accurate modeling of hydrologic process. Assessing the consequences of LU/LC changes on altered hydrologic processes is an emerging focus on long-term land use planning and management (DeFries and Eshleman, 2004). Several studies have been carried out to evaluate the impact of LU/LC changes on hydrologic processes at different catchment scale and climate using hydrologic modeling (Elfert and Bormann, 2010; Huang et al., 2010; Im et al., 2009; Wagner et al., 2013; Yan and Edwards, 2013; Zhou et al., 2013).

However, few studies have reported the assessment of hydrological impacts of LU/LC changes in the Upper Cauvery basin, especially in the upland regions located in the Western Ghats. Therefore, an effort was made in this study to use the developed

hydrological models to simulate the changes in hydrological processes arising out of hypothetical changes in the distribution of LU/LC in the basin.

1.7 STUDY OBJECTIVES

1. To analyze historical trends in rainfall and other hydroclimatic variables using ground-based observations made in the Upper Cauvery river basin
2. To exploit the benefits offered by satellite remote sensing based inputs and develop GIS based hydrological models with a more realistic representation of runoff generation mechanisms prevalent in heterogeneous basins
3. To compare the performances of hydrological models which incorporate infiltration-excess runoff generation with those which incorporate saturation-excess runoff generation mechanism in humid tropical watersheds
4. To explore the applicability of such distributed hydrologic modeling approaches to estimate spatial and temporal patterns of hydrological components within selected representative catchments in the Upper Cauvery Basin
5. To quantify the total uncertainty in estimated streamflow induced on account of uncertainties in model inputs, model parameters and model structure
6. To investigate the hydrologic impacts of hypothetical LU/LC change scenarios using the developed hydrologic models

1.8 OVERVIEW OF RESEARCH METHODOLOGY

Table 1.2 gives an overview of the overall methodology adopted in this research work. Depicted therein are the major tasks and specific activities undertaken to achieve the objectives of the study.

Table 1.2 Overview of research methodology adopted

Analysis of Hydrometeorological Data	Hydrological Modeling	Uncertainty Analysis	Impact of land cover changes
1) Statistical analysis ✓ Coefficients of variation ✓ Percentage departure 2) Significance of the trend ✓ Seasonal-Kendall method 3) Magnitude of a trend ✓ Sen's slope estimator 4) Long-term persistence ✓ Detrended fluctuation analysis	1) Develop and test a SWAT model with a wetness index derived from ✓ DEM ✓ Remote sensing data 2) Sensitivity analysis 3) Accuracy of daily streamflow predictions 4) Predictions of averaged annual water balance components 5) Differences in spatial patterns of source areas of surface runoff	1) Uncertainty analysis of developed hydrological models using ✓ GLUE ✓ SUFI-2	1) Hydrologic responses of developed models to simulate hypothetical land cover scenarios

1.9 ORGANIZATION OF THESIS

The thesis comprises of eight chapters, list of references and other annexures. A brief description of the each chapter is presented here.

Chapter 1 provides an introduction to the problem being considered for the study, the main objectives of the study and overview of the research methodology adopted.

Chapter 2 presents literature review of the previous works on analysis of hydrometeorological variables, development and application of SWAT model.

A description of the study area and the dataset used in this study is provided in **Chapter 3**.

Chapter 4 describes the analysis of historical hydroclimatic data to evaluate the significance and magnitude of trends over long periods.

Details of the distributed hydrological models used in this study are given in **Chapter 5**. The developed SWAT-MNDWI and available SWAT-VSA and SWAT models are applied to the Hemavathi and Harangi watersheds which are located in the Upper Cauvery Basin, Karnataka, India. Model performances are compared.

Chapter 6 provides uncertainty analysis of the developed models using two different techniques.

Chapter 7 is concerned with the application of the developed models to simulate the hydrological impacts of hypothetical land cover changes.

Finally, **Chapter 8** lists out overall conclusions, limitations and scope for further research.

CHAPTER 2

REVIEW OF LITERATURE

2.1 GENERAL

In following sections of this chapter, a review of available literature pertaining to the trend analysis of hydroclimatic variables, application and evaluation of SWAT model in various regions of the world, uncertainty analysis of hydrological models, hydrological impacts of LU/LC changes and modeling using VSA hydrology is provided.

2.2 ANALYSIS OF HYDROMETEOROLOGICAL VARIABLES

Burn and Hag Elnur (2002) developed a procedure for identifying trends in hydrologic variables. The Mann-Kendall non-parametric test was adopted to detect the variation in the trends and a permutation approach to estimate the trend distribution, and accounted for the correlation structure in the data in determining the significance level of the test results. The hydrologic variables were analyzed for a network of 248 Canadian catchments that were considered to reflect natural conditions. The study concluded that a greater number of trends were observed than were expected to occur by chance.

Gadgil et al. (2002) assessed that deficit in rainfall during 2002 was abnormal. This abnormality might be due to an unprecedented catastrophe or due to natural variability of the monsoon over India. From their study, it was concluded that the shortage in rainfall was due to the natural variation in the monsoon. Analysis of the past data suggested that there was a 78% chance that seasonal mean rainfall during that year would be 10% or more below the long-term average value. Also, they discussed briefly how forecasts for seasonal rainfall were generated, whether that event could have been foreseen.

Yue et al. (2002) used two non-parametric rank-based statistical tests, namely the Mann-Kendall test and Spearman's rho test for detecting monotonic trends in time series data. Also, their study investigated the power of these tests by Monte Carlo

simulation. The results indicated that their power depends on the pre-assigned significance level, magnitude of trend, sample size, and the amount of variation within a time. The simulation results also demonstrated that these two tests have similar power in detecting a trend, to the point of being indistinguishable in practice. The two tests were implemented to assess the significance of trends in annual maximum daily streamflow data of 20 pristine basins in Ontario, Canada. Results indicated that the P-values computed by these different tests were almost identical. By the binomial distribution, the field significant downward trend was assessed at the significance level of 0.05. Results indicated that a higher number of sites show evidence of decreasing trends than one might expect due to chance alone.

Archer (2003) investigated the characteristics of hydrological regimes using streamflow data from nineteen long-period stations in terms of annual and seasonal runoff. Regression between climatic variables and streamflow for three key basins, the River Hunza, River Astore and Khan Khwar were carried out followed by regional analysis of twelve further basins. Analysis showed distinct hydrological regimes with summer volume governed by: melt of glaciers and permanent snow, melt of seasonal snow, or winter and monsoon rainfall.

Chen et al. (2007) investigated the temporal trends of annual and seasonal runoff, precipitation and temperature from 1951 to 2003 in the Hanjiang basin using the Mann–Kendall and the linear regression methods and assessed the impact of climate change on water resources and predicted the future runoff change in the Danjiangkou reservoir basin using a two-parameter water balance model for the climate change forecasted by GCMs for the region for the period of 2021-2050. Simulated results indicated that during 2021-2050 annual runoff would increase by 8.18%, 7.78% and 2.14%, respectively, when the scenarios predicted by HadCM3, CSRIO and CCSRNIES were used as inputs to the water balance model. Sensitivity analysis showed that 1°C and 2°C increase in temperature reduced mean annual runoff by about 3.5% and 7%, respectively. A decrease/increase of mean monthly precipitation by 20 and 10% resulted in decreases/increase of mean annual runoff by about 30% and 15%, respectively.

George (2007) examined the long-term stream flow in the Winnipeg River basin, Canada during the last one hundred years. Result indicated that the mean annual flows had increased by 58% since 1924, primarily because of large increase in winter discharge. Increasing summer and autumn precipitation was the most probable cause of the changes in streamflow. The observed trends toward higher flows, combined with recent model projections, suggested that the potential threats to water supply faced by the Canadian Prairie provinces over the next few decades would not include decreasing streamflow in the Winnipeg River basin.

Hamed (2008) proposed a scaling hypothesis for the Mann–Kendall test to detect variability in hydrologic data. Exact expressions for the mean and variance of the test statistic were derived under the scaling hypothesis, and the normal distribution was shown to remain a reasonable approximation. A procedure for estimating the modified variance from observed data was also outlined. The modified test was applied to a group of 57 worldwide total annual river flow time series from the database of the Global Runoff Data Centre in Koblenz, Germany. The results showed a considerable reduction in the number of stations with significant trends when the effect of scaling is taken into account. These results indicated that the evidence of real trends in hydrologic data is even weaker than suggested by earlier studies, although highly significant increasing trends seem to be more common than negative ones.

Brabets and Walvoord (2009) analyzed the seasonal, monthly, and annual stream discharge data from 21 stations in the Yukon River Basin for trends over the entire period of record. Observed winter flow increased during the cold-PDO (Pacific Decadal Oscillation) phase and was generally limited to sites in the Upper Yukon River Basin. Positive trends in winter flow during the warm-PDO phase broadened to include stations in the Middle and Lower Yukon River drainage basins. Annual discharge remained relatively unchanged in the Yukon River Basin, but a few glacier-fed rivers demonstrated positive trends, which could be attributed to enhanced glacier melting.

Hamed (2009) developed a procedure for the calculation of the exact distribution of the Mann-Kendall trend test statistic for persistent data with an arbitrary correlation

structure. The application of this procedure was used to test the significance of recent trends starting in 1990 in 58 world river flow time series. Results confirmed the effect of scaling in small samples and the benefits of using the beta distribution as an approximation.

Kumar et al. (2009) evaluated the trends in 31 USGS gauging stations that have 50 years or more continuous unregulated streamflow records using four variations of the Mann-Kendall test. These variations include: (i) Mann-Kendall without autocorrelation, (ii) Mann-Kendall with lag-1 autocorrelation and trend-free pre-whitening, (iii) Mann-Kendall with complete autocorrelation structure, and (iv) Mann-Kendall with long term persistence. Mann-Kendall test was also applied to the precipitation data using the above four approaches to explore the relationship between precipitation and stream flow trends. Overall, there was an increasing trend in low and medium flow conditions across Indiana. They suggested that the subsurface drainage is playing a role in the observed streamflow trends in Indiana and its role needs to be further investigated.

Sahoo and Smith (2009) analyzed the trends in several hydro climatic variables in the rapidly urbanizing semi-arid San Antonio River Basin, particularly trends in freshwater inflows to the Guadalupe Estuary using the Mann-Kendall non-parametric test after removing serial and cross-correlations. The significance of detected trends was analyzed using a permutation method. Results of the analysis revealed a definitive line just below the City of San Antonio above which the influence of the increase in impermeable surfaces could be clearly seen. Above this line nearly all significant trends were negative (decreasing). The percent contribution of base flow to total streamflow in the upper watershed decreased for almost every season due to high, average, and low precipitation events. But, they observed that below this definitive line all significant trends were positive (increasing)

Boyer et al. (2010) assessed the magnitude of the hydrological alteration associated with climate change and examined the latitudinal component of the projected changes through the use of five watersheds on both shores of the St. Lawrence. Projected river discharges for the next century were generated with the hydrological model HSAMI

which was run with six climate series projections. The results showed that most of the hydrological simulations projected an increase in winter discharges and a decrease in spring discharges. Also, increase in mean temperature with the simultaneous decrease of the snow/precipitation ratio during the winter and spring period explained a large part of the projected hydrological changes.

Kumar et al. (2010) studied the monthly, seasonal and annual trends of rainfall using monthly data series of 135 years (1871–2005) for 30 sub-divisions (sub-regions) in India. Half of the sub-divisions showed an increasing trend in annual rainfall, but for only three (Haryana, Punjab and Coastal Karnataka), this trend was statistically significant. Similarly, only one sub-division (Chattisgarh) indicated a significant change in the trend out of the 15 sub-divisions showing decreasing trend in annual rainfall. For the whole of India, no significant trend was detected for annual, seasonal, or monthly rainfall. Annual and monsoon rainfall decreased, while pre-monsoon, post-monsoon and winter rainfall increased at the national scale. Rainfall in June, July and September decreased, whereas in August it increased, at the national scale.

Shao and Li (2011) developed a trend analysis tool by including a period component in the method. They observed that by doing this, the data dependence and seasonality would not be issues but become advantages due to information gain in each period. The proposed method treated the change in hydrological series as the interaction between long-term trend and seasonal variation. Unlike the traditional functional coefficient models which extend the threshold regression model, this functional coefficient model with periodic components enjoyed smoothing changes from year to year.

Tabari and Talaei (2011) analyzed the annual and seasonal precipitation trends of 41 stations in Iran for the period 1966–2005 using the Mann-Kendall test, the Sen's slope estimator and linear regression. The effective sample size method was applied to eliminate the effect of serial correlation on the Mann-Kendall test. The results indicated a decreasing trend in annual precipitation at about 60% of the stations. The decreasing trends were significant at seven stations at the 95% and 99% confidence levels. The magnitude of the significant negative trends in annual precipitation varied

from -1.999 mm/year at Zanzan station to -4.261 mm/year at Sanandaj station. The spatial distribution of the annual precipitation trends showed that significant negative trends occurred mostly in the northwest of Iran. On the seasonal scale, the trends in the spring and winter precipitations time series were negative. The highest number of stations with significant trends occurred in winter while no significant positive or negative trends were detected by the trend tests in autumn precipitation. In addition, the highest and lowest significant increases of precipitation values were obtained over Semnan and Mashhad in summer at the rates of +0.110 mm/year and +0.036 mm/year respectively.

Guerrero et al. (2012) studied the temporal variability and the uncertainty of the rating curve and its parameters through a Monte Carlo (MC) analysis on a moving window of data using the Generalised Likelihood Uncertainty Estimation (GLUE) methodology for six hydrometric stations in the upper Choluteca River basin, Honduras. The quotient in discharge volumes estimated from dynamic and static rating curves varied between 0.5 and 1.5. The difference between discharge volumes derived from static and dynamic curves was largest for sub-daily ratings but stayed large also for monthly and yearly totals. The relative uncertainty was largest for low flows but it was considerable also for intermediate and large flows.

Sonali and Nagesh Kumar (2013) studied the spatial and temporal trend of annual, monthly and seasonal maximum and minimum temperatures in India. Trends in annual, monthly, winter, pre-monsoon, monsoon and post-monsoon extreme temperatures were analyzed for three time slots viz. 1901–2003, 1948–2003 and 1970–2003. For this purpose, time series of extreme temperatures of India as a whole and seven homogeneous regions, viz. Western Himalaya (WH), Northwest (NW), Northeast (NE), North Central (NC), East coast (EC), West coast (WC) and Interior Peninsula (IP) were considered. Results revealed that the trend in minimum temperature is significant in the last three decades over India. Sequential MK test revealed that most of the trends both in maximum and minimum temperature began after 1970 either in annual or seasonal scales.

2.3 SOIL AND WATER ASSESSMENT TOOL (SWAT)

SWAT is a physically based distributed parameter model which has been developed to predict runoff, erosion, sediment and nutrient transport from agricultural watersheds under different management practices (Arnold et al., 1998). SWAT has been widely used in various regions and climatic conditions on daily, monthly and annual scale- and for watersheds of various sizes and scales. SWAT is suitable in the following contexts:

- Modeling watersheds with no monitoring data.
- Quantification of relative impact of alternative input data (e.g. change in management practices, climate, vegetation, etc) on water quality and other variables of interest.
- Modeling of various management strategies can be modelled without excessive investment in time or money.
- Studies which include long-term inputs.

Some of the hydrological water balance, uncertainty analysis, LU/LC change and VSA modeling studies using SWAT are discussed in the following sections.

2.3.1 Hydrological Water Balance Studies Using SWAT

In recent decades, the Soil and Water Assessment Tool (SWAT) model has proved to be one of the most popular models used world-wide for addressing a variety of water quantity and quality issues related to watershed hydrology. SWAT model has gained international acceptance as a robust interdisciplinary hydrological modeling tool. Based on the SWAT model, several hundreds of papers have been published in peer-reviewed journals and presented at international conferences (https://www.card.iastate.edu/swat_articles/).

Accordingly, this review is focused on only those SWAT model studies which are relevant to the objectives of the research – applications in humid watersheds.

Mamillapalli et al. (1996) found an improved accuracy in monthly flow predictions using the SWAT model for the 4,297 km² Bosque River Watershed in central Texas

as the number of sub watersheds increased. However, they did not present any method for determining the optimal sub watershed configuration for a watershed.

Bingner et al. (1997) suggested that sensitivity analyses should be conducted on land use, overland slope, and slope length for different subdivisions to decide the appropriate number of sub watersheds required for flow and sediment prediction, based on their study using SWAT for the 21.3 km² Goodwin Creek Watershed in northern Mississippi.

Murali Mohan (2000) applied physically based SWAT model to a 349.512 km² Yennehole river basin and the model was run as lumped, distributed and land use model. The performance of the SWAT model was assessed using stream flow values. The model showed good performance in tropical-humid catchments as well as sub-humid and semi-arid regions. The results indicated that the model could be applied to any ungauged catchments for simulating components of hydrological cycle.

Pikounis et al. (2003) used SWAT model to a 2976 km² catchment located in the Thessaly plain, in central Greece. The model was employed to simulate the main components of the hydrologic cycle in order to study the effects of land use changes. Three different land use change scenarios (expansion of agricultural land, complete deforestation of the Trikala sub-basin and expansion of urban areas in the Trikala sub-basin) were applied. All three scenarios showed increase in discharge during wet months and a decrease during dry periods.

Shrivastava et al. (2004) used distributed parameter SWAT model to estimate the daily and monthly surface runoff and sediment yield from a small watershed "Chhokeranala" in eastern India using satellite data and Geographical Information System (GIS). The results showed a good agreement between observed and simulated runoff and sediment yield during the study period. The results presented showed that the SWAT model could be used for satisfactory simulation of daily and monthly rainfall and runoff.

Tripathi et al. (2004) tested the SWAT model to simulate the runoff and sediment yield of a small agricultural watershed in eastern India using generated rainfall.

Results revealed that the SWAT model could generate monthly average rainfall satisfactorily and thereby could predict monthly average values of surface runoff and sediment yield close to the observed values.

White and Chaubey (2005) implemented the SWAT model to Beaver Reservoir Watershed of Northwest Arkansas. Results showed that calibration and validation of the model was a key factor in reducing uncertainty and increasing user confidence in its predictive abilities, which makes the application of the model effective.

Bekele and Nicklow (2007) studied the multi objective automatic calibration of a SWAT model to involve large number of calibration parameters, representing the spatial heterogeneity of inputs and various physical processes within a watershed. An automatic calibration method was developed using the Non-dominated Sorting Genetic Algorithm II (NSGA-II). The results showed that the approach was consistent and effective in estimating parameters of the model. The use of multiple objectives during the calibration process resulted in improved model performance.

Confesor and Whittaker (2007) investigated the application of Multi-Objective Evolutionary Algorithm (MOEA) and Pareto ordering optimization in the automatic calibration of the SWAT model. The NSGA-II, a fast and recent MOEA, and SWAT were processed in FORTRAN from a Parallel Genetic Algorithm library (PGAPACK) to determine the Pareto optimal set.

Kannan et al. (2007) illustrated some simple and efficient approaches for sensitivity analysis, calibration and identification of the best methodology within a SWAT modelling framework. The Hargreaves and Penman-Montieth methods of evapotranspiration estimation and the NRCS Curve Number (CN) and Green and Ampt infiltration methods for runoff estimation techniques were used, in four different combinations, to identify the combination of methodologies that best reproduced the observed data. Also, the calibration and validation periods were interchanged to test the impact of calibration using wet or dry periods. The curve number method performed better than the Green and Ampt method in predicting daily stream flow.

Misgana et al. (2007) showed that the accuracy of the raw model output (stream flow and sediment) was poor for all sub watershed delineations conducted on the Big Creek Watershed (133 km²), located in southern Illinois.

Nina et al. (2007) successfully used SWAT and spatial database to simulate stream flows and sediment yielding on a 5793 km² watershed in Gharasu watershed. This basin is located in the northwest of Karkheh river basin, in the far western corner of Iran. SWAT was successfully validated for stream flow and sediment loads for the Gharasu watershed. Finally, the SWAT model was used to predict the effect of changing land use and conversation practices on sediment yield within the basin. The study indicated that SWAT model is a capable tool for simulating hydrologic components and erosion in Gharasu river basin.

Gebriye (2007) assessed the impacts of land management practices on the surface runoff in Anjeni gauged watershed, Northern highlands of Ethiopia. Sensitivity analysis was done to identify the most sensitive flow parameters for the specific land use and agro-climatic condition of the Anjeni watershed. These sensitive model parameters were adjusted within their allowable ranges during calibration to optimize model prediction. The model was calibrated using eight years hydrometric measurements, from 01 January 1984 to 31 December 1991. Validation of the model was also done with independent measured stream flow data from 01 January 1992 to 31 December 1993. The model performance evaluation statistics such as $E_{NS} > 0.91$ and $R^2 > 0.92$ showed that the model can produce reasonable estimates of monthly discharge.

Somura et al. (2008) applied the SWAT model to the Hii River basin dataset collected from 1986 to 2005 at daily time step. The parameters were calibrated using data from 1993 to 1996 and validated using data from 1986 to 1992 and from 1997 to 2005. The calibrated parameters CANMX, ALPHA_BF, SOL_AWC, SOL_Z, CH_K2, SMFMX, GWQMN, CN₂, ESCO and SLOPE, were selected based on ranking by sensitivity analysis. The results of both calibration and validation represented the fluctuations of discharge relatively well, though some peaks were overestimated. During the calibration period, R^2 varied from 0.65 to 0.77 and E_{NS} from 0.64 to 0.76.

During the validation period from 1986 to 1992, R^2 varied from 0.58 to 0.74 and E_{NS} from 0.53 to 0.74 and for period from 1997 to 2005, R^2 varied from 0.51 to 0.71 and E_{NS} from 0.38 to 0.68.

Wenzhi et al. (2009) linked GIS with SWAT to calibrate and validate the historic flow data for the current land use conditions. Two additional land cover scenarios (a prehistoric land cover and a potential maximum plantation pine cover) were used to evaluate the impacts of land cover change on total water yields, groundwater flow and quick flow. The study area was Motueka river catchment New Zealand having an area of 2180 km². The results indicated that the annual total water yields, quick flow and base flow decreased moderately in the two scenarios when compared with current actual land use. They concluded that the simulated low flows for the prehistoric and potential pine land cover scenarios were both significantly lower than the low flows for the current land use.

Mythri (2010) predicted the impact of climate change in 3657 km² Netravathi River basin. Trend analysis of rainfall showed a decreasing trend, whereas temperature showed an increasing trend. The SWAT results reveal that the Netravathi flow would reduce up to 41% by 2071 and up to 44% by 2099 from the present average flow of 11502 Mm³. The temperature of the basin was increasing at rate of 0.1 % (over 30 years) i.e. 1.2⁰C. Predictions showed a maximum increase of temperature by 17% and a minimum increase by 1% from the present average value.

Santosh et al. (2010) applied ArcSWAT to assess stream flow in the Chaliyar river basin in Kerala with drainage area 2919 km². The model was initially calibrated for observed streamflow and then validated. Critical parameters identified for optimization during calibration were the CN_2 , ESCO, SOL_AWC, SLSUBBSN, and ALPHA_BF. Stream flow was estimated from parts of the basin at two different scales. Results of R^2 and E_{NS} indicated that the SWAT model could simulate stream flow at both scales reasonably well with very little difference between the observed and computed values. The study indicated that there is a larger uncertainty in SWAT streamflow estimates at larger scales. The study also revealed that the accuracy of

meteorological and hydrologic data influenced the accuracy of model simulation results.

Xiang (2010) used distributed hydrological model, SWAT, to study the seasonal and interannual variation of the runoff in upstream Dagu River watershed and the governing processes. The model output was found sensitive to five parameters (e.g., CN_2 , ESCO, and SOL_AWC). The modeled results showed maximum monthly runoff occurring in August and minimum in February, consistent with the observation. The runoff depth was deep in the eastern and western areas, while it was relatively shallow in the southern and northern areas.

Mohan Kumar (2011) applied the SWAT model using inputs derived from available global datasets such as topography, land use, and soil map. The applicability of the SWAT model for the humid tropical Netravathi catchment was explored. The resolutions adopted in this study were large, coarse resolutions for which applicability and effectiveness of the SWAT model was studied. This was compared with model application made with conventional ground-based inputs. The R^2 and E_{NS} were used to evaluate model calibration. The Study showed satisfactory results for the daily, monthly, and yearly time steps using global datasets.

Bitew and Gebremichael (2011) assessed the suitability of commonly used high-resolution satellite rainfall products (CMORPH, TMPA 3B42RT, TMPA 3B42 and PERSIANN) as input to SWAT model for daily streamflow simulation in two watersheds (Koga at 299 km² and Gilgel Abay at 1656 km²) of the Ethiopian highlands. Results revealed that the utility of satellite rainfall products as input to SWAT for daily streamflow simulation strongly depended on the product type. The 3B42RT and CMORPH simulations showed consistent and modest skills in their simulations but underestimated the large flood peaks, while the 3B42 and PERSIANN simulations had inconsistent performance with poor or no skills. Increasing the watershed area from 299 km² to 1656 km² improved the simulations obtained from the 3B42RT and CMORPH (i.e. products that were found more reliable and consistent) rainfall inputs while it deteriorated the simulations obtained from the 3B42

and PERSIANN (i.e. products that were found unstable and inconsistent) rainfall inputs.

Chen et al. (2011) examined the potential for improving SWAT model hydrologic predictions of root-zone soil moisture, evapotranspiration, and stream flow within the 341 km² Cobb Creek Watershed in south-western Oklahoma through the assimilation of surface soil moisture observations using an Ensemble Kalman filter (EnKF). In a series of synthetic twin experiments, assimilating surface soil moisture was shown to effectively update SWAT upper-layer soil moisture predictions and provide moderate improvement to lower layer soil moisture and evapotranspiration estimates. Comparison against ground-based observations suggested that SWAT significantly under-predicted the magnitude of vertical soil water coupling at the site, and this lack of coupling impeded the ability of the EnKF to effectively update deep soil moisture, groundwater flow and surface runoff.

Singh and Gosain (2011) applied GIS based hydrological modeling for a multijurisdictional Indian River basin. Study showed that water yield of the basin was inversely proportional to the amount of forest cover and SWAT efficiently predicted the streamflow. The study demonstrated that simulation modeling can play a very significant role in water resources management by generating a series of scenarios.

Akiner and Akkoyunlu (2012) developed a new approach using an Artificial Neural Network (ANN) technique to improve precipitation missing value predictions and the future precipitation value estimations over the Melen watershed located in Western Black Sea region of Turkey. The monthly river flow rate from the Melen watershed was modeled and forecasted through the SWAT Model using the generated precipitation data. Results showed that there was a considerable good relation between the simulated and observed results.

Chen and Wu (2012) studied the integration of the SWAT model and the TOPographic MODEL (TOPMODEL) features for enhancing the physical representation of hydrologic processes. In SWAT, four hydrologic processes, surface runoff, base flow, groundwater re-evaporation and deep aquifer percolation were modeled by using a group of empirical equations. They found that the empirical

equations usually constrain the simulation capability of relevant processes. To replace these equations and to model the influences of topography and water table variation on streamflow generation, the TOPMODEL features were integrated into SWAT, and a new model, termed as SWAT-TOP was developed. In the new model, the process of deep aquifer percolation was removed, the concept of re-evaporation of groundwater was refined, and the processes of surface runoff and base flow were re-modeled. SWAT-TOP and SWAT were applied to the East River basin in South China, and the results revealed that, compared with SWAT, the new model could provide a more reasonable simulation of the hydrologic processes of surface runoff, groundwater re-evaporation, and base flow.

Karcher et al. (2013) modified the SWAT model to enable the identification of areas where implementation of best management practices would likely result in the most significant improvement in downstream water quality. Model results obtained using the new land-use cover was compared to those obtained using a more conventional land-use cover. Results indicated that stream flow and nutrient loadings were similar at the basin outlet, confirming the overall consistency of the approach. These results suggested that the alternative, crop-rotation-specific method could be used to provide additional information for spatially resolved decision making regarding nutrient loading and downstream nutrient concentrations.

Kushwaha and Jain (2013) tested the suitability of SWAT model for estimation of runoff and to assess the sensitiveness of model input parameters in a predominantly forested watershed (Dabka) in Kumaun region of Himalaya. Sensitivity analysis was performed on 13 input variables in terms of model outputs such as water yield, surface runoff and base flow to gain in depth understanding of the role of different model parameters for their proper selection. The study concluded that model performed well during calibration and validation period.

Adeogun et al. (2014) estimated the water yield and water balance of upstream Jebba hydropower dam catchment in Nigeria using SWAT model. The model output showed a good agreement between the observed flow and simulated flow as indicated by E_{NS} and R^2 , which were greater than 0.7 for both calibration and validation periods. The

performance obtained with SWAT model suggested that the model could be a promising tool to predict water balance and water yield in sustainable management of water resources.

Ahmadi et al. (2014) developed a computational framework for incorporation of disparate information from observed hydrologic responses at multiple locations into the calibration of watershed models. The proposed framework was applied for calibration of the SWAT model for the Eagle Creek watershed, USA using three single objective optimization methods and one multi objective optimization method. Solutions were classified into behavioral and non-behavioral using percent bias and NS. The results showed that aggregation of stream flow and NO_x ($\text{NO}_3\text{-N} + \text{NO}_2\text{-N}$) information measured at multiple locations within the watershed into a single measure of weighted errors resulted in faster convergence to a solution with a lower overall objective function value than using multiple measures of information. However, the DREAM (DiffeREntial Evolution Adaptive Metropolis) method solution was the only one among the three single objective optimization methods considered in this study that satisfied the conditions defined for characterizing system behaviour.

Bannwarth et al. (2014) developed a new calibration method, named ANSELM (A Nash-Sutcliffe Efficiency Likelihood Match), which allowed the assignment of optimal parameters to different hydrological response units in simulations of stream discharge with the SWAT model to overcome calibration difficulties related to the mountainous topography. ANSELM performed better than the Parasol calibration tool built into SWAT in terms of model efficiency and computation time. The coupling of SWAT with ANSELM yielded reasonable simulations of both wet- and dry-season storm hydrographs.

Bieger et al. (2014) simulated surface runoff and sediment yields for the Xiangxi Catchment using SWAT model. The study allowed for a more precise targeting of BMPs than analysis at the coarser sub basin level and provided an opportunity to validate simulated amounts of surface runoff and sediment yield by evaluating the plausibility of their spatial variation within the watershed. Results indicated that satisfactory model performance at the gauge does not guarantee plausible results at

HRU level. Both surface runoff and sediment yields varied reasonably with land use and soil types, but not with slope.

Hari Krishna et al. (2014b) studied the characterization of the hydrologic processes of the Upper Manair catchment and assess crop water productivity using SWAT to evolve irrigation management plans to sustain the use of groundwater resources for irrigation. The biological and economical yield of different field crops, viz. Rice, Maize, Cotton, Sugarcane and sunflower were predicted successfully. Water productivity for Rice, Maize, Cotton, Sugarcane and sunflower were estimated to be 0.61, 1.27, 0.41, 8.04 and 1.05 kg/m³, respectively, which were significantly lower than the potential.

Mosbahi et al. (2014) conducted a sensitivity analysis for flow in a semi-arid catchment, located in northwestern of Tunisia, using SWAT model. The simulation results revealed that among eight selected parameters, CN₂, ESCO, SOL_AWC and GWQMN were found to be the most sensitive parameters. Results of calibration showed that the SWAT model could accurately predict streamflow.

2.3.2 Uncertainty Analysis Studies Using SWAT

Chaubey et al. (2005) studied the effect of DEM data resolution on predictions from the SWAT model. The effect of input data resolution was evaluated by running seven scenarios at increasing DEM grid sizes (30 x 30 m, 100 x 100 m, 150 x 150 m, 200 x 200 m, 300 x 300 m, 500 x 500 m, 1000 x 1000 m). Results of this study showed that the grid size effected the watershed delineation, stream network and sub-basin classification in the SWAT model. A decrease in grid size resulted in decreased stream flow predictions. However, choice of input grid size depended on the watershed response of interest. Minimum DEM data resolution ranged from 100 to 200 m to achieve less than 10% error in SWAT output of stream flow.

Muleta and Nicklow (2005) developed an automatic approach for calibrating daily streamflow and daily sediment concentration of watershed located in southern Illinois using SWAT model. The automatic calibration method was developed on a hierarchy of three techniques, namely screening, parameterization, and parameter sensitivity analysis, at the parameter identification stage of model calibration. Latin hypercube

sampling was used to generate input data from the assigned distributions and ranges, and parameter estimation was performed using genetic algorithm. The Generalized Likelihood Uncertainty Estimation (GLUE) methodology was subsequently implemented to investigate uncertainty of model estimates, accounting for errors due to model structure, input data and model parameters.

Abbaspour et al. (2007) used SWAT model to simulate the related processes effecting water quantity, sediment, and nutrient loads in the Thur River catchment, which is located in the north-east of Switzerland. Model calibration and uncertainty analysis were performed with Sequential Uncertainty Fitting algorithm (SUFI-2). The percentage of data bracketed by the 95% prediction uncertainty and the d-factor measures were used to assess the goodness of calibration. These statistics showed excellent results for discharge and nitrate and quite good results for sediment and total phosphorous and concluded that watersheds similar to Thur with good data quality and relatively small model uncertainty it is feasible to use SWAT as a flow and transport simulator.

Arabi et al. (2007) developed a computational framework for analyzing the uncertainty in model estimates of water quality benefits of best management practices (BMPs) in two small watersheds in Indiana. SWAT was integrated with Monte Carlo-based simulations to adjust the suggested range of model parameters to more realistic site-specific ranges based on observed data and computing a scaled distribution function to assess the effectiveness of BMPs. Results indicated that the suggested range of some SWAT parameters, especially the ones that were used to determine the transport capacity of channel network and initial concentration of nutrients in soils, required site-specific adjustment. It was evident that uncertainties associated with sediment and nutrient outputs of the model were too large, perhaps limiting its application for point estimates of design quantities.

Tolson and Shoemaker (2008) developed an alternative methodology to the GLUE technique in which pseudo likelihood functions are utilized, instead of a traditional statistical likelihood functions to improve the efficiency of uncertainty analysis. The study showed how the new Dynamically Dimensioned Search (DDS) optimization

algorithm could be used to independently identify multiple acceptable or behavioral model parameter sets in two ways. They developed a new, practical, and efficient uncertainty analysis methodology called DDS–Approximation of Uncertainty (DDS-AU) that quantified prediction uncertainty using prediction bounds rather than prediction limits. Results showed that for the same limited computational effort, DDS-AU prediction bounds could simultaneously be smaller and contain more of the measured data in comparison to GLUE prediction bounds.

Yang et al. (2008) implemented five uncertainty analysis techniques (GLUE, Parameter Solution (ParaSol), SUFI-2, and a Bayesian framework using Markov chain Monte Carlo (MCMC) and Importance Sampling (IS)) for the SWAT model to determine the differences and similarities. The results with respect to the posterior parameter distributions, performances of their best estimates, prediction uncertainty, conceptual bases, computational efficiency, and difficulty of implementation were compared. Also, if computationally feasible, Bayesian-based approaches were recommended because of their solid conceptual basis, but construction and test of the likelihood function required critical attention.

Shen et al. (2012) studied the parameter uncertainty of the stream flow and sediment simulation in the Daning River Watershed of the Three Gorges Reservoir Region (TGRA), China using GLUE technique with the SWAT model. The results showed that sediment simulation presented greater uncertainty than stream flow, and uncertainty was even greater in high precipitation conditions (from May to September) than during the dry season. Also, the main uncertainty sources of stream flow came from the catchment process while a channel process impacts the sediment simulation greatly.

Datta and Bolisetti (2013) adopted the second order autoregressive likelihood method (AR(2)) to calibrate the SWAT model for the Canard River watershed, south-western Ontario, Canada. The Bayesian approach was used for uncertainty analysis of SWAT modeling. The results were compared with the simple least square (SLS) method of calibration. The study revealed that the AR(2) method parameter uncertainty was high and there exists local optimum values in the parameter space. The reliability of

streamflow simulation uncertainty due to parameter uncertainty was increased when AR(2) model is implemented in the calibration process. Therefore, this study suggests applying separate statistical error models in the likelihood function for representing the modeling errors in low-flow and high-flow periods

Shi et al. (2013) evaluated the performance of the SWAT model for hydrologic modeling in the Xixian basin using three methods of calibration and uncertainty analysis (SUFI-2, GLUE, ParaSol). The results showed that SWAT performed well in the Xixian River basin, in performing the hydrological water balance analysis which indicated that base flow was an important aspect of the total discharge within the study area, and that more than 60% of the annual precipitation is lost through evapotranspiration.

Athira and Sudheer (2014) quantified the uncertainty in the simulations from SWAT model using GLUE on a watershed in the USA. The number of simulations required for the uncertainty analysis was reduced by 90% in the proposed method compared to existing methods. The proposed method also resulted in an uncertainty reduction in terms of reduced average band width and high containing ratio.

Xue et al. (2014) tested the two uncertainty analysis methods, the SUFI-2 and GLUE to analyze the uncertainty of surface flow and sediment yield modeling using SWAT model. The results showed that the SUFI-2 method was capable of examining the uncertainty by using the Latin hypercube sampling scheme. The GLUE method was specialized in reflecting parameter correlations and uncertainties associated with parameters and predictants.

Yen et al. (2014) examined the sensitivity of the latent variables for SWAT model to know the potential impact of input uncertainty on model predictions. Results showed that the increase in the range of latent variables poses a significant influence to streamflow and ammonia predictions while the impact was less significant in sediment responses. The performance of SWAT in predicting streamflow and ammonia declined with wider ranges of latent variables. In addition, the increase in the range of latent variables did not present noticeable effect on the corresponding predictive uncertainty in sediment predictions.

Zhang et al. (2014) implemented four different uncertainty approaches Particle Swarm Optimization (PSO) techniques, GLUE, SUFI-2 and ParaSol to perform a comparative study with SWAT model applied to Peace River Basin, Central Florida. The accuracies of simulation were analyzed and compared based on the statistical results of the four uncertainty methods, difficulty level of each method, the number of runs and theoretical basis and the reasons thereof. Furthermore, for the four uncertainty methods with SWAT model in the study area, the pair-wise correlation between parameters and the distributions of model fit summary statistics computed from the sampling over the behavioral parameter and entire model calibration parameter feasible spaces were identified and examined. It provided additional insight into the relative identifiability of the four uncertainty methods.

2.3.3 LU/LC Change Studies Using SWAT

Breuer et al. (2006) quantified the uncertainty in hydrological response for a set of land use change scenarios by varying plant parameters within realistic uncertainty bounds in a Monte Carlo analysis using SWAT model over Dill catchment (60 km²) in Germany. The results showed that simulated hydrological fluxes significantly change after the introduction of out wintering suckler cow management, despite the presence of a significant amount of output uncertainty due to uncertainty in the plant parameterization. The key to proper uncertainty assessment was to consider the uncertainty in the difference between the scenarios instead of the absolute uncertainty of each single scenario. Additionally, a sensitivity analysis showed that changing soil properties in response to land use change does not result in significantly different results in the scenario analysis.

Bormann et al. (2009) studied the effect of spatial resolution and distribution of model input data on the results of regional-scale land use scenarios using three different hydrological catchment models. A 25 m resolution data set of a meso-scale catchment and three land use scenarios were used. SWAT was more sensitive to input data aggregation, simulating constant water balances between 50 m and 200 m grid size. The study concluded that spatial discretisation was more important than spatial distribution and accuracy of data sets was much more important than a high spatial resolution.

Githui et al. (2009) used the SWAT model to investigate the impact of land-cover changes on the runoff of the River Nzoia catchment, Kenya. Land-cover change scenarios were generated, namely the worst and best-case scenarios. A comparison between 1970–1975 and 1980–1985 showed that land-cover changes accounted for a difference in surface runoff ranging from 55% to 68% between the two time periods. Compared to the 1980–1985 actual runoff, the land-cover scenarios generated changes in runoff of about –16% and 30% for the best and worst case scenarios respectively.

Du et al. (2013) used the SWAT model to analyse and quantify the hydrological processes in rapid urbanization regions of the Qinhuai River basin. A varied parameterization strategy was developed by establishing regression equations with selected SWAT parameters as dependent variables and catchment impermeable area as independent variable. The performance of the newly developed varied parameterization approach was compared with the conventional fixed parameterization approach in simulating the hydrological processes under LU/LC changes. The results showed that the model simulation with varied parameterization approach had a large improvement over the conventional fixed parameterization approach in terms of both long-term water balance and flood events simulations.

Li et al. (2013) used SWAT model to simulate land-use change effects on water quantity in the upper Huaihe River basin in China. The land-use change effects on spatio-temporal change patterns of runoff, rainfall-runoff relationship, the sensitivity of rainfall-runoff relationship to rainfall for different types of land use, and impact of land-use patterns on rainfall-runoff relationships were investigated. The results revealed that under the same condition of soil texture and terrain slope, the runoff generation and sensitivity of rainfall-runoff relationship to rainfall decreased for farmland, paddy field, and woodland.

Wagner et al. (2013) analyzed past land use changes between 1989 and 2009 and their impacts on the water balance in the Mula and Mutha Rivers catchment, upstream of Pune, India, using SWAT model. Land use changes were identified from three Rivers catchment multitemporal land use classifications for the cropping years 1989/1990,

2000/2001, and 2009/2010. Results showed that urbanization led to an increase of the water yield by up to 7.6%, and a similar decrease of evapotranspiration, whereas the increase of cropland resulted in an increase of evapotranspiration by up to 5.9%.

Bossa et al. (2014) incorporated the scale-dependent parameter to SWAT model for simulating climate and land use change impacts on water-sediment-nutrient yields in Benin at a regional scale (49,256 km²). Land use change scenarios in which the population growth was translated into a specific demand for settlements and croplands according to the development of the national framework, were considered. Surface runoff, groundwater flow, sediment and organic N and P yields were affected by land use change (as major effects) of -8% to +50%, while water yield and evapotranspiration were dominantly affected by climate change of -31% to +2%.

Deng et al. (2014) used the SWAT model to evaluate the impact of land use/cover change on surface runoff and evapotranspiration in the upper reaches of the Hanjiang Basin. Results indicated that the area of paddy field, dry land, shrubbery and construction land by 2020 will have increased; however, woodland, grassland and water areas will have decreased. Results showed that there was an increasing trend in the annual average runoff flowing into the Danjiangkou Reservoir, and that land use change had more influence on runoff throughout the year than during the flood season. The annual average evapotranspiration, annual runoff variation coefficient and annual runoff distribution coefficient were predicted to increase.

Hari Krishna et al. (2014a) applied the SWAT model to Upper Manair catchment, Andhra Pradesh, India to determine the impact of land management practices and change in land use on water yield for sustainable use. To obtain sustainability of ground water resources in the watershed, it was tried to simulate the water balance components by reducing the area under paddy cultivation through three alternate cropping scenarios. The evaluation of three scenarios clearly demonstrated the impact of conversion of paddy (water intensive crop) on the hydrology of watershed. The study concluded that converting paddy area to dry land crops will enhance availability of surface water resources and decrease ground water resources.

Ridwansyah et al. (2014) examined the applicability of SWAT model for modeling mountainous catchments, focusing on Cisadane catchment Area in west Java Province, Indonesia. The SUFI-2 uncertainty technique was used for automatic calibration of streamflow. This study showed SWAT model can be a potential monitoring tool especially for watersheds in Cisadane catchment area or in the tropical regions.

2.3.4 VSA Modeling Using SWAT

VSA hydrology is the concept that the majority of runoff exiting a watershed is driven by a relatively small portion of the watershed. The original concept of saturation excess process was developed by the U.S. Forest Service and the Tennessee Valley Authority, the term VSA is usually attributed to Hewlett and Hibbert (1967). Dunne and Black (1970), Hewlett and Nutter (1970), and Dunne et al. (1975) are also commonly noted for their early, foundational contributions to the VSA hydrology concept. Steenhuis et al. (1995) showed that SCS-CN can be interpreted in terms of saturation excess process. Distributed Curve Number -Variable Source Area (CN-VSA) method was first developed by Lyon et al. (2004) and it was re-conceptualized to SWAT-VSA by Easton et al. (2008).

SWAT-VSA model incorporates VSA hydrology in terms of CN-VSA equation for capturing the spatial pattern of saturation excess runoff source areas. This re-conceptualization of SWAT helps in modeling the saturation excess runoff from VSAs without any modification in code base of SWAT model and thus provides efficient and easy way of capturing spatially variant saturation excess runoff processes from the landscape.

Easton et al. (2008) re-conceptualized the SWAT model to distribute overland flow in ways consistent with VSA hydrology by modifying how the CN and available water content were defined. Both original SWAT and re-conceptualized SWAT (SWAT-VSA) model were applied to a sub-watershed in the Cannonsville basin in upstate New York to compare model predictions of integrated and distributed responses, including surface runoff, shallowly perched water table depth, and stream phosphorus loads against direct measures. Results showed that event runoff was predicted

similarly well for both SWAT-VSA and SWAT. However, the distribution of shallowly perched water table depth was predicted better by SWAT-VSA and it is this shallow groundwater that governs VSAs.

Singh (2009) discussed about three hydrological models to assess the runoff and sediment yield in a watershed of Himalayan region. The three models namely, SWAT, SWAT-VSA and modified SWAT-VSA (SWAT-HIM) were used. All the three models differed in terms of Hydrological Response Units (HRU's) were generated and distribution of CN. Soil Wetness Index (SWI), which signifies the saturation level in the area was detrimental in runoff modeling by the SWAT-VSA and SWAT-HIM. The study addresses SWAT model by modifying runoff generation mechanism accounting CN distribution based on soil wetness index and land cover types to suit the runoff generation process in the Himalayan landscape. The SWAT-HIM model resulted in satisfactory output in the watershed dominated by saturation excess. It was concluded that SWAT created HRU's from the combination of land use/soil types and runoff was modeled on the basis of CN defined for HRU.

White et al. (2011) developed a physically based water balance that was coded in the SWAT model to replace the CN method of runoff generation. To compare this new water balance SWAT (SWAT-WB) to the original CN-based SWAT (SWAT-CN), two watersheds (Blue Nile in Ethiopia, Catskill Mountains of New York) were considered. Results showed that spatial distribution of runoff-generating areas differed greatly between the two models, with SWAT-WB reflecting the topographical controls imposed on the model. Also, water balance provided results equal to or better than the CN, but with a more physical based approach.

Dahlke et al. (2012) compared saturated runoff contributing areas predicted with the VSA interpretation of the SCS-CN method with field-measured VSAs in a 0.5 ha hillslope in central New York State. They found that the SCS-CN method accurately predicted the observed VSA and showed best agreement if the VSA was defined as the area where the water table was within 10 cm of the soil surface. Also, results not only demonstrate that the VSA interpretation of the SCS-CN method accurately

predicts VSA extents in small watersheds but also that the transient water table does not necessarily need to intersect the land surface to cause a storm runoff response.

Prasena and Pika Shrestha (2013) assessed the effects of land use change on runoff in the Bedog sub watershed. Soil and Water Assessment Tool-Water Balance (SWAT-WB) hydrological modeling was used to predict runoff. Sensitivity analysis revealed that soil properties were the most sensitive parameters on runoff generation. The result showed an acceptable performance in runoff simulation. Changes in land use were responsible for an increase in the annual runoff between 3.42% to 4.67%. This study showed that dynamics of runoff could be predicted by forecasting and simulating future land use.

Cheng et al. (2014) applied the three likelihood functions - NS, Generalized Error Distribution with Box-Cox transformation (BC-GED) and Skew Generalized Error Distribution with BC (BC-SGED) for SWAT-WB-VSA (Soil and Water Assessment Tool – Water Balance – Variable Source Area) model calibration for the Baocun watershed, Eastern China. Performance of calibrated models were compared using the observed river discharges and groundwater levels. The results showed that the minimum variance constraint can effectively estimate the BC parameter. The form of the likelihood function significantly impacted on the calibrated parameters and the simulated results of high and low flow components.

Pezet et al. (2014) evaluated the contribution of several aquifers with specific storage capacities to global catchment storage to its dynamics; and subsequent effects on VSA and non-point-source pollution. The SWAT-mVSA (SWAT-multi VSA) was used to calculate soluble reactive phosphorus (SRP) fluxes in a catchment representative of the agricultural conditions of large perialpine lakes. SWAT-mVSA predicted components of the hydrological balance and SRP fluxes more accurately than SWAT-VSA.

Woodbury et al. (2014) tested two different versions of SWAT model to simulate the hydrology and biogeochemical response of the Cannonsville Reservoir watershed, in New York. The first version distributed overland flow in ways that were consistent with VSA hydrology driven by saturation excess runoff, whereas the second version

was the standard version of SWAT. The two models were used to determine the maximum upper bound on the reduction in phosphorus loading by removing all of the corn in the watershed. The average reductions between the two models were 65 and 37% for PP and TDP, respectively. Also, SWAT-VSA model was used to estimate the effect of moving corn land in the watershed from the wettest, most runoff prone areas to the driest, least runoff prone areas, which cannot be done directly with the standard SWAT model.

2.4 SUMMARY

From the review of literature, the following observations can be made with regard to the status of knowledge on the objectives of the present study:

1. The SWAT model has proved to be extremely popular in simulating the hydrology of catchments over various sizes, possessing a variety of LU/LC types and located in diverse hydroclimatic regions of the world. However, there appears to be a further scope for comprehensive performance evaluation of the model in humid tropical watersheds in India.
2. Also, SWAT has not been tested using the paired catchment approach – that is, application and comparison in two watersheds located close to each other and exposed to the same type of hydroclimatic conditions but differing in the LU/LC composition.
3. Very few hydrological models seem to have incorporated the VSA mechanism of runoff generation. There appears to be a need to use this mechanism in thickly vegetated watersheds with steep topography.
4. Existing VSA hydrology models use a topography-based index to identify runoff areas. Whether satellite remote sensing can be used to derive a more realistic wetness index?
5. Comprehensive testing and evaluation of VSA hydrology models appear to be lacking for humid tropical watersheds, with most reported studies having been carried out in humid temperate regions.

6. Also, how do performances of models with and without VSA compare when applied to the same watershed?
7. Although a large number of hydrological modeling studies using SWAT have been carried out, only a small portion of them covered uncertainty analysis and reported uncertainty in model estimates.
8. Although a few studies have carried out trend analysis of hydroclimatic observations in the Upper Cauvery basin, these have been applied at coarse spatial and temporal scales. Given the importance of possible climate change imposing constraints on further water resources development in the basin, there is a need to carry out trend analysis at finer spatial (station) and temporal (monthly) scales.
9. Since the Cauvery basin is already facing a variety of water problems on account of anthropogenic activities, evaluating the hydrological impacts of further changes in LU/LC in the basin is extremely important. Few studies seem to have addressed this issue.

CHAPTER 3

STUDY AREA AND DATA

3.1 DESCRIPTION OF THE STUDY AREA

The Cauvery River, also known as the Dakshin Ganga, is one of the major interstate peninsular rivers of India. Cauvery River rises in the Talakadu region of Western Ghats and flows in an eastwardly direction passing through the states of Karnataka, Kerala, Tamil Nadu and union territory of Pondicherry before it drains into the Bay of Bengal. The Cauvery basin lies between latitudes $10^{\circ}05'N$ and $13^{\circ}30'N$ and longitudes $75^{\circ}30'E$ and $79^{\circ}45'E$. The total length of the river is about 800 km, of which 320 km is in Karnataka, 416 km is in Tamil Nadu and 64 km forms the common boundary between Karnataka and Tamil Nadu states. There are 21 principal tributaries each exceeding a watershed area of 250 km^2 of which the important ones are Hemavathi, Harangi, Kabini, Suvarnavathi, Shimsha, Arkavathi, Chinnar, Palar, Bhavani, Noyil, Tirumanimuttar, Amaravathi and Ponnana Ar. The Cauvery basin extends over an area of $81,155 \text{ km}^2$ (Jain et al., 2007; WRDO, 1976).

The present study considers the portion of the Cauvery basin up to the Billigundulu gauge site located in Karnataka on the border with Tamil Nadu. The basin up to Billigundulu is known as the Upper Cauvery Basin and has an area of $36,682 \text{ km}^2$ with many tributaries, including the Shimsha, Hemavathi, Harangi, Arkavati, Lakshmanathirtha and Kabini (Table 3.1). The river originates from Talakadu at an elevation of 2028 m above MSL (Mean Sea Level) and reaches Billigundulu at an elevation of 257 m above MSL.

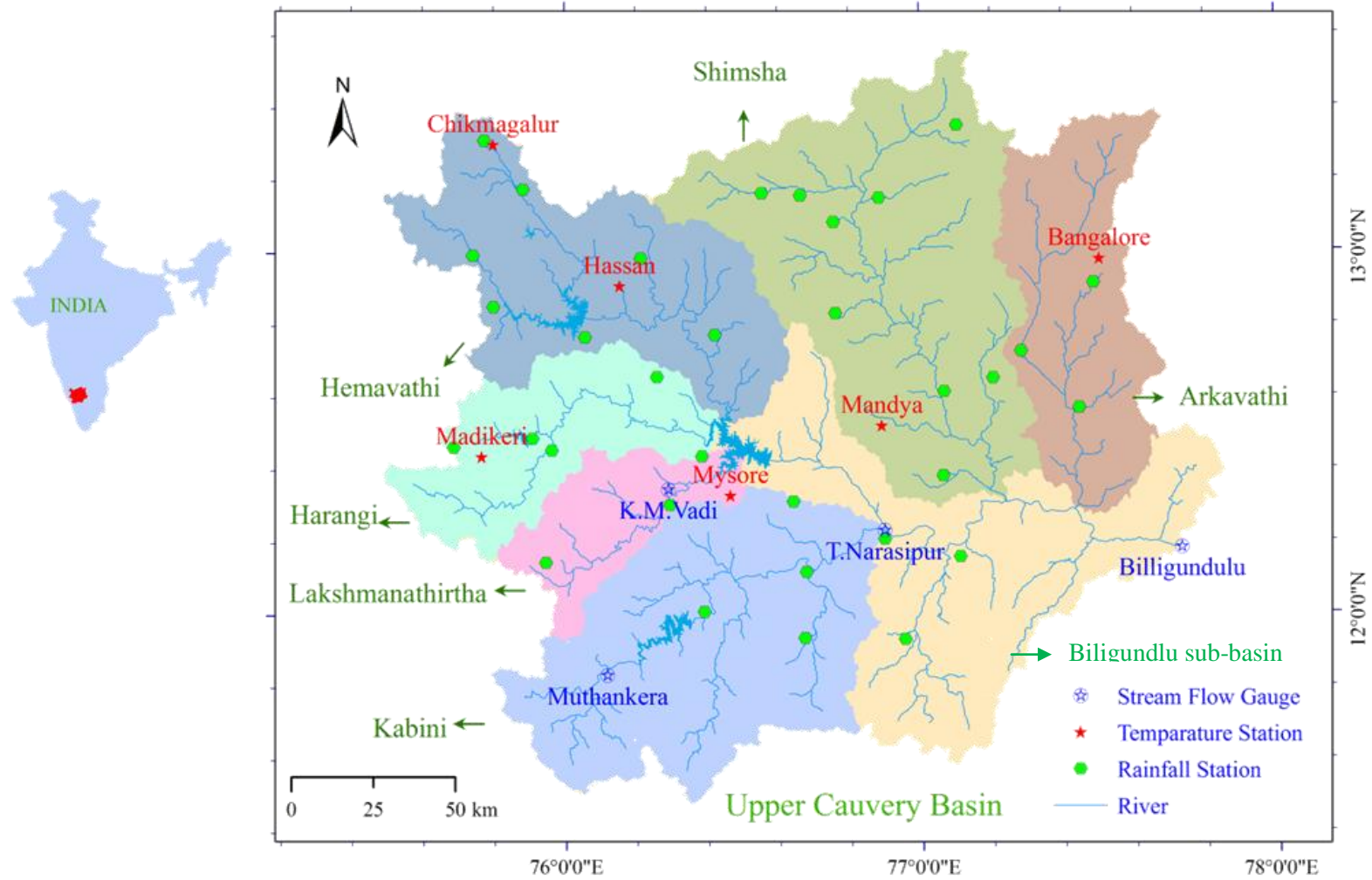


Fig. 3.1 Map of Upper Cauvery Basin showing locations of rainfall, temperature and streamflow gauging stations

The location of rainfall, temperature and streamflow gauging stations used in this study and major tributaries of the Upper Cauvery Basin are shown in Fig. 3.1. Table 3.1 summarises the drainage area of each major tributary of the Upper Cauvery Basin.

Table 3.1 Tributaries of the Upper Cauvery Basin

Sl. No.	Sub basin Name	Drainage Area (km²)
1	Hemavathi	5548.32
2	Harangi	3209.20
3	Lakshmanathirtha	1912.45
4	Kabini	7021.33
5	Shimsha	8646.89
6	Arkavathi	4123.84
7	Biligundlu sub-basin	6219.97
	Upper Cauvery	36682.00

3.2 CLIMATE

The climate of the basin is of tropical transitional zone. The mean daily temperature ranges from 4.8°C in the highlands to 39°C in the lower semi-arid regions. The average annual rainfall varies from 621 mm in the lowlands to a 4137 mm in the highlands. Fig. 3.2 shows the distribution of monthly mean maximum and minimum daily temperature for the climate stations while Fig. 3.3 shows the distribution of monthly mean rainfall for the various sub basins. The southwest monsoon generally sets in the month of June. Heavy rainfall occurs during this season with maximum rainfall in July and August in the highlands. The major rainfall occurs during this season and contributes 80% of the total annual rainfall. Rainfall in the winter season (January and February) is less than one percent of the annual total, in the hot pre-monsoon season (March to May) about 7% and in the post-monsoon season about 12%. The basin experiences considerable evaporation. Evaporation is found to be very high in the summer months of the year and moderate to low in the monsoon and post monsoon seasons. Average values are about 5 mm/day during summer and 2.5 mm/day during winter. Winds are mainly westerly or south westerly during the

southwest monsoon period. During the rest of the year, winds blow north easterly during forenoons and westerly or north westerly during afternoons.

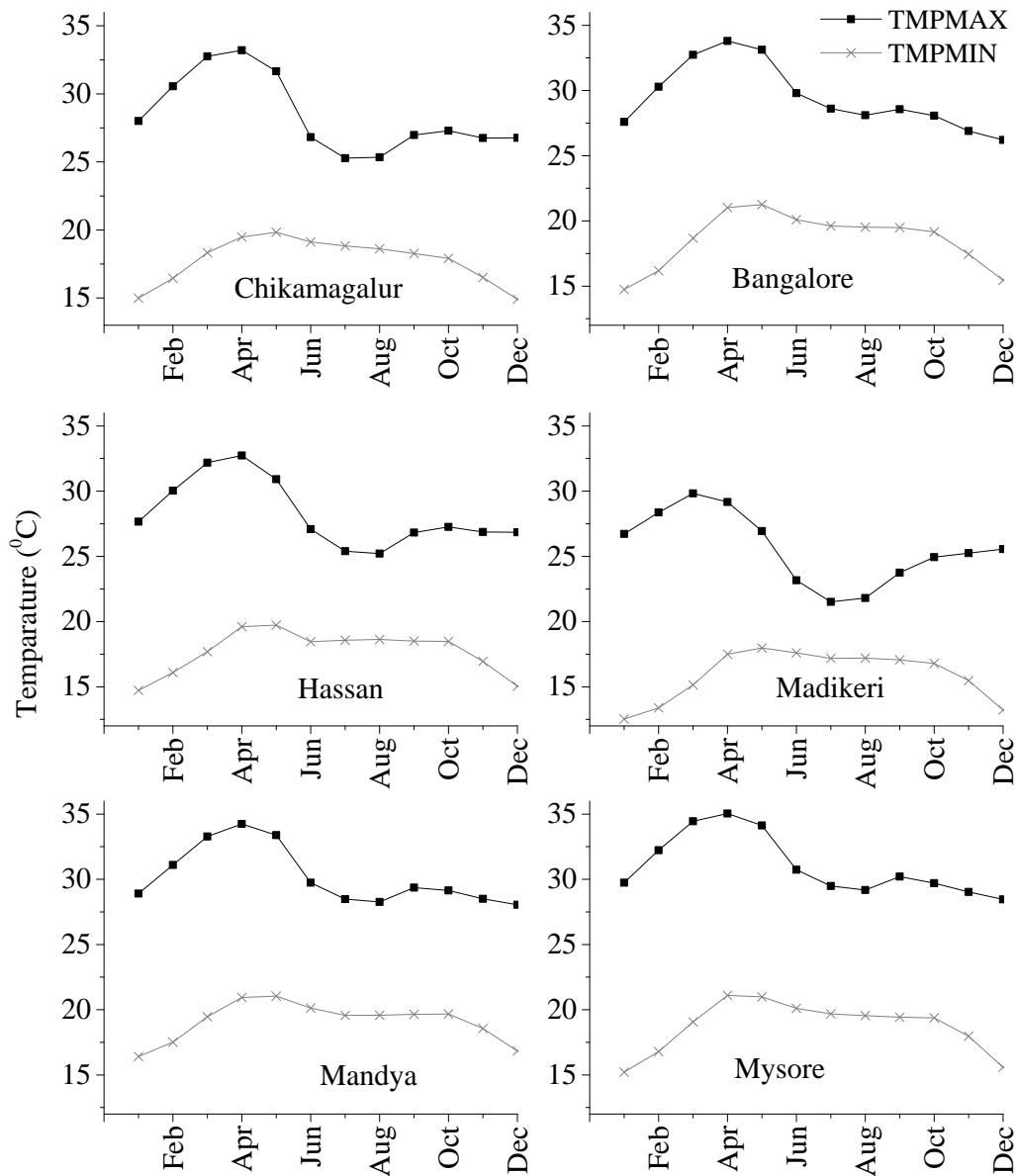


Fig. 3.2 Monthly mean minimum and maximum daily temperature for climate stations in the Upper Cauvery Basin

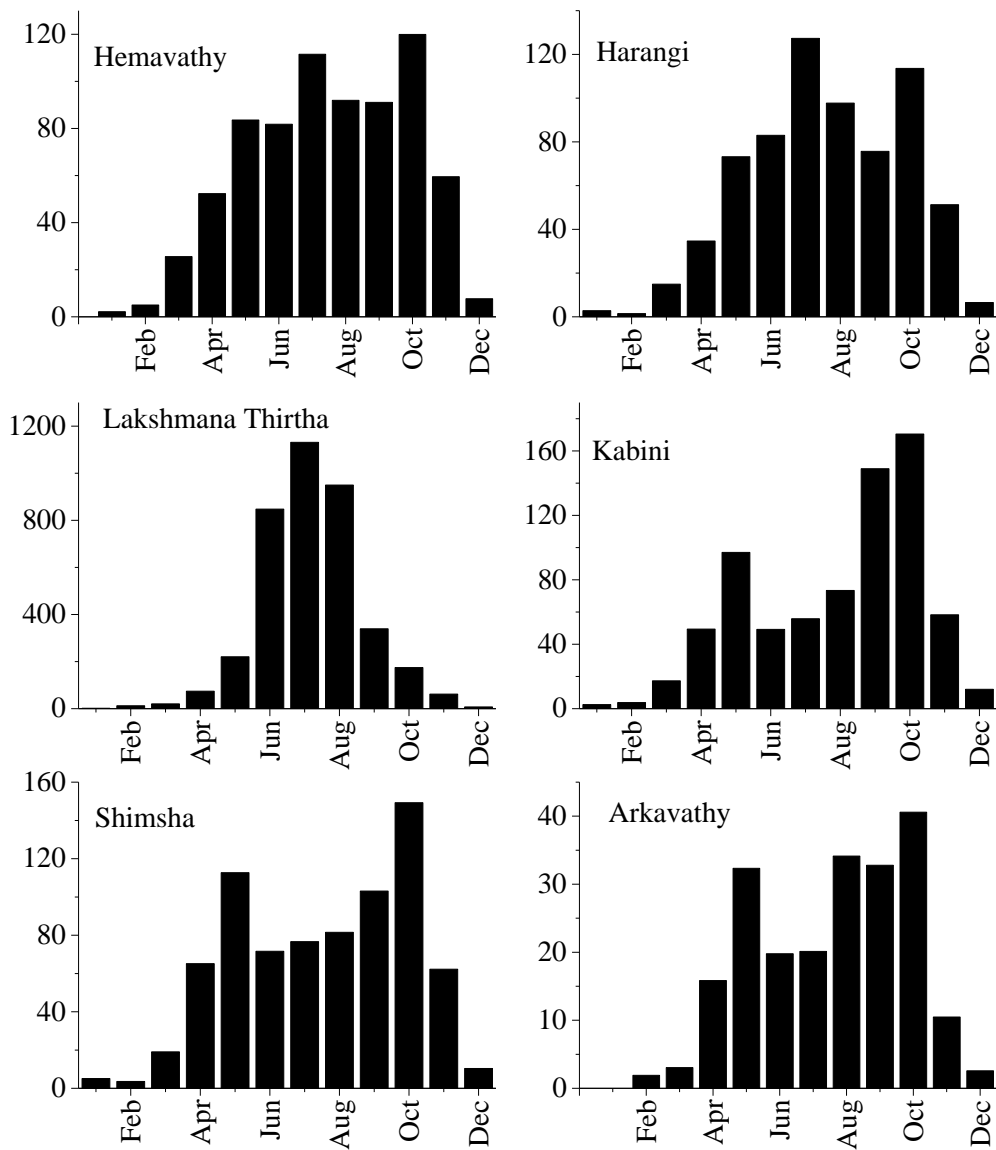


Fig. 3.3 Monthly mean rainfall (mm) for sub basins in the Upper Cauvery Basin

3.3 LAND USE/LAND COVER

The heavy rainfall in the upper areas favors luxurious growth of vegetation. The upper portion of the basin lies in the Western Ghats region, which is covered with mostly dense moist deciduous forests. Forests of different types, in varying stages from evergreen to scrub can be seen in the basin. Paddy and sugar cane are the major crops in the canal commanded areas. Coffee, tea, cardamom and other spices are found

mainly in the hilly region. The predominant land use in the basin is agriculture and food crops include paddy, raagi and mixed type of vegetables and fruits while the cash crops consist of coffee, sugar cane, sunflower and horticultural crops. The 1:50,000 scale LU/LC data was collected from The Karnataka State Remote Sensing and Application Center (KSRSAC). Agricultural fields and forest areas cover 64.17% and 24.47% of the basin respectively. The water bodies include reservoirs and tanks which cover 3.9% of the basin. The barren rocky and scrub land covers 4.51% of the basin. The urban areas, industrial area and villages cover 2.95% of the basin. The map of the LU/LC is shown in Fig. 3.4 and characteristics are shown in Table 3.2.

Table 3.2 Characteristics of LU/LC in the Upper Cauvery Basin

Land use	Class	Area (km²)	Watershed area (%)
Residential	URBN	421.32	1.13
Residential-Low Density	URLD	456.69	1.23
Agricultural Land-Close-grown	AGRC	19258.29	51.77
Agricultural Land-Generic	AGRL	263.16	0.71
Agricultural Land-Row Crops	AGRR	4351.43	11.70
Forest-Evergreen	FRSE	307.40	0.83
Forest-Deciduous	FRSD	6623.89	17.81
Forest-Mixed	FRST	2163.19	5.81
Pasture	PAST	1677.76	4.51
Wetlands-Non-Forested	WETN	7.48	0.02
Industrial	UIDU	57.86	0.16
Water	WATR	1452.14	3.90
Indian grass	INDN	159.68	0.43

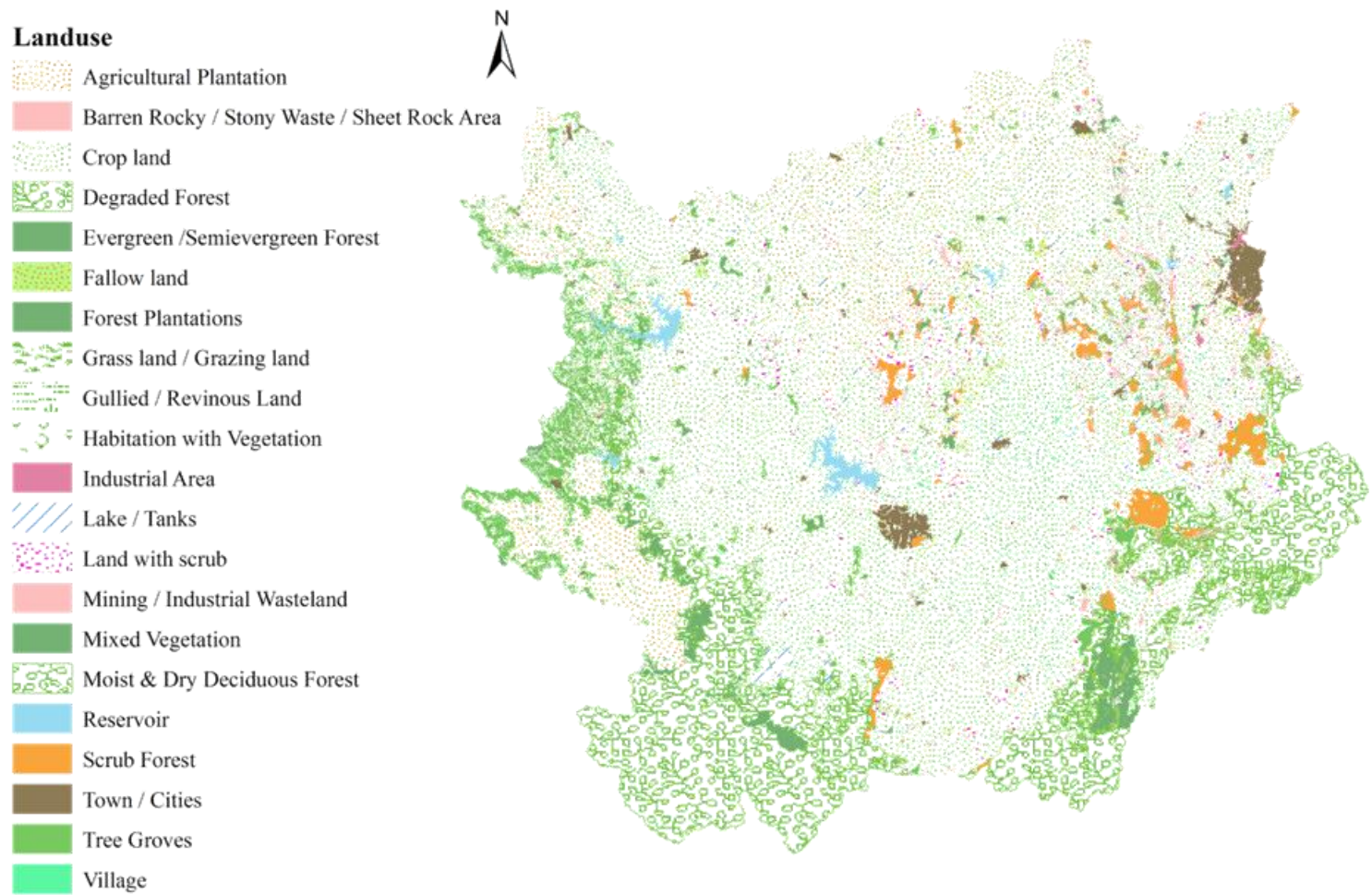


Fig. 3.4 LU/LC map of the Upper Cauvery Basin (KSRSAC)

3.4 SOILS

The soil map of the basin was obtained from the National Bureau of Soil Survey and Land Use Planning (NBSS and LUP) and is shown in Fig 3.5. The basin is characterized by clayey, gravelly clay, loamy and rock outcrops types of soils. The major types are deep, moderately well drained, clayey soils of valleys, with problems of drainage and slight salinity in patches (22.56%) and deep, well drained, clayey soils on undulating uplands, with moderate erosion (6.18%) and rock outcrops (6.59%) occupy the basin. Detailed description of the soil classes are given in Appendix 1 and their spatial extents are listed in Table 3.3.

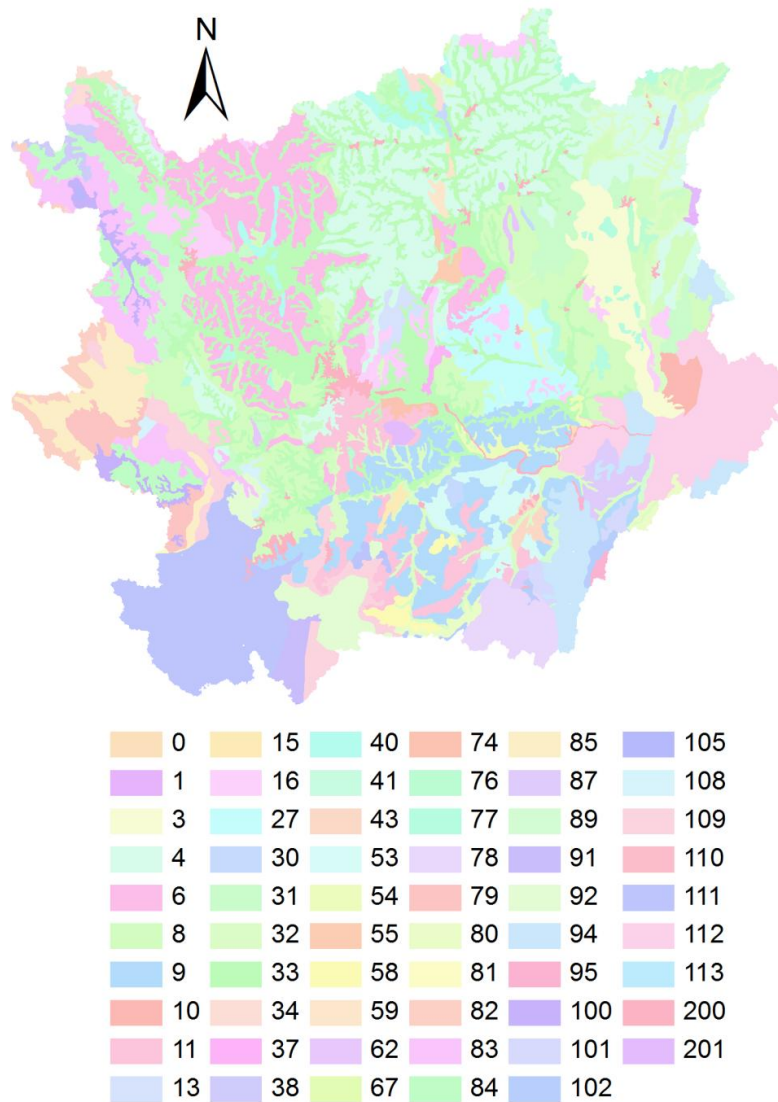


Fig. 3.5 Soil map of the Upper Cauvery Basin (NBSS and LUP)

Table 3.3 Characteristics of soil in the Upper Cauvery Basin

* Descriptions of soil class are given in the Appendix I

Soil class*	Area (km²)	% Watershed area	Soil class*	Area (km²)	% Watershed area
33	8393.53	22.56	79	244.17	0.66
77	2450.73	6.59	87	245.76	0.66
111	2300.32	6.18	82	196.73	0.53
8	2009.91	5.4	34	192.77	0.52
32	1988.51	5.35	101	193.33	0.52
4	1970.18	5.3	58	172.53	0.46
6	1452.30	3.9	91	168.41	0.45
9	1146.32	3.08	102	154.64	0.42
94	1076.61	2.89	55	125.50	0.34
31	1057.31	2.84	54	127.40	0.34
109	1048.76	2.82	43	123.53	0.33
84	1021.41	2.75	13	116.82	0.31
200	953.67	2.56	108	114.24	0.31
85	861.86	2.32	59	103.02	0.28
27	846.59	2.28	62	103.88	0.28
11	819.30	2.2	37	96.20	0.26
83	716.72	1.93	201	94.70	0.25
16	697.65	1.88	38	70.66	0.19
3	664.27	1.79	30	61.74	0.17
53	553.04	1.49	89	55.55	0.15
100	529.52	1.42	15	46.59	0.13
40	485.81	1.31	95	42.99	0.12
92	458.59	1.23	67	36.20	0.1
78	457.30	1.23	105	15.40	0.04
80	324.30	0.87	1	8.78	0.02

3.5 HYDROMETEOROLOGICAL DATA

Observed records of daily rainfall, daily minimum and daily maximum air temperature and daily runoff were obtained for the historical 30 year period 1981-2010. Daily rainfall data was collected from the Karnataka Irrigation Investigation Division for 33 rain gauge stations located in and around the basin. Station name, latitude, longitude, elevation and average annual rainfall are shown in Table 3.4. Daily minimum and maximum temperature data was collected from the India Meteorological Department (IMD). Details of the 6 climate stations are shown in Table 3.5. Table 3.6 provides location details of 4 major dams where inflow and outflow records are available. Locational details of 4 Central Water commission (CWC) stream gauging sites in the Upper Cauvery Basin are shown in Table 3.7.

Table 3.4 Rain gauge stations in the Upper Cauvery Basin

Sl. No.	Station Name	Longitude	Latitude	Elevation (m)	Avg. yearly rainfall (mm)
1	Arkalgud	76.06	12.77	911	910
2	Begur	76.67	11.93	741	719
3	Belur	75.88	13.18	977	1106
4	Chamarajanagar	76.95	11.93	690	810
5	Chandrasekarpur	76.89	13.15	767	598
6	Channapatana	77.20	12.65	673	1162
7	Chikmagalur	75.77	13.31	1020	985
8	Galibeedu	75.69	12.46	1107	4137
9	Hallimysore	76.26	12.66	865	720
10	Hanbal	75.74	12.99	893	2697
11	Harangi	75.91	12.49	859	1768
12	Hunsur	76.29	12.30	753	846
13	K R Nagar	76.38	12.44	802	621
14	Kanakapura	77.45	12.57	638	1107
15	Kengeri	77.49	12.91	788	1073
16	Kikkeri	76.42	12.77	828	691
17	Kollegal	77.11	12.16	634	854

18	Kushalanagar	75.96	12.46	842	1045
19	Maddur	77.07	12.61	627	790
20	Malavally	77.06	12.38	622	670
21	Mayasandra	76.76	13.08	775	700
22	Mysore	76.64	12.31	745	881
23	Nagamangala	76.76	12.83	777	860
24	Nanjanagud	76.68	12.12	656	820
25	Nonavinakere	76.56	13.16	802	795
26	Ponnampet	75.95	12.15	852	2258
27	Ramanagaram	77.28	12.72	687	1106
28	Sargur	76.39	12.01	674	934
29	Shantigrama	76.21	12.98	937	798
30	Sukravarasanthé	75.80	12.85	968	1578
31	T Narasipur	76.90	12.21	653	838
32	Tumkur	77.10	13.35	813	922
33	Turuvekere	76.66	13.16	785	861

Table 3.5 Climatic Station in the Upper Cauvery Basin

Sl. No.	Station Name	Longitude	Latitude	Elevation (m)	Avg. max Temp (°C)	Avg. min Temp (°C)
1	Chikmagalur	75.80	13.30	1069	27.63	17.84
2	Hassan	76.20	12.58	918	28.53	15.26
3	Madikeri	75.44	12.25	1152	25.97	17.62
4	Mandya	76.89	12.52	682	30.87	19.76
5	Mysore	76.42	12.18	760	29.82	21.08
6	Bangalore	77.60	13.00	907	29.67	17.84

Table 3.6 Major Dams in the Upper Cauvery Basin

Sl. No.	Dam Name	Longitude	Latitude	Elevation (m)
1	Hemavathi Dam	76.06	12.83	876
2	Kabini Dam	76.35	11.98	695
3	Harangi Dam	75.90	12.49	854
4	KRS Dam	76.57	12.43	716

Table 3.7 Stream gauge Sites in the Upper Cauvery Basin

Sl. No.	Site Name	Longitude	Latitude	Elevation (m)	Drainage Area (km ²)
1	K.M.Vadi	76.29	12.35	767	1330
2	Muthankera	76.12	11.83	705	1260
3	T.Narasipur	76.90	12.23	635	7000
4	Billigundulu	77.73	12.18	255	36682

3.6 TOPOGRAPHIC DATA

Topographic data was obtained in the form of Digital Elevation Model (DEM) at 90 m resolution from the Shuttle Radar Topography Mission (SRTM). DEM data was used to delineate the basin and sub basins and calculate basin parameters such as slope and slope length. The SRTM 90 m resolution DEM data was used in this study (Fig. 3.6).

3.7 SATELLITE IMAGERY

Global remote sensing datasets like Indian Remote Sensing (IRS) series, Landsat series, Advanced Very High Resolution Radiometer (AVHRR) and Moderate Resolution Imaging Spectrometer (MODIS) data are available for the study area. These datasets are helpful for studying the spatial and temporal variations of the different bio physical parameters like Leaf Area Index (LAI), Normalized Differential Vegetation Index (NDVI), Wetness index, land surface temperature and surface albedo. In this study Landsat 7 image (Enhanced Thematic Mapper Plus (ETM+) sensor) was chosen as it provides the necessary information with high quality and moderate resolution. ETM+ sensor provides eight channels (3 visible, 1 near infrared, 2 mid infrared, 1 thermal infrared and 1 panchromatic) at 28.5 resolutions (60 m

resolution for the thermal infrared and 15 m resolution for panchromatic band). The available cloud free Landsat image archives are up to the year 2002. The MODIS image provides similar spectral bands and temporal coverage every one to two days. However, at 1 km spatial resolution it is difficult to delineate saturated areas because in small watersheds saturated areas tend to expand in extent of few square meters. Hence, December 20, 2000 Landsat 7 image was used to calculate the wetness index. Rainfall data for 10 days average before satellite passed were analysed which gave 10 mm and 37 mm averaged rainfall over the Hemavathi and Harangi watersheds respectively. This means that when satellite passed on the study area, saturated areas were visible.

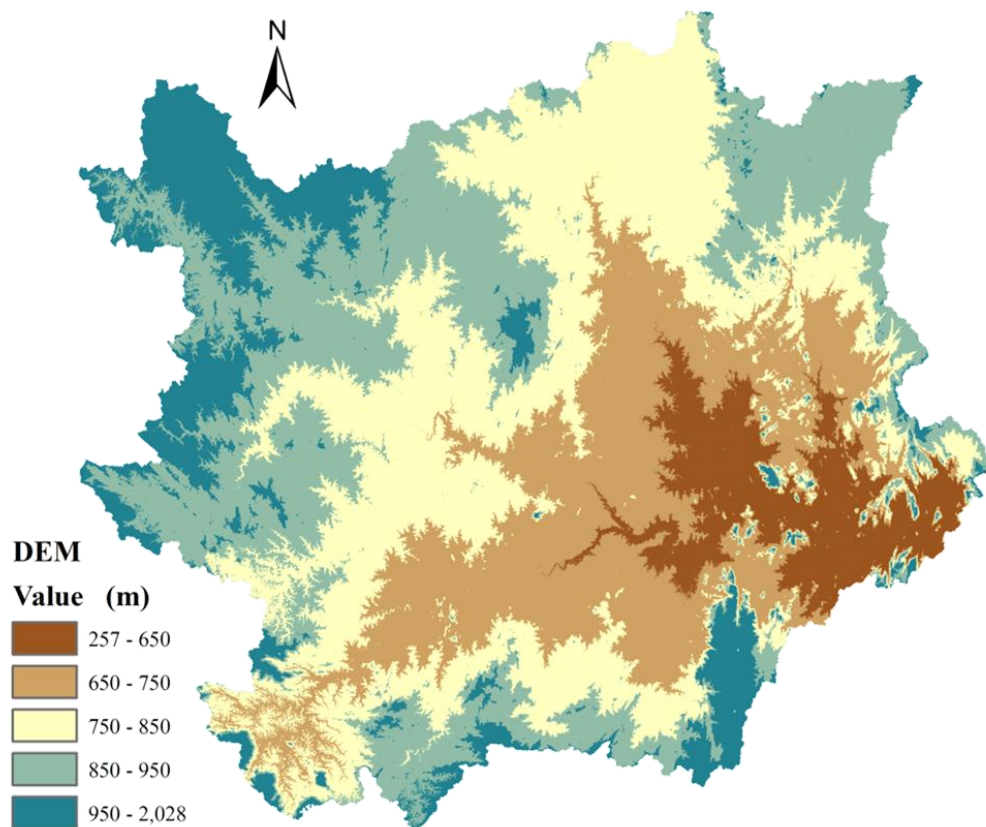


Fig. 3.6 Topography map of the Upper Cauvery Basin

ANALYSIS OF HYDROMETEOROLOGICAL DATA

4.1 GENERAL

The need for carrying out analysis of trend in the historical hydroclimatic records of the Upper Cauvery basin has been highlighted in Section (1.5). Also, a detailed review of previous trend analysis studies carried out in India, in the Upper Cauvery basin and in other regions of the world has been provided in Section (2.2).

Most studies carried out earlier have implemented the conventional Mann-Kendall test to identify trends in data sets created for monthly or seasonal time steps. In this work however, the Seasonal Kendall test (Hirsch et al., 1982) was implemented thereby circumventing the need to separately analyse monthly or seasonal data. The Seasonal Kendall test accounts for seasonality by computing the Mann-Kendall test on each of the months/seasons separately, and then combining the results. Also, very few earlier studies have tried to identify long-term persistence in time series of hydro-climatic variables. In this study, the the Detrended Fluctuation Analysis (DFA) proposed by Kantelhardt et al. (2001) was implemented for the purpose of detecting long-term persistence.

Hence, this study seeks to determine whether rainfall, maximum and minimum air temperatures and streamflow exhibit trends over a long period of record. Also, percentage departures in monthly mean values of the variables considered were characterized for different decades. In order to calculate existence of a trend and magnitude of trend in rainfall, streamflow and temperature data, the Seasonal-Kendall test (Hirsch et al., 1982) and Sen's slope (Sen, 1968) estimator were used. To find long-term persistence in the time series data Detrended Fluctuation Analysis (DFA) method was used (Kantelhardt et al., 2001). A brief description of these methods is provided in subsequent Section s.

4.2 SEASONAL-KENDALL TEST

The Seasonal-Kendall method (Hirsch et al., 1982) is a non-parametric test used for finding the significance of increasing or decreasing trends in time series. It accounts for seasonality by computing the Mann-Kendall test on each of the seasons or months separately, and by combining the results. The Kendall statistic for each month S_i , is summed over the years (1 to m years) to form the overall statistic S_k .

$$S_k = \sum_{i=1}^m S_i \quad (4.1)$$

S_i is calculated by considering the variable (Y) (hydrometeorological data) and time (T)

$$S_i = P_i - M_i \quad (4.2)$$

where P = the number of times the Y's increase as the T's increase

M = the number of times the Y's decrease as the T's increase

The distribution of S_k can be approximated quite well by a normal distribution with expectation (μ_{sk}) equal to the sum of the expectations (zero) of the individual S_i under the null hypothesis, and variance equal to the sum of their variances. Standardized S_k is evaluated against a table of the standard normal distribution.

$$Z_{sk} = \begin{cases} \frac{S_k - 1}{\sigma_{sk}} & \text{if } S_k > 0 \\ 0 & \text{if } S_k = 0 \\ \frac{S_k + 1}{\sigma_{sk}} & \text{if } S_k < 0 \end{cases} \quad (4.3)$$

where $\mu_{sk} = 0$

$$\sigma_{sk} = \sqrt{\sum_{i=1}^m (n_i / 18)(n_i - 1)(2n_i + 5)} \quad (4.4)$$

n = number of data points in i^{th} season or month

If the calculated value of $|Z| > Z_{\alpha/2}$, the null hypothesis is rejected at significance level α .

4.3 SEN'S SLOPE ESTIMATOR

The magnitude of trend in time series can be determined using the Sen's slope estimator (Sen, 1968). The Sen's slope estimator has been widely used for finding change in slope per unit time in the time series. In this method the slope (Q_i) of all data pairs is first calculated using the equation

$$Q_i = \frac{x_j - x_k}{j - k} \quad \text{for } i = 1, 2, 3, \dots, N \quad (4.5)$$

where X_j and X_k are data value at time j and k ($j > k$) respectively. The median of these N values of Q_i Sen's slope estimator is calculated as

$$Q = \begin{cases} Q_{\left[\frac{N+1}{2}\right]} & \text{if } N \text{ is odd} \\ Q = \frac{1}{2} \left(Q_{\left[\frac{N}{2}\right]} + Q_{\left[\frac{N+2}{2}\right]} \right) & \text{if } N \text{ is even} \end{cases} \quad (4.6)$$

A positive value of Q indicates an increasing trend and a negative value indicates a decreasing trend in time series.

4.4 DETRENDED FLUCTUATION ANALYSIS

The determination of trends in the hydro-meteorological time series is influenced by the existence of long-term persistence. The long-term persistence in time series can be quantified by using DFA (Kantelhardt et al., 2001). In DFA the time series is initially integrated and the integrated time series is divided into subseries of equal length 'm'. In each subseries, local trend is estimated and this trend is subtracted from the subseries to obtain a detrended subseries. The root mean square fluctuation of this integrated and detrended subseries is calculated using the equation

$$F(m) = \sqrt{\frac{1}{N} \sum_{k=1}^N [Y_k - y_m(k)]^2} \quad (4.7)$$

The above component is computed for all subseries data. The fluctuation can be characterized by a scaling exponent (d). The slope of linear relation of $\log F(m)$ versus $\log(m)$ gives the 'd'. Using 'd', DFA exponent (α) is estimated using the equation

$$\alpha = 2d - 1 \quad (4.8)$$

The $\alpha \leq 0.5$ for uncorrelated time series and $\alpha > 0.5$ indicates long range correlation.

4.5 METHODOLOGY

The hydro-climatic variables selected for analysis were: daily maximum temperature, daily minimum temperature, rainfall depth and streamflow. Daily observations of these variables for the historical 30 year period 1981-2010 were used and aggregated to monthly totals for rainfall depth and rainy days and averages for temperature and streamflow. Data of 33 rain gauge stations, 6 climate stations and 4 stream gauging sites located within the Upper Cauvery Basin were used in the analysis (Section 3.5). Statistical trend analysis of the selected hydro-climatic variables was carried out in four phases. In the first phase the statistical parameters of Coefficient of Variation (CV) and percentage of departure from mean were calculated. The second phase involved identification of the significance of increasing or decreasing trend using the Seasonal-Kendall test (Hirsch et al., 1982). In the third phase, the slope of the linear trend was calculated using Sen's slope estimator (Sen, 1968). Long-term persistence of time series data was detected using the Detrended Fluctuation Analysis (DFA) (Kantelhardt et al., 2001) method in the fourth phase. With regard to rainfall depth, the analysis was performed separately for individual rain gauge sites and also for areal rainfall calculated over six sub-basins (Fig. 3.1)

Historical data of all the hydro-climatic variables were tested for consistency and missing records. Outliers were eliminated and missing data were filled-in using linear interpolation for temperature and streamflow variables and nearest neighbor values for rainfall. Using a monthly time step, basic statistical parameters of mean, standard deviation and coefficient of variation (CV) were computed for each of the variables. Data for maximum and minimum temperature and rainfall were further segregated into the 3 separate decades of 1981-1990, 1991-2000 and 2001-2010. For these variables, percentage departure of monthly values were computed with reference to the mean for each decade. To determine areal average rainfall over each sub basin Thiessen polygon technique was used. In this study SWAT model (Arnold et al., 1998) was used for computing areal average rainfall for each sub basin and for entire basin using the influencing rain gauge stations.

4.6 RESULTS AND DISCUSSION

4.6.1 Statistical Analysis of Hydrometeorological Variables

Values of CV for monthly mean rainfall, maximum and minimum temperatures and streamflow data for the period 1981-2010 are shown in Table 4.1. While CV values for monthly rainfall averaged over each sub-basin and also for the entire Upper Cauvery basin are shown in Table 4.1, CV values for rainfall recorded at each of the individual rain gauge stations are shown in Table 4.2.

For all sub basins considerable variation was observed in rainfall during the winter season (December to March) ranging from 14% to as high as 71%. However, it must be noted that these months contribute less than 3% of annual rainfall. Rainfall variability across the sub-basins is typically less than 10% during the other months including the monsoon season (June to September). Maximum daily temperature displayed very small variability (5% to 10%) across all stations and months, with slightly higher CV values being recorded for the monsoon months (Table 4.1). On the other hand, minimum daily temperatures were more variable at all stations especially during the winter months of November, December, January and February. Values of CV were also low for streamflow, except at the K.M. Vadi gauging station where streamflows exhibited slightly higher variability especially during the monsoon season (Table 4.1). As regards CV values for monthly rainfall at individual stations, Table 4.2 clearly highlights the fact that variabilities are much higher during all months of the year in comparison to variabilities when the same rainfall is spatially averaged over sub-basins (Table 4.1). CV values for stations are particularly high during months of December, January, February and March, with highest variability of 95% recorded at the Sukravarasanthe station during February. CV values start decreasing to the range of 5%-15% from April onwards up to the month of November. These results highlight the need to analyze historical rainfall records for individual stations rather than spatially averaged values if the true variabilities are to be captured.

Figs. 4.1 to 4.5 show the percentage departure of average monthly maximum and minimum daily temperature and average monthly total rainfall and streamflow for the three decades (1981-1990, 1991-2000 and 2001-2010) from their corresponding 30-

year normal values. Considering maximum temperature, Fig (4.1) indicates that the departures for all stations and all decades were within $\pm 3\%$. Except for the Hassan climate station, all other stations exhibited low departures during all months and all decades. The maximum daily temperature at the Hassan station appeared to lower than the normal value for all months during the decade 1991-2000, but during the more recent decade (2001-2010), temperatures appeared to have increased during most of the months. At the Madikeri station, maximum temperatures seemed to have reduced during 2001-2010.

With regard to monthly average daily minimum temperature (Fig. 4.2), departures were small at Chikmagalur, Bangalore and Mysore climate stations during all months and all three decades. While the Hassan and Mandya stations exhibited high departures in minimum temperatures during all months, the Madikere station had high departures during the non-monsoon months only. Higher minimum temperatures were recorded at the Hassan station during the decade 1991-2000 and lower temperatures were recorded during 2001-2010. On the other hand, the Mandya station experienced higher minimum temperatures during all months for the decade 2001-2010 and lower temperatures during 1981-1990.

Table 4.1 Coefficients of variation for rainfall (a), maximum temperature (b), minimum temperature (c) and streamflow (d)

a) Rainfall												
	CV											
Sub basin Name	Jan	Feb	Mar	Apr	May	Jun	Jul	Aug	Sep	Oct	Nov	Dec
Hemavathi	0.26	0.36	0.19	0.07	0.06	0.04	0.04	0.04	0.05	0.07	0.09	0.21
Harangi	0.27	0.20	0.14	0.07	0.05	0.04	0.03	0.03	0.04	0.22	0.08	0.17
Lakshmanathirtha	0.30	0.26	0.16	0.08	0.06	0.05	0.05	0.05	0.05	0.05	0.10	0.22
Kabini	0.34	0.22	0.14	0.07	0.06	0.05	0.05	0.05	0.06	0.06	0.10	0.25
Shimsha	0.33	0.24	0.24	0.09	0.06	0.08	0.07	0.06	0.06	0.05	0.09	0.18
Arkavathi	0.71	0.28	0.16	0.10	0.08	0.10	0.07	0.06	0.07	0.07	0.11	0.21
Upper Cauvery	0.26	0.16	0.15	0.05	0.04	0.04	0.04	0.03	0.04	0.04	0.07	0.15

b) Maximum temperature												
	CV											
Station Name	Jan	Feb	Mar	Apr	May	Jun	Jul	Aug	Sep	Oct	Nov	Dec
Chikmagalur	0.05	0.05	0.05	0.05	0.08	0.09	0.07	0.07	0.06	0.06	0.05	0.05
Hassan	0.07	0.06	0.06	0.07	0.10	0.11	0.09	0.08	0.08	0.07	0.07	0.07
Madikeri	0.06	0.06	0.07	0.07	0.09	0.09	0.07	0.08	0.08	0.07	0.06	0.05
Mandya	0.05	0.05	0.05	0.05	0.07	0.07	0.06	0.05	0.05	0.05	0.06	0.06
Mysore	0.05	0.06	0.06	0.05	0.06	0.09	0.07	0.05	0.05	0.05	0.05	0.05
Bangalore	0.06	0.06	0.05	0.05	0.06	0.06	0.06	0.05	0.05	0.05	0.06	0.06

c) Minimum temperature		CV										
Station Name	Jan	Feb	Mar	Apr	May	Jun	Jul	Aug	Sep	Oct	Nov	Dec
Chikmagalur	0.11	0.11	0.08	0.07	0.08	0.05	0.04	0.04	0.05	0.07	0.11	0.12
Hassan	0.14	0.13	0.13	0.11	0.10	0.11	0.07	0.06	0.07	0.07	0.13	0.15
Madikeri	0.23	0.22	0.17	0.10	0.07	0.06	0.05	0.05	0.06	0.09	0.14	0.22
Mandya	0.16	0.17	0.15	0.10	0.10	0.10	0.09	0.10	0.10	0.10	0.12	0.16
Mysore	0.13	0.12	0.11	0.08	0.06	0.06	0.06	0.06	0.06	0.07	0.10	0.13
Bangalore	0.14	0.13	0.11	0.07	0.06	0.05	0.04	0.04	0.04	0.06	0.11	0.14

d) Streamflow		CV										
Site Name	Jan	Feb	Mar	Apr	May	Jun	Jul	Aug	Sep	Oct	Nov	Dec
K.M.Vadi	0.07	0.08	0.07	0.07	0.05	0.17	0.11	0.10	0.15	0.10	0.07	0.05
Muthankera	0.02	0.02	0.08	0.04	0.09	0.05	0.03	0.02	0.03	0.02	0.02	0.03
T.Narasipur	0.04	0.05	0.02	0.02	0.03	0.07	0.04	0.03	0.03	0.03	0.02	0.02
Billigundulu	0.02	0.03	0.02	0.02	0.02	0.05	0.05	0.03	0.03	0.03	0.02	0.01

Table 4.2 Sen's slopes, significant of trend using the Seasonal-Kendall method, DFA exponent and coefficients of variation for rainfall stations

(Raw = Raw time series, Ds = Deseasonalised time series)

Station Name	Sen's slope	p-value	Kendall's tau	DFA exponent		CV											
				Raw	Ds	Jan	Feb	Mar	Apr	May	Jun	Jul	Aug	Sep	Oct	Nov	Dec
Arkalgud	0	0.263	0.047	0.407	0.483	0.64	0.87	0.31	0.15	0.11	0.09	0.07	0.07	0.11	0.10	0.15	0.37
Begur	0	0.649	0.031	0.463	0.668	0.56	0.37	0.20	0.12	0.10	0.11	0.09	0.11	0.10	0.08	0.13	0.28
Belur	0	0.163	-0.050	0.684	0.784	0.41	0.52	0.24	0.12	0.10	0.08	0.09	0.08	0.10	0.10	0.16	0.32
Chamarajanagar	0	0.759	0.015	0.470	0.517	0.48	0.56	0.21	0.11	0.09	0.13	0.12	0.12	0.09	0.08	0.11	0.23
Chandrasekarpur	0	0.073	-0.057	0.585	0.531	0.47	0.52	0.35	0.18	0.12	0.16	0.12	0.11	0.11	0.11	0.15	0.35
Chikmagalur	0	0.499	0.021	0.429	0.550	0.49	0.51	0.24	0.13	0.10	0.08	0.09	0.08	0.10	0.09	0.15	0.30
Galibeedu	0	0.216	-0.040	0.291	0.457	0.42	0.27	0.19	0.13	0.08	0.04	0.03	0.04	0.06	0.07	0.12	0.25
Hallimysore	0	0.331	0.040	0.468	0.630	0.45	0.59	0.31	0.13	0.10	0.10	0.08	0.09	0.10	0.08	0.15	0.34
Hanbal	0	0.796	-0.001	0.246	0.409	0.52	0.72	0.27	0.12	0.11	0.05	0.05	0.05	0.07	0.08	0.12	0.40
Harangi	0	0.753	-0.010	0.275	0.429	0.69	0.46	0.21	0.12	0.10	0.06	0.05	0.05	0.09	0.16	0.14	0.30
Hunsur	0	0.824	0.012	0.408	0.558	0.41	0.33	0.26	0.13	0.09	0.08	0.08	0.07	0.09	0.08	0.16	0.31
K R Nagar	0	0.867	0.008	0.422	0.614	0.47	0.41	0.28	0.14	0.10	0.13	0.12	0.12	0.10	0.09	0.15	0.30
Kikkeri	0	0.643	-0.001	0.319	0.471	0.68	0.49	0.31	0.14	0.10	0.12	0.11	0.11	0.10	0.09	0.14	0.38

Kollegal	0	0.448	-0.032	0.497	0.588	0.47	0.54	0.34	0.13	0.10	0.15	0.13	0.11	0.10	0.09	0.12	0.27
Kushalanagar	0	0.602	0.019	0.433	0.611	0.52	0.40	0.21	0.11	0.09	0.06	0.06	0.06	0.08	0.08	0.12	0.32
Maddur	0	0.279	-0.048	0.391	0.563	0.60	0.54	0.28	0.14	0.10	0.14	0.11	0.10	0.09	0.08	0.12	0.23
Malavally	-0.04	0.005	-0.086	0.438	0.507	0.54	0.48	0.28	0.14	0.10	0.14	0.12	0.11	0.10	0.09	0.12	0.22
Mayasandra	0	0.649	-0.008	0.381	0.415	0.61	0.56	0.71	0.20	0.13	0.18	0.15	0.13	0.10	0.10	0.18	0.40
Mysore	0.04	0.113	0.053	0.447	0.629	0.69	0.49	0.25	0.12	0.10	0.10	0.09	0.09	0.09	0.08	0.13	0.24
Nagamangala	0	0.893	0.012	0.371	0.548	0.44	0.46	0.27	0.12	0.09	0.14	0.12	0.11	0.08	0.08	0.12	0.24
Nanjanagud	0	0.411	0.034	0.346	0.594	0.50	0.37	0.24	0.12	0.09	0.09	0.08	0.08	0.09	0.08	0.12	0.28
Nonavinakere	0	0.437	0.029	0.331	0.497	0.58	0.54	0.43	0.17	0.11	0.14	0.13	0.10	0.10	0.09	0.14	0.30
Ponnampet	0	0.622	0.021	0.342	0.454	0.47	0.45	0.20	0.12	0.10	0.07	0.06	0.06	0.07	0.08	0.14	0.33
Sargur	0	0.503	0.032	0.593	0.740	0.59	0.35	0.21	0.12	0.10	0.09	0.07	0.08	0.10	0.09	0.13	0.48
Shantigrama	0	0.204	-0.039	0.481	0.588	0.51	0.45	0.43	0.16	0.10	0.10	0.09	0.10	0.10	0.09	0.14	0.38
Sukravarsanthe	0	0.863	0.017	0.278	0.436	0.59	0.95	0.25	0.12	0.09	0.05	0.04	0.04	0.06	0.08	0.12	0.37
T Narasipur	0	0.842	0.009	0.362	0.527	0.45	0.47	0.24	0.11	0.10	0.12	0.11	0.10	0.11	0.09	0.12	0.24
Tumkur	0	0.620	0.015	0.338	0.462	0.58	0.41	0.29	0.16	0.11	0.11	0.10	0.09	0.10	0.09	0.15	0.41
Turuvekere	0	0.547	-0.024	0.322	0.497	0.66	0.48	0.37	0.17	0.11	0.14	0.11	0.10	0.09	0.09	0.13	0.35

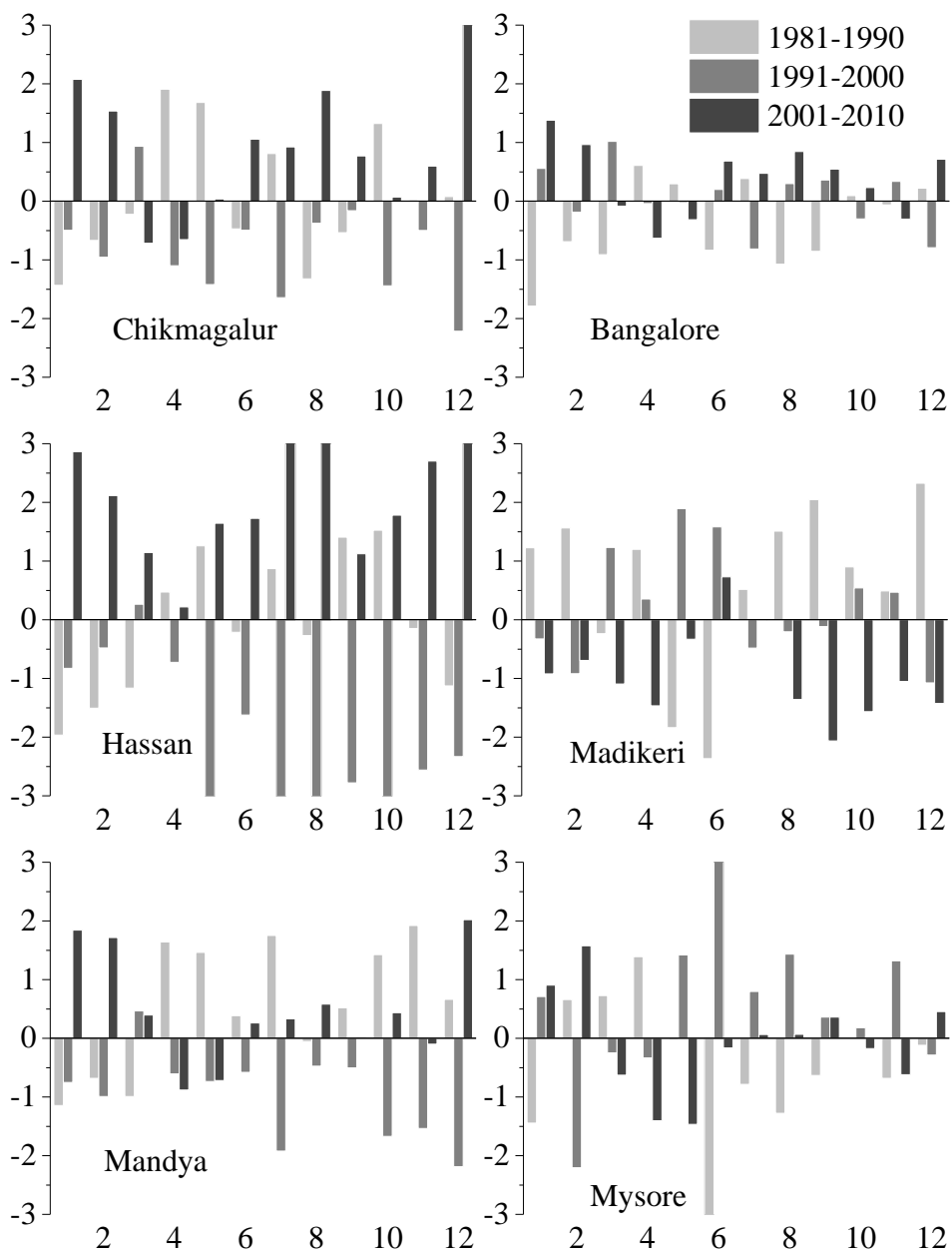


Fig. 4.1 Percentage departure of monthly maximum temperature of different decades from 30 years normal value

Note: x-axis : months, y-axis : percentage departure

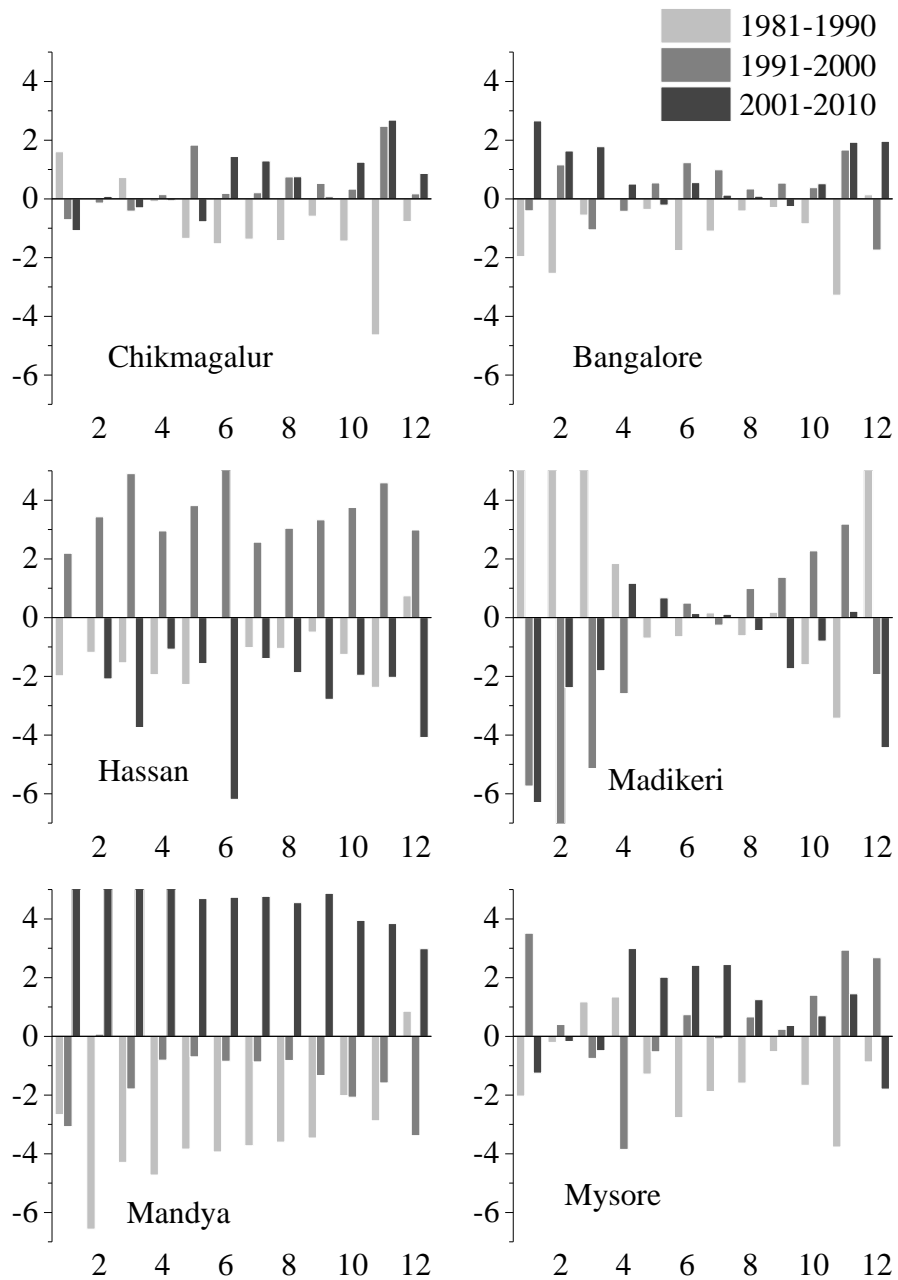


Fig. 4.2 Percentage departure of monthly minimum temperature of different decades from 30 years normal value

Note: x-axis : months, y-axis : percentage departure

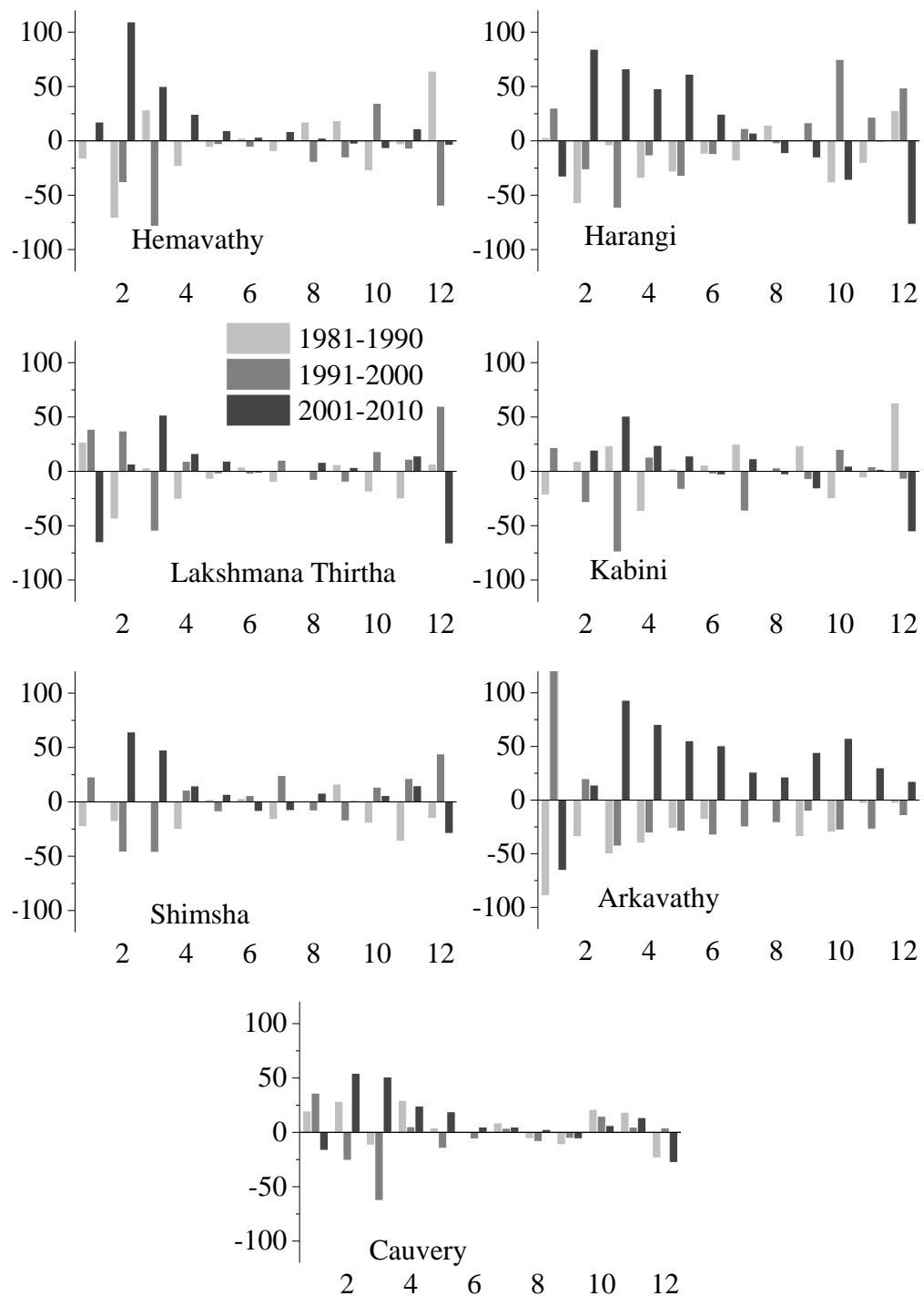
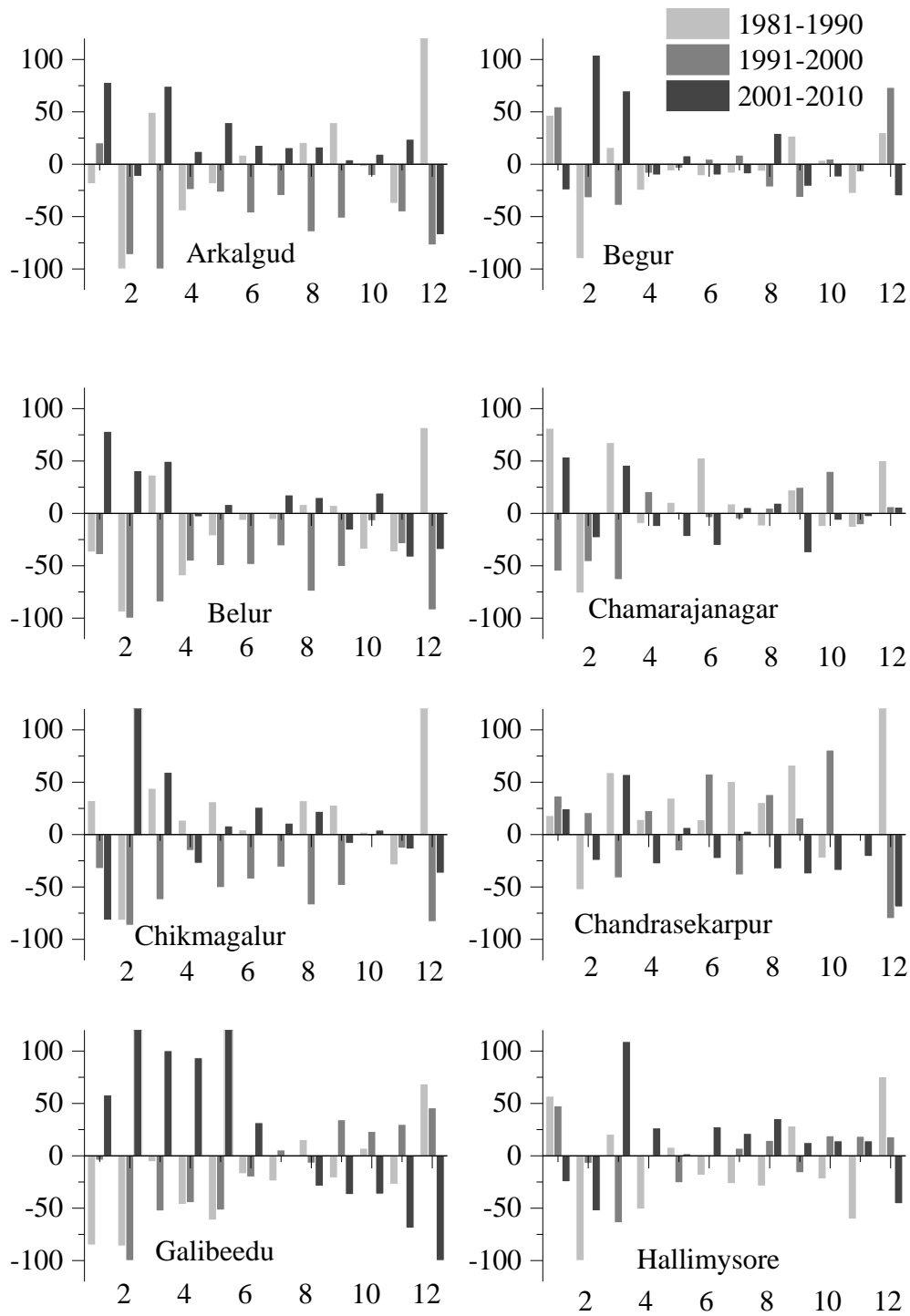
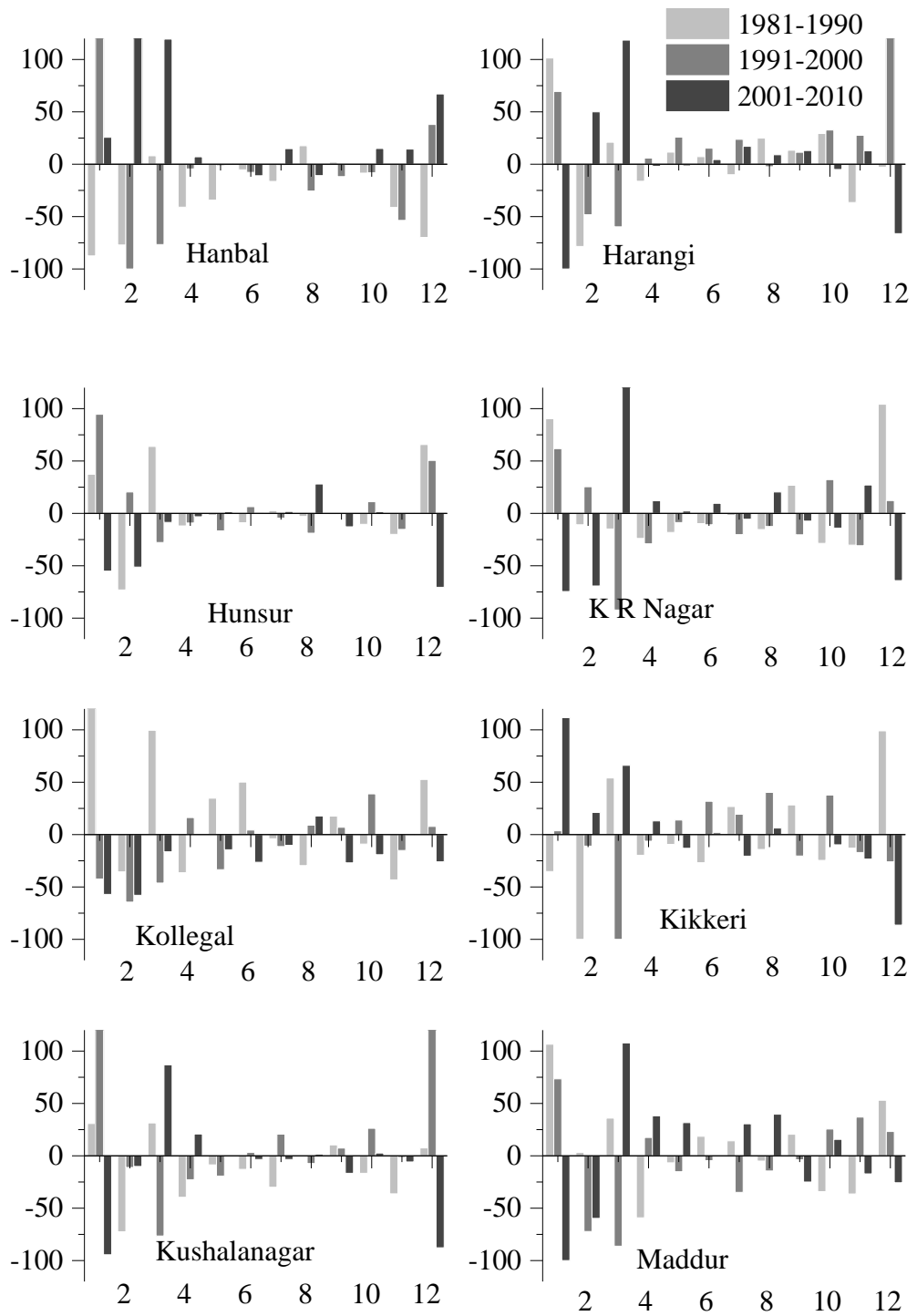


Fig. 4.3 Percentage departure of monthly rainfall of different decades from 30 years normal value for sub basins

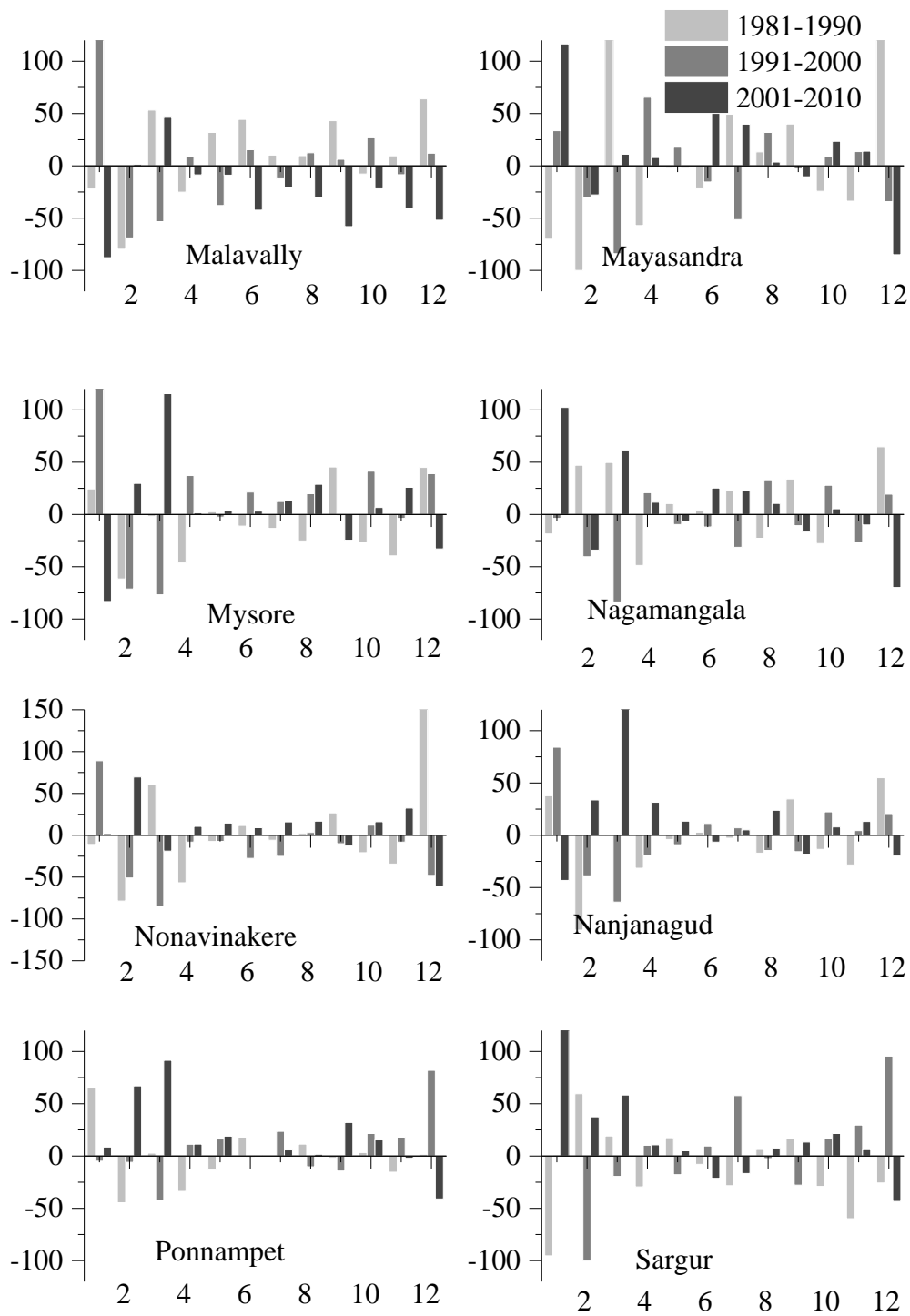
Note: x-axis : months, y-axis : percentage departure



contd.



contd.



contd.

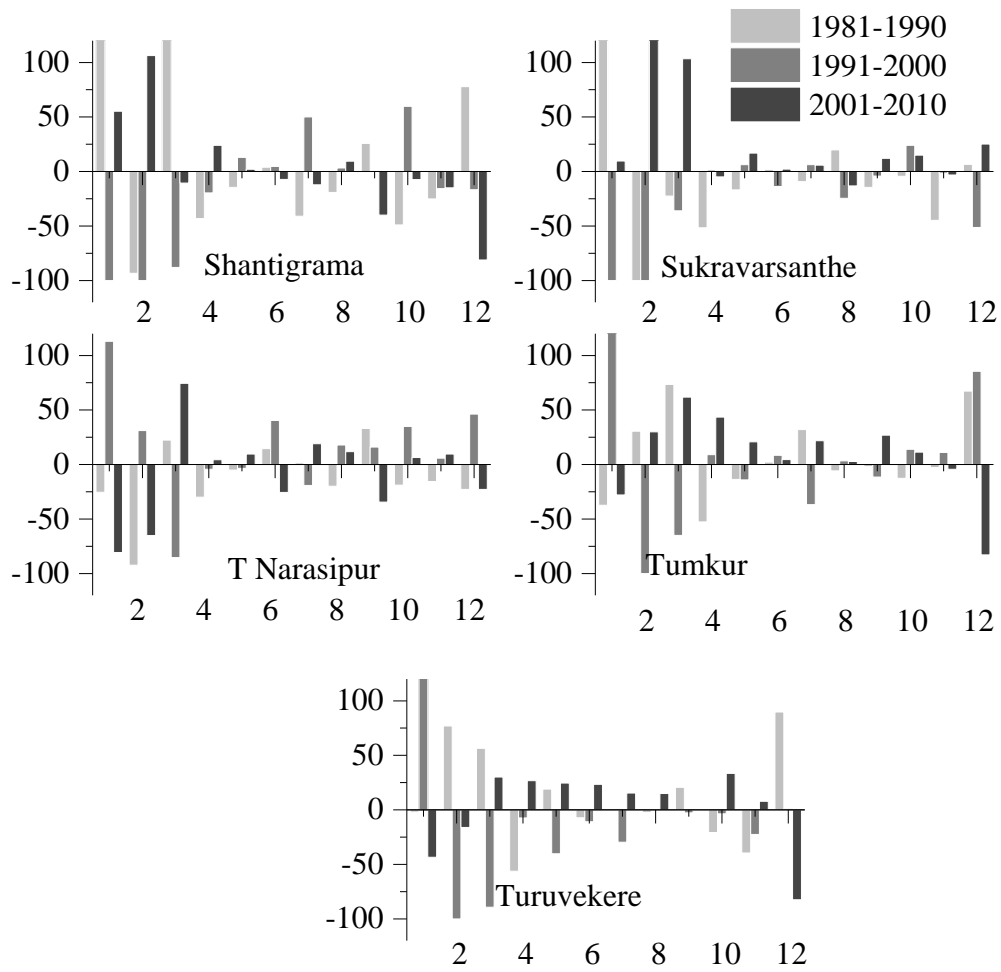


Fig. 4.4 Percentage departure of monthly rainfall of different decades from 30 years normal value for different rainfall stations.

Note: x-axis : months, y-axis : percentage departure

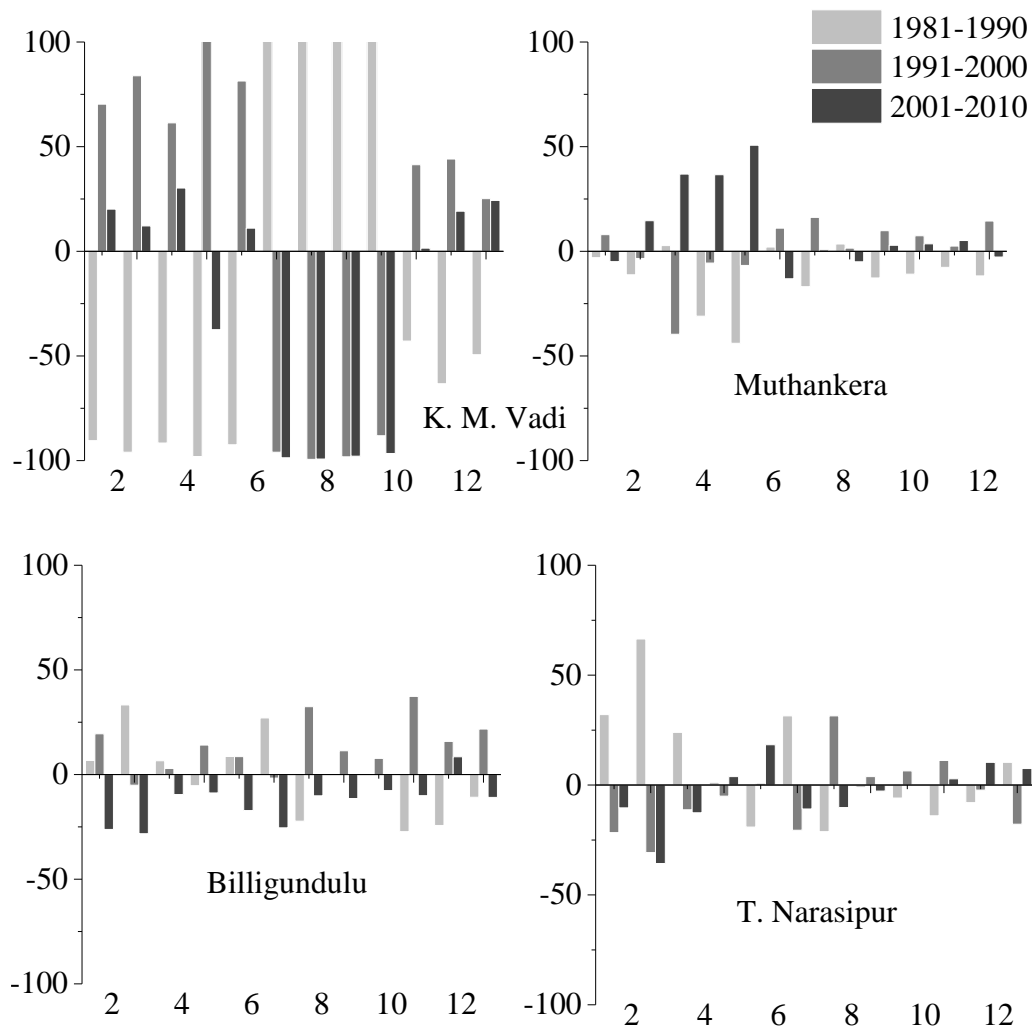


Fig. 4.5 Percentage departure of monthly streamflow of different decades from 30 years normal value.

Note: x-axis : months, y-axis : percentage departure

Considering Fig. 4.3, it can be seen that areal rainfall across the sub-basins exhibited high departures (exceeding $\pm 50\%$) during the non-monsoon months during certain decades. However, departures in rainfall were quite small during the monsoon season for all the sub-basins except Arakavathi where insignificant departures occurred even during the monsoon months.

Similar behaviour of low departures during monsoon months and somewhat high departures during the summer months can be seen with regard to rainfall at all individual rain gauge stations (Fig. 4.4). From Fig.4.5, it can be seen that the streamflow

of K M Vadi station exhibited high departures for all the months compare to other streamflow gauge stations.

4.7 TREND ANALYSIS OF HYDROMETEOROLOGICAL TIME SERIES

Results of trend analysis (Sen's slope, p-value and Kendall's tau) with regard to rainfall at individual stations and areal average rainfall for each of the sub basins are presented in Tables 4.2 and 4.3a. No statistically significant trend was observed at any of the rain gauge stations. Out of total 6 sub basins, Arkavathi sub basin showed significant increasing trends at 5% significance level. No trend was observed for the other sub basins. Regional Sen's slope analysis for monthly rainfall over the entire Upper Cauvery basin resulted in a trend of 0.005 mm/year; but this was not statistically significant at 5% significance level.

The results of the Seasonal-Kendall and Sen's slope analysis performed for monthly average daily minimum and maximum temperatures are shown in Table 4.3b. Out of 6 climatic stations, Hassan station showed statistically significant increasing trend for both minimum and maximum temperature. The Chikmagalur station showed a significant increasing trend for maximum temperature but there is no significant trend for minimum temperature. The Bangalore station exhibited a significant increasing trend in minimum temperature with no significant trend for maximum temperature. The Madikeri station has shown significant decreasing trend for minimum temperature at 5% significance level.

Streamflow data was analyzed for the 4 gauge sites in the Upper Cauvery Basin for quantifying the magnitude of trend and results are presented in Table 4.3c. The T. Narasipur gauge site showed significant decreasing trends at 5% significance level for streamflow. The T. Narasipur gauge site indicated an annual decrease of $-0.778 \text{ m}^3/\text{s}$ /year in the decade 1981-2010. No significant trend was observed for the other three gauge sites.

Table 4.3 Sen's slopes and significant of trend using the Seasonal-Kendall method for a) rainfall, b) temperature and c) streamflow

a) Rainfall						
Sub basin Name	Sen's slope		p-value		Kendall's tau	
Hemavathi	0.00		0.456		-0.29	
Harangi	0.08		0.481		0.027	
Lakshmanathirtha	0.05		0.344		0.036	
Kabini	0.04		0.416		0.031	
Shimsha	0.00		0.631		-0.018	
Arkavathi	0.37		0.0002		0.166	
Upper Cauvery	0.06		0.462		0.029	
b) Maximum and minimum temperatures						
Station Name	Sen's slope		p-value		Kendall's tau	
	Max	Min	Max	Min	Max	Min
Chikmagalur	0.04	0.01	0.0001	0.566	0.162	0.020
Hassan	0.02	0.04	0.0001	0.0001	0.153	0.153
Madikeri	-0.02	-0.04	0.928	0.0001	0.003	-0.164
Mandya	0.00	0.00	0.292	0.637	0.036	-0.016
Mysore	0.02	0.01	0.007	0.193	0.094	0.045
Bangalore	0.00	0.02	0.563	0.0001	0.020	0.229
c) Streamflow						
Site Name	Sen's slope		p-value		Kendall's tau	
K.M.Vadi	0.00		0.055		0.072	
Muthankera	0.98		0.978		0.001	
T.Narasipur	-9.34		0.0004		-0.160	
Billigundulu	-9.92		0.273		-0.056	

4.8 LONG-TERM PERSISTENCE IN HYDROMETEOROLOGICAL TIME SERIES

To check whether hydrometeorological time series exhibit long range dependency or not, the DFA method was applied. Monthly rainfall and streamflow data for the period 1981-2010 was used for this purpose. The long range dependence was checked for raw and deseasonalised time series. From Table 4.4, a weak persistence was observed for rainfall and streamflow raw time series using the DFA method, although slightly stronger persistence was evident for the deseasonalised time series. The DFA exponent (α) for rainfall was in the range 0.25 to 0.57 and for streamflow was 0.38 to 0.55 for the raw time series. The DFA exponent (α) ranged between 0.51 to 0.68 for rainfall and between 0.41 to 0.58 for streamflow when the deseasonalised time series were considered.

Table 4.4 DFA exponent for monthly (a) rainfall and (b) streamflow time series

a) Rainfall			
Sl. No.	Sub basin Name	DFA exponent (α)	
		Raw time series	Deseasonalised time series
1	Hemavathi	0.40	0.59
2	Harangi	0.31	0.52
3	Lakshmanathirtha	0.38	0.58
4	Kabini	0.46	0.67
5	Shimsha	0.25	0.51
6	Arkavathi	0.57	0.68
	Upper Cauvery	0.36	0.60
b) Streamflow			
Sl. No.	Site Name	DFA exponent (α)	
		Raw time series	Deseasonalised time series
1	K.M.Vadi	0.43	0.41
2	Muthankera	0.38	0.46
3	T.Narasipur	0.50	0.56
4	Billigundulu	0.55	0.58

4.9 SUMMARY AND CONCLUSIONS

Historical records of hydroclimatic variables in the Upper Cauvery basin were analysed to identify possible changes and trends over the 30-year period 1981-2010. The variables analysed were monthly averages of daily maximum temperature, daily minimum temperature, rainfall depth and streamflows recorded at 33 rain gauge stations, 6 climate stations and 4 stream gauging stations located within the basin. In addition to analysing rainfall at individual rain gauge stations, areal rainfall depths for 6 sub-basins and the entire Upper Cauvery basin also were computed and subjected to analysis. For each of the variables, historical data was analysed to compute coefficient of variation (CV) and percentage departures in monthly mean values from the normal values separately for 3 different decades. In order to calculate existence of a trend and magnitude of trend in these variables, the Seasonal-Kendall (Hirsch et al., 1982) and Sen's slope (Sen, 1968) estimator were used. To find long-term persistence in the time series data Detrended Fluctuation Analysis (DFA) method was used (Kantelhardt et al., 2001).

Overall, monthly rainfall over sub basins and also at individual stations did not exhibit statistically significant trends by any of the methods employed. However, somewhat large values of CV and departures were noted for rainfall in non-monsoon months. Not much variation was observed for maximum daily temperature except in the months of May and June for the Hassan climate station. Statistically significant trend was observed in maximum temperature only for Chikmagalur and Hassan stations. The CV of minimum temperature show a large variability from November to March for all climate stations and also a significant increasing trend for Hassan and Bangalore stations, while for Madikeri a decreasing trend was observed with a variation of $-0.16\text{ }^{\circ}\text{C}/\text{year}$. Not much variation was found for stream flow except for the T.Narasipur gauge site which showed a significant decreasing trend of $-0.778\text{ m}^3/\text{s}/\text{year}$. Long range dependence analysis indicated a weak persistence for both rainfall and stream flow. Results of this study can provide important inputs to climate/hydrology modelers and also to decision makers concerned with developing adaptation/mitigation plans for climate change. However, it needs to be pointed out that the results may be influenced by the monthly time step chosen for analysis.

Adoption of a daily time step and analysis of extreme events may provide additional information on trends in these hydroclimatic variables.

CHAPTER 5

HYDROLOGICAL MODELING

5.1 GENERAL

The main focus of the present study was to evaluate the relative performances of hydrological models incorporating VSA mechanism of runoff generation with that of a model which incorporates the infiltration-excess runoff generation mechanism. Accordingly, three models – SWAT (incorporating infiltration-excess mechanism), SWAT-VSA model (Easton et al., 2008) (VSA mechanism) and the proposed SWAT-MNDWI (VSA mechanism) were used. All three models were applied to two watersheds (Hemavathi and Harangi) located in the humid tropical Upper Cauvery Basin, Karnataka, India using historical records of relevant climate variables and other data related to topography, LU/LC and soils.

The present chapter is devoted to a detailed description of the hydrological models used, the study watersheds, data inputs, methodology adopted in applying the models and a detailed discussion of results obtained.

5.2 DESCRIPTION OF MODELS USED

5.2.1 SWAT

SWAT is a comprehensive model designed to simulate hydrological processes, nutrient dynamics and sediment transport at river basin-scale (Arnold et al., 1998). The model can be applied using a daily time step in a distributed manner by delineating the catchment into sub-basins which are further discretized into Hydrological Response Units (HRUs). The HRUs are unique intersections of land use and soil types and all model computations are performed at the level of individual HRUs. Predictions from each HRU are aggregated for each sub-basin and subsequently routed through the channel network to the catchment outlet. The hydrology component of the model requires inputs of rainfall, climate, LU/LC, soils

and elevation data. Simulation of hydrological processes for each HRU is based on the water balance equation:

$$SW_t = SW_0 + \sum_{i=1}^t R_{day} - Q_{surf} - E_a - w_{seep} - Q_{gw} \quad (5.1)$$

where SW_t is the final soil water content (mm H₂O), SW_0 is the initial soil water content on day i (mm H₂O), i is time in days for the simulation period t . R_{day} , Q_{surf} , E_a , W_{seep} , and Q_{gw} are the daily precipitation, surface runoff, evapotranspiration, percolation and return flow respectively. Surface runoff (Q_{surf}) for each HRU is calculated by using SCS-CN method. The general form of the SCS-CN method (USDA-SCS, 1972), is given by following equation

$$Q_{surf} = \frac{P_e^2}{(P_e + S_e)} \quad (5.2)$$

where P_e (mm) is the depth of effective precipitation (precipitation minus initial abstraction), S_e (mm) is the depth of effective available storage in the watershed when runoff begins and it is defined as

$$S_e = 25.4 * \left(\frac{1000}{CN} - 10 \right) \quad (5.3)$$

Curve Number (CN) is a function of the land use, soil permeability and antecedent soil water conditions.

5.2.2 SWAT-VSA

The SWAT-VSA model (Easton et al., 2008) incorporates VSA hydrology in terms of CN-VSA equation for capturing the spatial pattern of saturation excess runoff from source areas. The re-conceptualization of SWAT model helps in modeling VSAs without any modification in the code of the original model and thus provides an efficient and easy way of capturing spatially variant saturation excess runoff processes from the landscape. CN-VSA hydrology distinguishes between unsaturated and saturated areas in the catchment and assumes that all rainfall infiltrates in the unsaturated areas and all rain falling on saturated areas is converted into runoff. Based on this assumption, Steenhuis et al. (1995) derived the following equation for the fractional runoff contributing area for a rainfall event (A_f):

$$A_f = 1 - \frac{S_e^2}{(P_e + S_e)^2} \quad (5.4)$$

According to the Eq. (5.4) given by Schneiderman et al. (2007), runoff only occurs when and where local effective storage (σ_e) is less than effective precipitation and substituting σ_e for P_e in Eq.(5.4), the relationship for the fraction of watershed area (A_s) can be expressed as-

$$A_s = 1 - \frac{S_e^2}{(\sigma_e + S_e)^2} \quad (5.5)$$

According to Schneiderman et al. (2007), runoff for an area, q_i (mm), can be expressed as

$$q_i = P_e - \sigma_e \quad \text{for } P_e > \sigma_e, \quad (5.6)$$

For $P_e \leq \sigma_e$ the unsaturated portion of the watershed, $q_i=0$. To avoid changing the SWAT code, Easton et al. (2008) proposed approximating Eq. (5.6) with the CN equation,

$$Q_{surf} = \frac{P_e^2}{(P_e - \sigma_e)} \quad (5.7)$$

The SWAT-VSA model uses Soil Topographic Index (STI) in place of soil input and the area of each HRU is defined by the concurrence of land use and STI. STI classifies each unit of a watershed into a relative tendency to become saturated and producing a saturation excess response to runoff. The STI map is generated by using the following equation,

$$STI = \ln\left(\frac{a}{T \tan \beta}\right) \quad (5.8)$$

where 'a' is the upslope contributing area for the cell per unit of contour line (m), $\tan\beta$ is the topographic slope of the cell and T is the transmissivity of the uppermost soil layer (m^2/d). The local storage deficit of each wetness class ($\sigma_{e,i}$) is determined by integrating Eq. (5.7) over the fraction of the watershed represented by that wetness class (Schneiderman et al., 2007)

$$\sigma_{e,i} = \int_{A_{s,i}}^{A_{s,i+1}} \sigma_e * d\bar{A}_s$$

$$= \frac{2S_e \left(\sqrt{1 - A_{s,i}} - \sqrt{1 - A_{s,i+1}} \right)}{\left(A_{s,i+1} - A_{s,i} \right)} - S_e \quad (5.9)$$

where the fractional area ($A_{s,i}$) corresponded to each wetness index class that is bounded one side by the fraction of watershed that is wetter and other side by the fraction of the watershed that is dryer.

5.2.3 SWAT-MNDWI

In SWAT-MNDWI, the STI is replaced with a remote sensing based wetness index and each HRU is defined by a unique intersection of land use and remote sensing based wetness index. De Alwis et al. (2007) delineated hydrologically active areas within a catchment using a wetness index derived from the Normalized Difference Water Index (NDWI) developed by Gao (1996). Xu (2006) proposed a Modified Normalized Difference Water Index (MNDWI) to enhance open water features while efficiently suppressing and even removing built-up land noise as well as vegetation and soil noise. In this study, MNDWI proposed by Xu (2006) is used to define the distribution of wetness indices and it is expressed as follows

$$MNDWI = \frac{(Green - MIR)}{(Green + MIR)} \quad (5.10)$$

where Green is a green band such as ETM+ (Enhanced Thematic Mapper Plus sensor) band 2, and MIR is a middle infrared band such as ETM+ band 4.

The multi-spectral Landsat 7 ETM+ (Enhanced Thematic Mapper plus sensor) imagery was used to calculate wetness index over the study areas. Cloud-free Landsat images are archived only up to the year 2002. After search and preliminary analysis of available images, good quality cloud-free data available for 20 December 2000 was selected and used to calculate MNDWI using Eq. (5.10). Since significant rainfall had occurred over the study areas prior to this date, saturated areas could be identified.

The ArcSWAT version of the SWAT model which has been developed as an extension to ArcGIS-ArcView[®] software to provide a convenient graphical user interface was used in the present study. Executables, source codes and input/output documentation of the SWAT and ArcSWAT models can be found at <http://swat.tamu.edu>. As regards the SWAT-VSA and SWAT-MNDWI, the model

application procedure proposed by Easton et al. (2008) was adopted so that the same SWAT code could be used for applying these two models as well.

5.3 DESCRIPTION OF WATERSHEDS

5.3.1 Hemavathi Watershed

The Hemavathi located in Karnataka State, is a tributary to the Cauvery river and originates in the mountainous Western Ghats region. Hemavathi watershed has an area of 2974.20 km² (Fig. 5.1a) up to Hemavathi Dam. The major LU/LC classes in the Hemavathi consist of forest (14.56%), agricultural (72.51%) and urban (2.74%). Water bodies and reservoirs comprise 5.3% of the watershed area. Elevation in the watershed ranges from 843 m at the outlet to 1795 m in the upland areas. The average annual rainfall exceeds 1500 mm. Mean daily maximum and minimum air temperatures are 37°C and 10°C respectively. Daily streamflow output from the watershed is monitored as inflow into the Hemavathi dam (Fig. 5.1). The map of the LU/LC is shown in Fig. 5.2 and characteristics are given in Table 5.1. The soil map of the watershed is shown in the Fig 5.3.

5.3.2 Harangi Watershed

The Harangi river originates in the Pushpagiri Hills of Western Ghats and joins the Cauvery near Kudige in Madkeri. The watershed is located in Karnataka State and has an area of 538.8 km² (Fig. 5.1b) up to Hemavathi Dam. Elevation in the Harangi watershed ranges from 818 m to 1635 m. While average annual rainfall exceeds 3000 mm, the mean maximum and minimum temperatures are 36°C and 4.8°C respectively. The major LU/LC categories in the Harangi watershed include forest (53.52%), agricultural (32.86%), urban (1.57%) and water bodies/reservoirs (3.24%). Daily streamflow output from the watershed is monitored as inflow into the Harangi dam (Fig. 5.1). The LU/LC map and characteristics of the Harangi watershed are shown in Fig 5.4 and Table 5.2 respectively. The soil map of the watershed is shown in the Fig 5.5.

Table 5.1 Characteristics of LU/LC in the Hemavathi watershed

Land use	Class	Area (km²)	Watershed area (%)
Residential	URBN	26.21	0.88
Residential-Low Density	URLD	55.35	1.86
Agricultural Land-Close-grown	AGRC	1455.03	48.92
Agricultural Land-Generic	AGRL	14.21	0.48
Agricultural Land-Row Crops	AGRR	687.41	23.11
Forest-Evergreen	FRSE	5.34	0.18
Forest-Deciduous	FRSD	13.98	0.47
Forest-Mixed	FRST	419.79	14.11
Pasture	PAST	75.52	2.54
Industrial	UIDU	0.97	0.03
Water	WATR	157.24	5.29
Indian grass	INDN	63.15	2.12

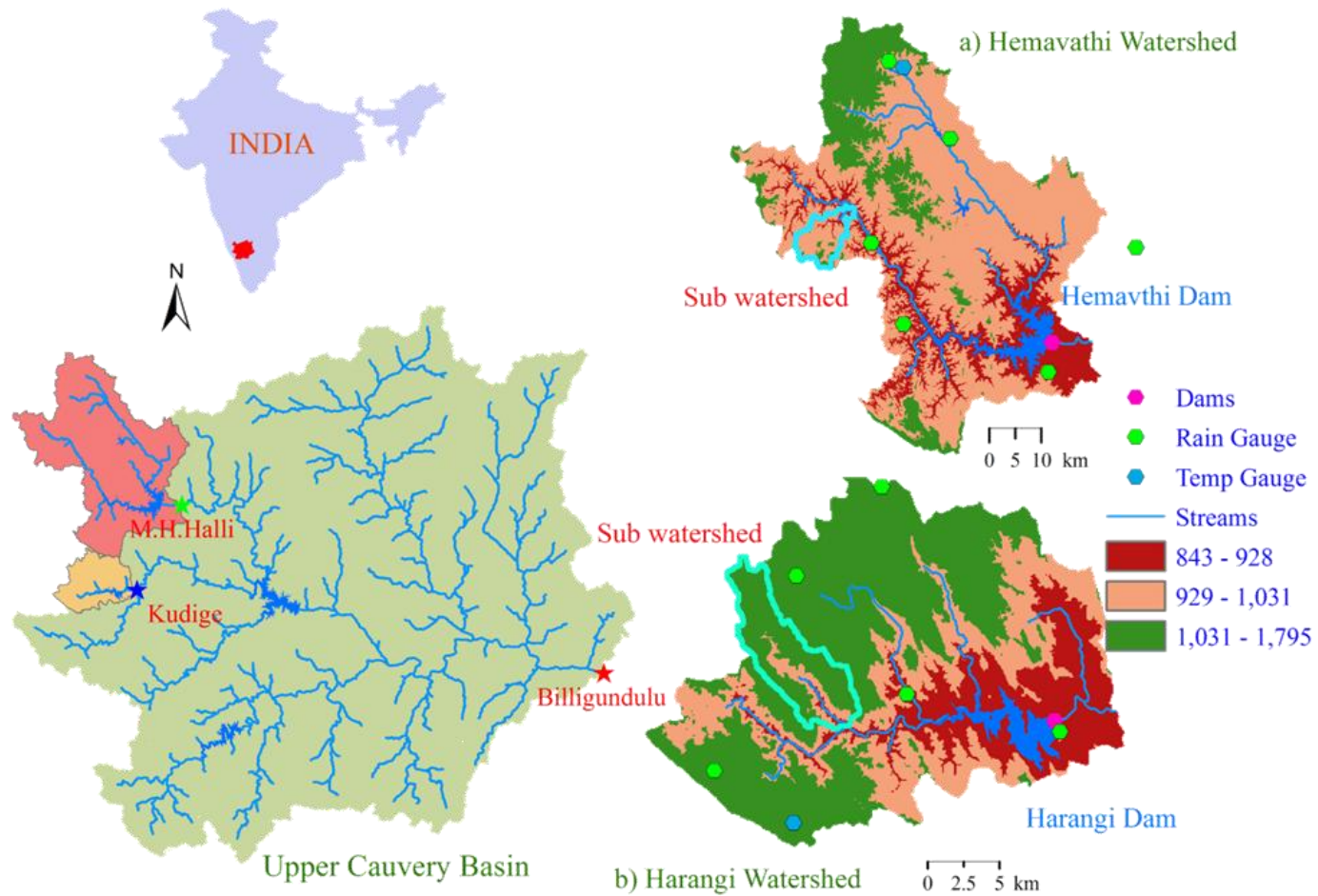


Fig. 5.1 Location Maps of (a) Hemavathi and (b) Harangi watersheds showing elevations, stream network and location of dams, rain gauges and climate stations

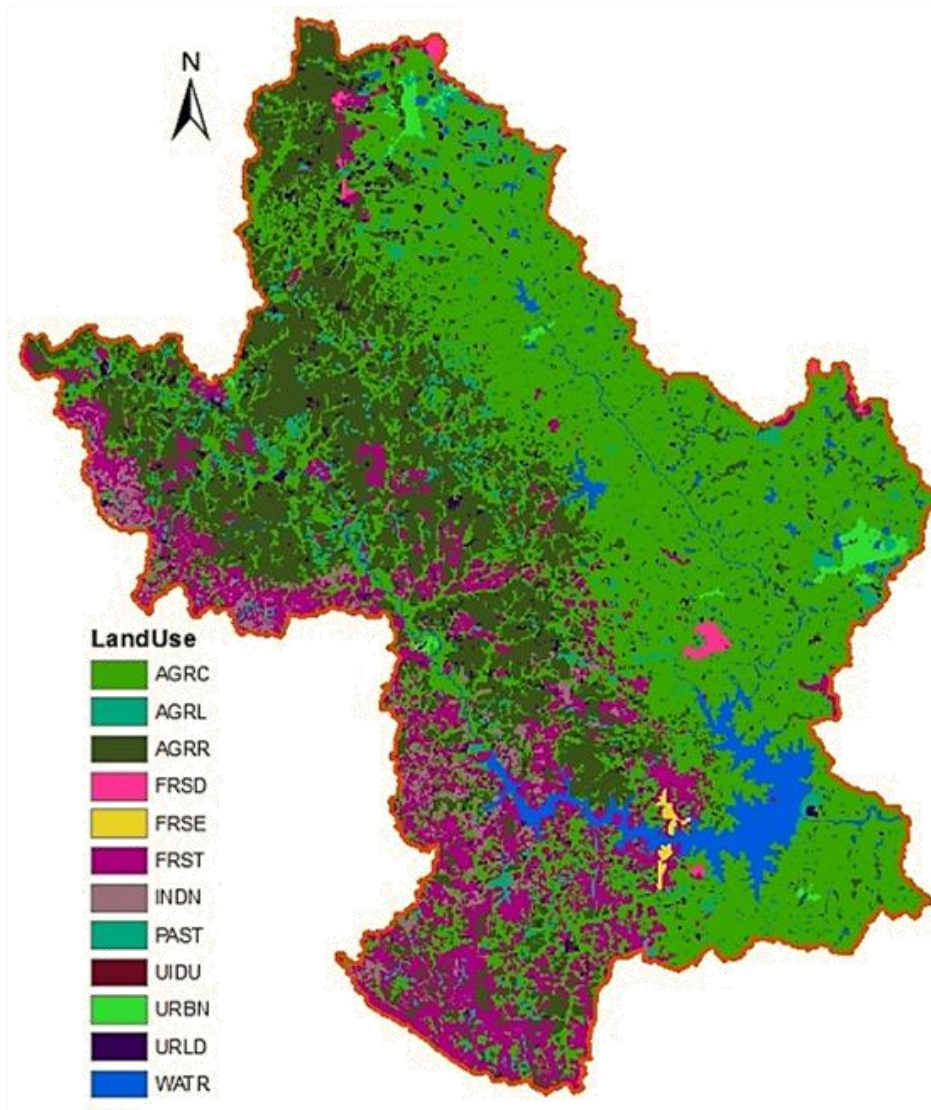


Fig. 5.2 LU/LC of the Hemavathi watershed

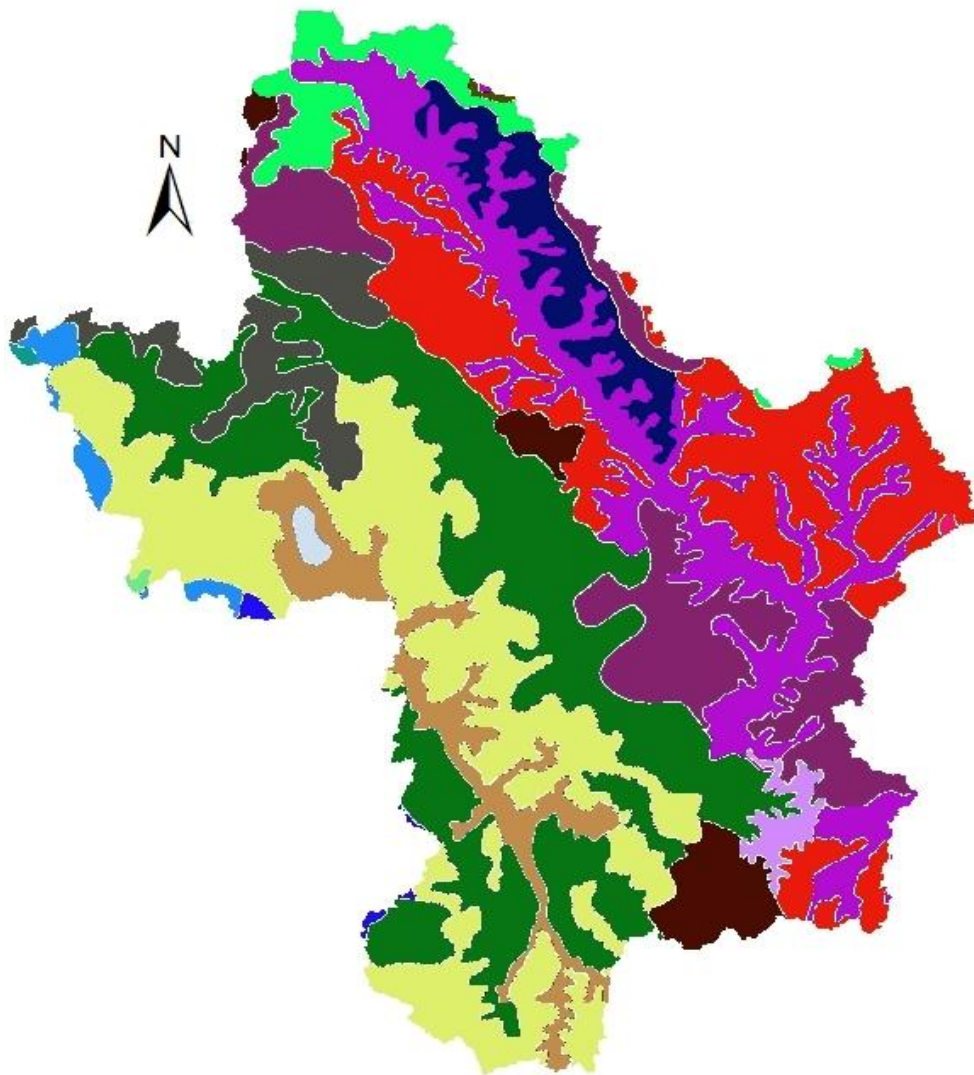


Fig. 5.3 Soil map of the Hemavathi watershed

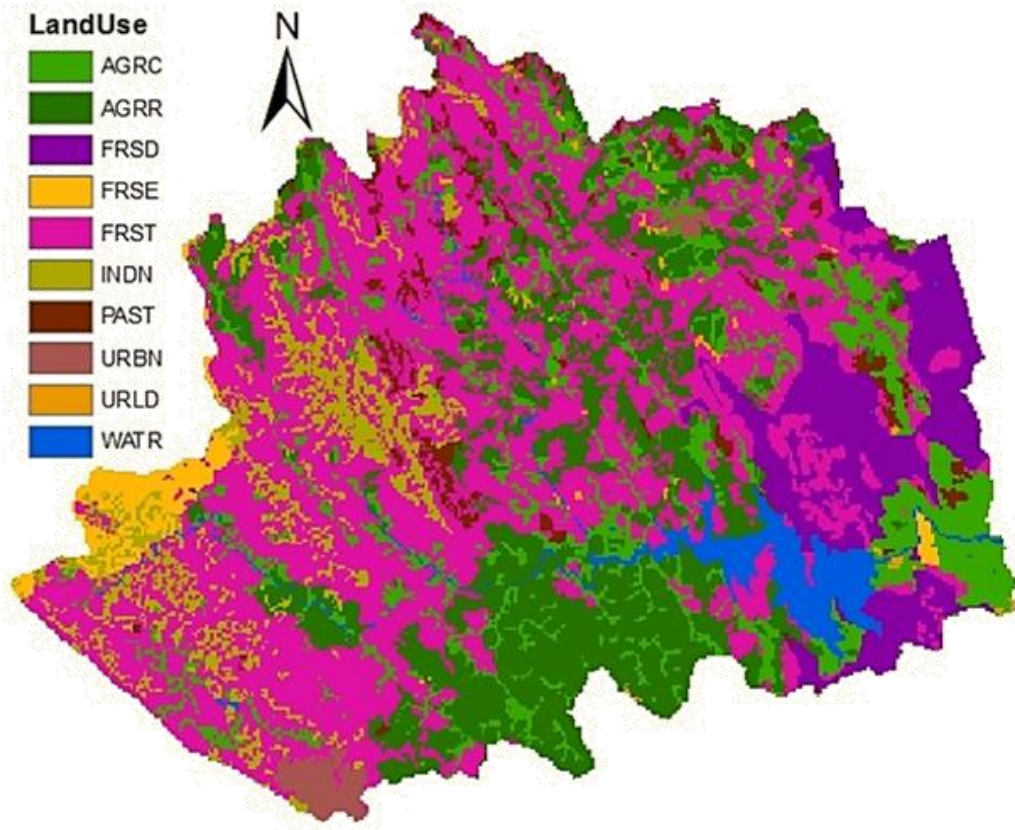


Fig. 5.4 LU/LC of the Harangi watershed

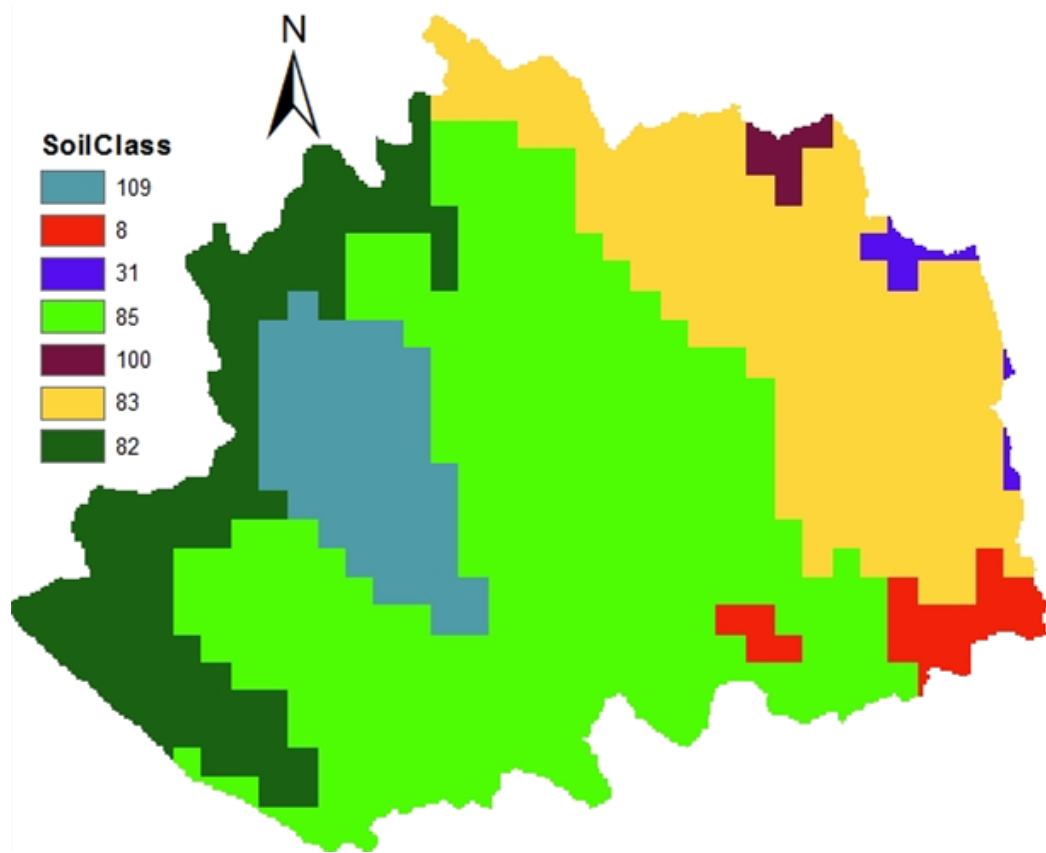


Fig. 5.5 Soil map of the Harangi watershed

Table 5.2 Characteristics of LU/LC in the Harangi watershed

Land use	Class	Area (km ²)	Watershed area (%)
Residential	URBN	6.07	1.13
Residential-Low Density	URLD	2.46	0.46
Agricultural Land-Close-grown	AGRC	72.21	13.40
Agricultural Land-Row Crops	AGRR	104.87	19.46
Forest-Evergreen	FRSE	10.46	1.94
Forest-Deciduous	FRSD	45.08	8.37
Forest-Mixed	FRST	232.84	43.21
Pasture	PAST	13.59	2.52
Water	WATR	17.45	3.24
Indian grass	INDN	33.77	6.27

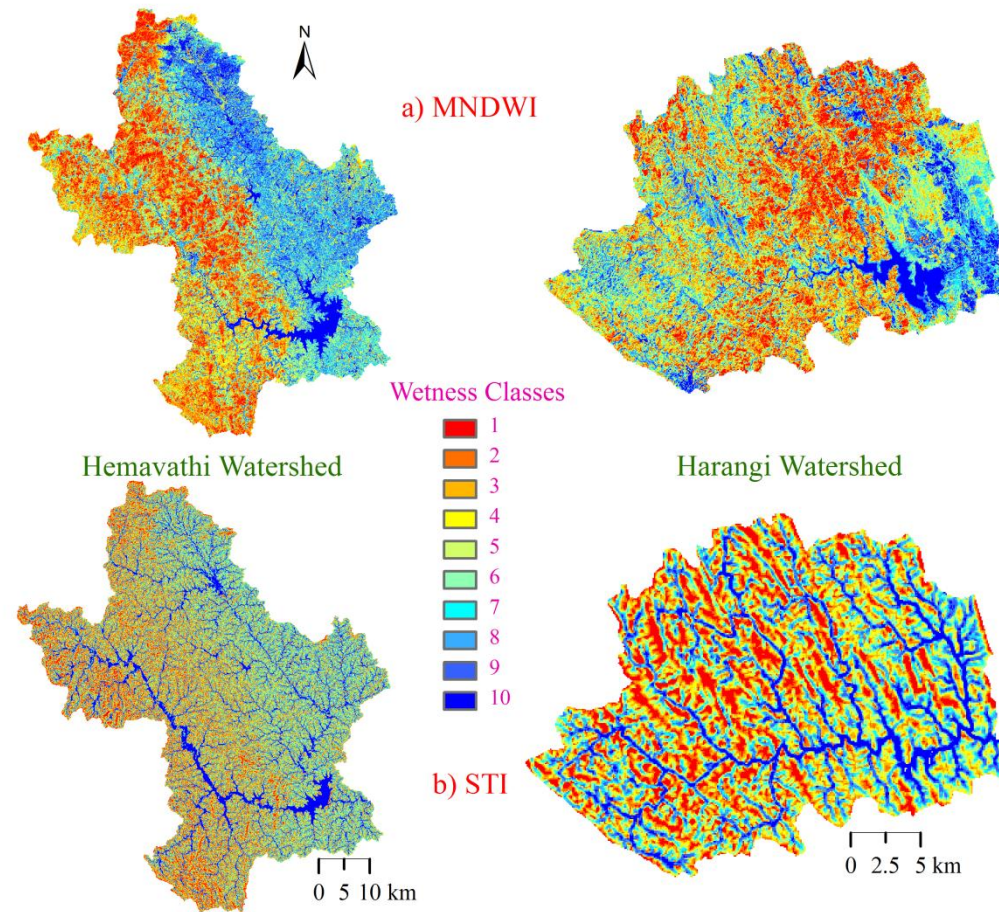


Fig. 5.6 Spatial distribution of wetness classes derived from (a) MNDWI and (b) STI for Hemavathi and Harangi watersheds

5.4 METHODOLOGY

5.4.1 Input Data

Basic input data required for the SWAT hydrological model includes topography, weather, rainfall, land use and soil data. Topographic data was obtained in the form of DEM (Digital Elevation Model) at 90 m resolution from the SRTM (Shuttle Radar Topography Mission) and it was used to delineate the watersheds into multiple sub watersheds. Topography-based parameters such as slope class and stream length were calculated from the DEM. Land use data at 1:50,000 scale was collected from KRSAC (Karnataka State Remote Sensing Application Centre) and soil maps along with the associated physical properties database were obtained from the National Bureau of Soil Survey and Land Use Planning (NBSS and LUP). Daily rainfall data was collected from Karnataka Irrigation Investigation Division (KIID) for 10 rain gauge stations located in and around the watersheds. Daily minimum and maximum air temperature data was collected from the Indian Meteorological Department (IMD) climate stations located at Chikamagalur and Madkeri. Daily inflow records for the major dams in the watersheds were collected from respective dam divisions of the Karnataka State Irrigation Department.

5.4.2 HRU Definitions

HRUs are a unique combination of land use, soil and slope class in the SWAT model. In SWAT-VSA and SWAT-MNDWI, soil data is replaced by STI and MNDWI respectively. The STI used in SWAT-VSA model was calculated from Eq. (5.8) using DEM. MNDWI was derived from the Landsat 7 (ETM+ sensor) satellite image using Eq. (5.10). Wetness indices of STI and MNDWI were divided into equal area intervals ranging from 1 to 10 using the ArcGIS reclassify raster tool by the quantile classification method, with class 1 having lowest tendency to saturate and class 10 having highest tendency to saturate (Fig. 5.6). Spatial distributions of the fractional areas were based on wetness class as defined by the STI and MNDWI. The STI and MNDWI values relate to a location's probability to attain saturation and subsequently contribute to surface runoff. Fig 5.7 shows flowchart for the creation of HRUs and

defining curve number according to SCS-CN method for SWAT and CN-VSA method for SWAT-VSA and SWAT-MNDWI.

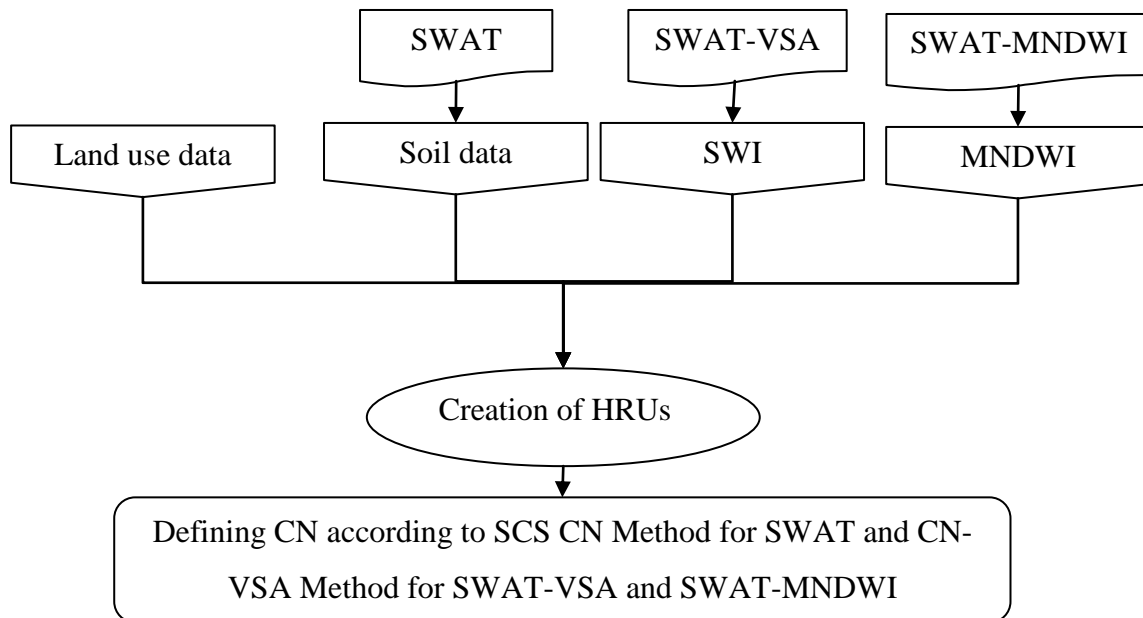


Fig. 5.7 Flowchart for creating HRUs and defining CN for SWAT-MNDWI, SWAT-VSA and SWAT models

5.4.3 Sensitivity Analysis

Sensitivity analysis is crucial in obtaining a better assessment of the impact of change in an individual input parameter on the model response. The ArcSWAT interface combines the Latin Hypercube (LH) and One-factor-At-a-Time (OAT) sampling (Van Griensven et al., 2006) to determine the global sensitivity rank of each of the selected model parameters. Using this approach, sensitivity analysis was performed on 16 different hydrological parameters for all three versions of SWAT considered in this study separately for Hemavathi and Harangi watersheds (Table 5.3). By using default upper and lower boundary parameter values, the parameters were tested for sensitivity using observed daily dam inflow data for the period 2000-2003.

Table 5.3 Parameter and their ranges considered in the sensitivity analysis

(Gw = groundwater, Evap = evaporation and Geom = geomorphology)

Name	Min	Max	Definition	Process
Alpha_Bf	0	1	Base flow alpha factor (day)	Gw
Blai	-20	20	Leaf area index*	Crop
Canmx	0	10	Maximum canopy index	Runoff
Ch_K2	0	150	Effective hydraulic conductivity in main channel alluvium (mm/h)	Channel
Ch_N	-20	20	The Manning coefficient for channel*	Channel
CN ₂	-20	20	SCS runoff curve number for moisture condition II*	Runoff
Epc0	-20	20	Plant evaporation compensation factor*	Evap
Esco	0	1	Soil evaporation compensation factor	Evap
Gw_delay	0	100	Groundwater delay	Gw
Gw_revap	0.02	0.2	Groundwater revap coefficient	Gw
Gwqmn	0	1000	Threshold depth of water in the shallow aquifer required for return flow to occur (mm)	Soil
Revapmn	0	500	Threshold depth of water in the shallow aquifer for revap to occur (mm)	Gw
Sol_Awc	-20	20	Available water capacity (mm/mm)*	Soil
Sol_K	-20	20	Soil conductivity (mm/h)*	Soil
Sol_Z	-20	20	Soil depth*	Soil
Surlag	0	10	surface runoff lag coefficient	Runoff

*Relative percent change.

5.4.4 Model Calibration and Validation

Model calibration entails the modification of parameter values and subsequent comparison of simulated stream flow with observed data until a defined objective function is minimized. In this study, the manual and automatic calibration was carried out using the dataset of observed daily dam inflow records for the period 2000-2003. Observed daily dam inflow data of Hemavathi dam for Hemavathi watershed and Harangi dam for Harangi watershed were used. The parameters obtained from the

sensitivity analysis using LH-OAT were chosen for manual and automatic calibration. To calibrate SWAT model, auto-calibration tool in the ArcSWAT interface was used with Parasol mode.

In the case of SWAT-VSA and SWAT-MNDWI models, parameters CN_2 and Soil_Awc were calibrated as per procedures described in detail by Lyon et al. (2004) and Easton et al. (2008). Broadly the approach involves two steps: 1) prediction of fractional area of watershed that is saturated through determination of amount of water storage available (S) in the entire catchment from observed rainfall-runoff data and 2) prediction of saturated areas within the watershed using an appropriate wetness index such that the error between estimated and observed runoff is minimized. The calibrated models at Hemavathi dam and Harangi dam were validated using daily dam inflow data for the period 2004 to 2006.

5.4.5 Model Performance Evaluation

Streamflow predictions by the three models were evaluated for the calibration and validation periods using four statistical measures: Nash–Sutcliffe efficiency (E_{NS}) (Nash and Sutcliffe, 1970), coefficient of determination (R^2), percent bias (PBIAS) (Yapo et al., 1996) and Root Mean Square Error (RMSE) as defined by the following equations:

$$E_{NS} = \left[1 - \frac{\sum (Y - X)^2}{\sum (Y - Y_{avg})^2} \right] * 100 \quad (5.11)$$

$$R^2 = \left[\frac{N \sum XY - \sum X \sum Y}{\sqrt{[N \sum X^2 - (\sum X)^2] \times [N \sum Y^2 - (\sum Y)^2]}} \right]^2 \quad (5.12)$$

$$PBIAS = \frac{\sum (Y - X)}{\sum Y} * 100 \quad (5.13)$$

$$RMSE = \sqrt{\frac{\sum (X - Y)^2}{N}} \quad (5.14)$$

where X represents daily observed streamflow, Y represents simulated streamflow values and N is the total number of records.

The E_{NS} value measures how well the simulated values coincide with the observed values. The strength of the relationship between the observed and simulated values is indicated using the R^2 value. PBIAS shows how much the simulated data is larger or smaller than their observed values. According to Gupta et al. (1999), PBIAS can be utilized as an indicator of under or over estimation by the model. The RMSE values can be used to compare the performance of a given model with other predictive models.

5.5 RESULTS AND DISCUSSION

5.5.1 Sensitivity Analysis

Results of the global sensitivity analysis for the 6 cases considered – SWAT, SWAT-VSA and SWAT-MNDWI models applied separately to the Hemavathi and Harangi watersheds are presented in Fig. 5.8. Sensitivity ranks with respect to the 16 hydrological parameters according to their magnitude of response are shown there. Parameters may be categorized based on the relative magnitudes of ranks (Van Griensven et al., 2006) and for this analysis, parameters with rank 1 were classified as ‘very important’, those with ranks between 2-6 as ‘important’, parameters with ranks between 7-11 as ‘slightly important’ and those with rank greater than 12 as ‘unimportant’.

Accordingly, considering the Hemavathi watershed first, it can be seen from the results shown in Fig. 5.8 that the parameter representing the threshold depth of water in the shallow aquifer required for return flow to occur (Gwqmn) was a very important parameter (rank 1) for two cases except for the SWAT model where it ranked as important (rank 2). This result indicates the importance of significantly large baseflow contributions to runoff in tropical regions with shallow unconfined aquifers. Given its importance in determining the magnitude of surface runoff, the SCS runoff curve number for moisture condition II (CN_2) was also a very important parameter for the SWAT model, but fell under the important category for the other two versions of the SWAT model. Available water capacity (Sol_Awc) and soil evaporation compensation factor (Esco) proved to be important parameters for all three versions of models highlighting the role of evapotranspiration in tropical climates. Four parameters, depth of soil layer (Sol_Z), delay in groundwater flow

(Gw_delay), effective hydraulic conductivity in main channel alluvium (Ch_K2) and maximum canopy index (Canmx) were slightly important with the remaining parameters being unimportant.

For the Harangi watershed, differences in parameter sensitivity between the three models were less pronounced (Fig. 5.8). Gwqmn was the only very important parameter and as in the earlier case, Sol_Awc, CN₂ and Esco were important parameters for all three models. Base flow alpha factor (Alpha_Bf) also proved to be an important parameter for all models. Parameters falling under the slightly important and unimportant categories were similar to those for the Hemavathi watershed. Overall, it appears that for both watersheds and all three models, parameters related to shallow groundwater and unsaturated zone significantly affected streamflow responses.

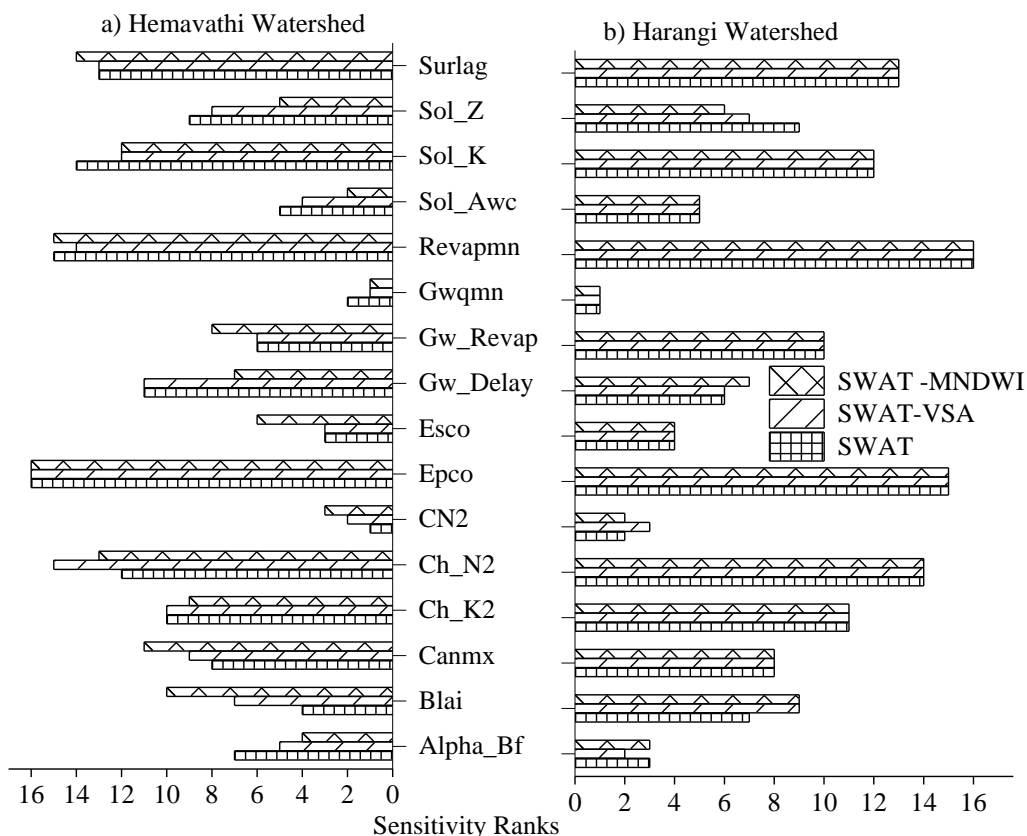


Fig. 5.8 Sensitivity ranks for hydrological parameters of SWAT-MNDWI, SWAT-VSA and SWAT models for (a) Hemavathi (b) Harangi watersheds

5.5.2 Model Calibration Results

Implementation of both SWAT-MNDWI and SWAT-VSA models requires initial determination of a lumped value for the retention parameter (S_e) as per the procedure described by Steenhuis et al. (1995). This permits subsequent computation of fractional saturated area (A_f) for a rainfall event. The data from 2000 to 2004 was used to calculate S_e value and to calibrate CN_2 values for SWAT-MNDWI's and SWAT-VSA's wetness classes. Fig. 5.9 showing a plot of effective rainfall versus corresponding observed runoff at the outlet was used to determine a lumped value of S_e separately for the Hemavathi and Harangi watersheds. Resulting values of S_e were 91 mm and 129 mm for the Hemavathi and Harangi watersheds respectively. Using the procedure described by Easton et al. (2008), lumped S_e was used to distribute the $\sigma_{e,i}$ values in the watershed according to the wetness index, which resulted in average CN_2 values of 69.27 and 63.47 for the Hemavathi and Harangi watersheds. To calculate the basin average CN_2 for SWAT model the same S_e of 91 mm and 129 mm was used for the Hemavathi and Harangi watersheds. Spatially weighted average CN_2 values of 70.79 and 67.95 were obtained for the Hemavathi and Harangi watersheds respectively. Table 5.4 summarizes the calibrated CN_2 values for each combination of soil and land use.

To reduce the RMSE between predicted and observed stream flow, for Hemavathi watershed, the CN_2 values were evenly adjusted by adding 1.52 units. The optimized average CN_2 , for overall wetness index classes, was 70.79. Similarly, for Harangi watershed, average CN_2 of 63.47 was obtained for the entire watershed which was uniformly adjusted by adding 4.48 units. The optimized average CN_2 for overall wetness index classes was found to be 67.95. Soil_Awc parameter was used to compute the allowable water flow among HRUs in SWAT-MNDWI and SWAT-VSA models. The Soil_Awc parameter was computed using the equation proposed by (Easton et al., 2008). Table 5.4 summarizes the adjusted CN_2 and Soil_Awc values for each wetness index class for Hemavathi and Harangi watersheds.

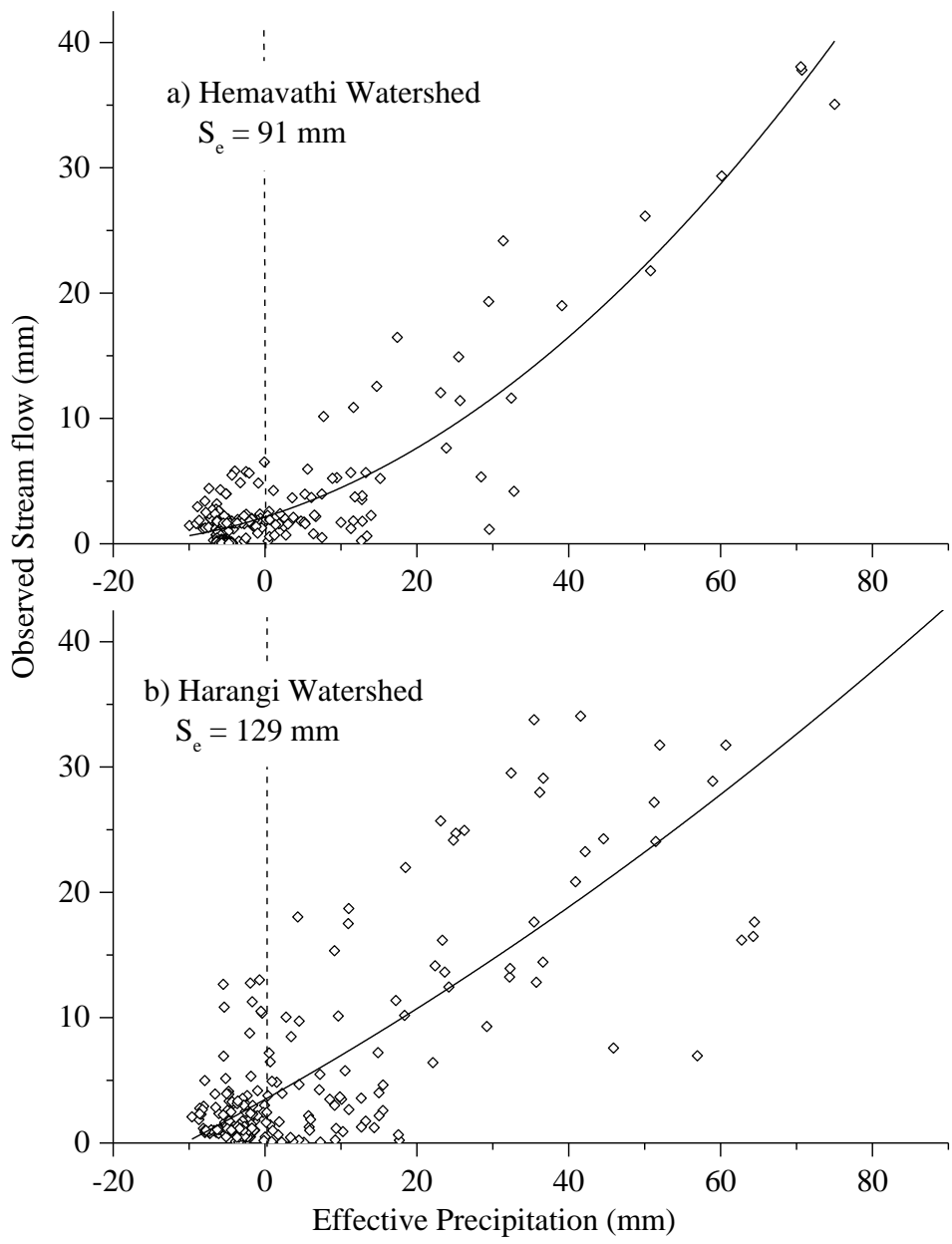


Fig. 5.9 Relation between effective precipitation and observed stream flow for (a) Hemavathi and (b) Harangi watersheds

Table 5.4 Adjusted parameters for SWAT-MNDWI, SWAT-VSA and SWAT models for Hemavathi and Harangi watersheds

Wetness index	SWAT-MNDWI and SWAT-VSA				SWAT					
	Hemavathi Watershed		Harangi Watershed		Hemavathi Watershed			Harangi Watershed		
	CN ₂ ^a	Soil_ Awc	CN ₂ ^a	Soil_ Awc	Soil	Land use	CN ₂ ^b	Soil	Land use	CN ₂ ^b
1	20.62	0.06	15.49	0.05	B	AGRC	65.78	B	AGRC	64.54
2	40.17	0.11	32.14	0.10	C	AGRR	82.90	C	AGRR	80.93
3	55.06	0.16	46.36	0.15	C	FRSE	63.21	C	FRSE	68.67
4	65.84	0.19	57.62	0.19	B	FRSD	71.85	B	FRSD	62.89
5	72.26	0.21	64.75	0.21	B	FRST	66.39	B	FRST	59.91
6	79.38	0.23	73.08	0.24	B	PAST	74.62	B	PAST	70.76
7	83.83	0.24	78.52	0.25						
8	87.55	0.25	83.22	0.27						
9	91.22	0.26	87.99	0.28						
10	96.81	0.28	95.54	0.31						
Average	69.27		63.47				70.79			67.95
Calibrated	70.79		67.95							

^a CN₂ values were calculated with the VSA methodology.

^b The average CN₂ values were calibrated from the observed runoff/rainfall relationship at the watershed outlet. Soil, Soil hydrologic group.

5.5.3 Accuracy of Streamflow Predictions

The SWAT, SWAT-VSA and SWAT-MNDWI models were calibrated using daily observed dam inflow data of Hemavathi dam for Hemavathi watershed and Harangi dam for Harangi watershed using procedures described in Section (5.4.4) for the period January 01, 2000 to December 31, 2003. Daily observed dam inflow data from January 01, 2004 to December 31, 2006 was used to validate the models. Fig. 5.10 and 5.11 show the time series and scatter plots of simulated and observed flows (m³/s) for the three models. From these figures it is noticed that during the calibration and

validation phases, observed streamflow is simulated reasonably well by all three model versions for both the Hemavathi and Harangi watersheds. In the case of Hemavathi watershed, the scatter plots indicate that all models simulated low and medium flows better than high flows with the SWAT-MNDWI model being slightly better in this regard. In the case of the Harangi watershed, which possesses higher proportion of forest land cover, scatter plots indicate slightly superior performance of the SWAT-VSA and SWAT-MNDWI models for medium flows probably on account of using the variable source area mechanism. Model performances evaluated using four statistical measures: E_{NS} , R^2 , RMSE and PBAIS are shown both for calibration and validation phases in Table 5.5. The E_{NS} and R^2 values are reasonably high for both calibration and validation periods. The PBIAS statistic indicates that SWAT model under predicted flows whereas the SWAT-MNDWI and SWAT-VSA model over predicted for both the watersheds during calibration and validation periods respectively. Similarly under prediction of flow for Indian basins by the SWAT model has been reported in earlier studies (Jayakrishnan et al., 2005; Tripathi et al., 2003).

For all cases shown in Table 5.5, the SWAT-MNDWI model yielded the least RMSE followed by the SWAT-VSA model. For the Hemavathi watershed, SWAT resulted in RMSE values which were significantly higher than the other two models. Overall, from the results shown in Table 5.5, it appears that the SWAT-MNDWI performed best both in calibration and validation phases for both watersheds.

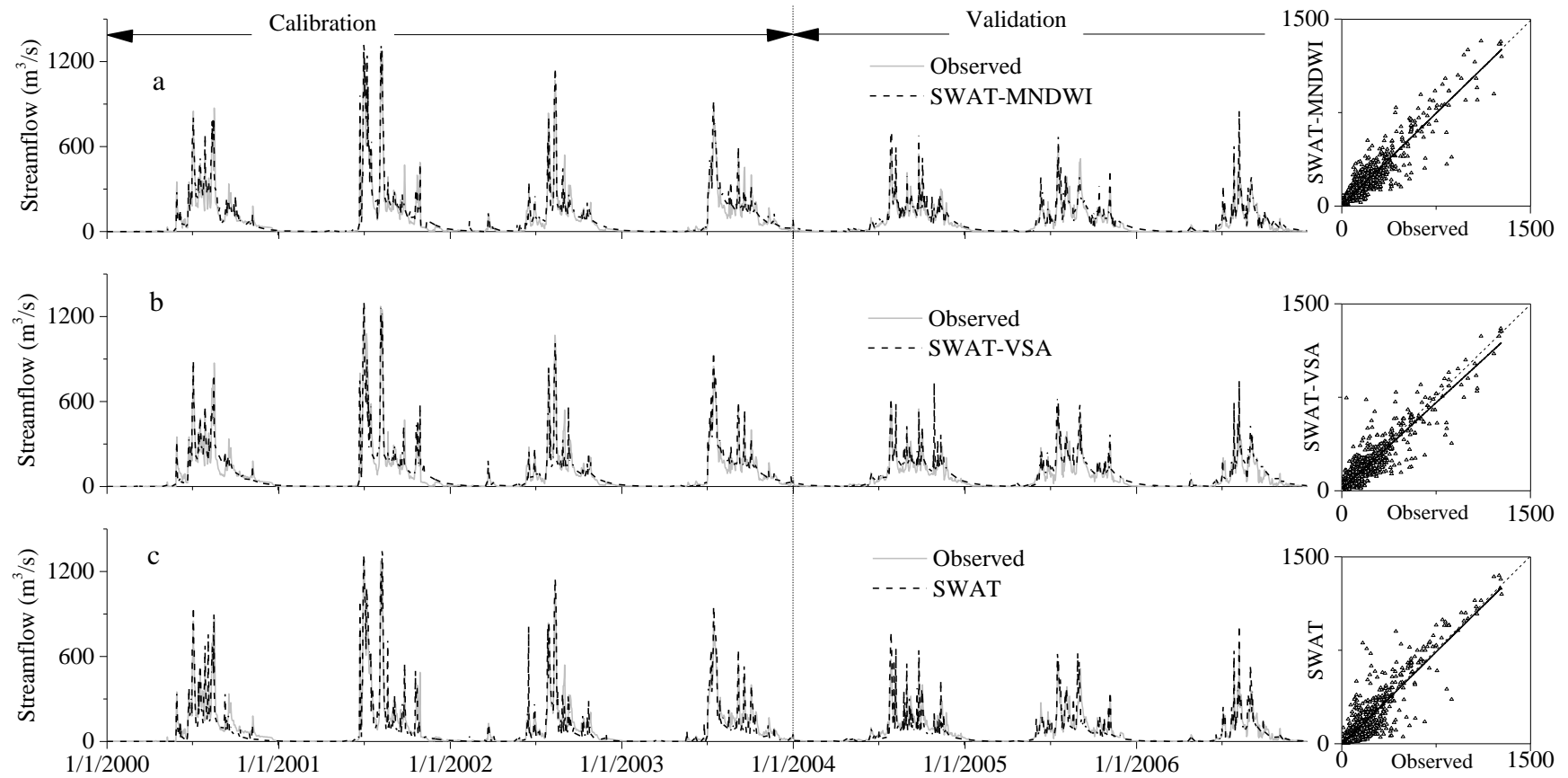


Fig. 5.10 Time Series and scatter plots of observed and simulated daily stream flow inflow in the Hemavathi watershed using SWAT-MNDWI (a), SWAT-VSA (b) and SWAT (c) at the Hemavathi dam gauge site.

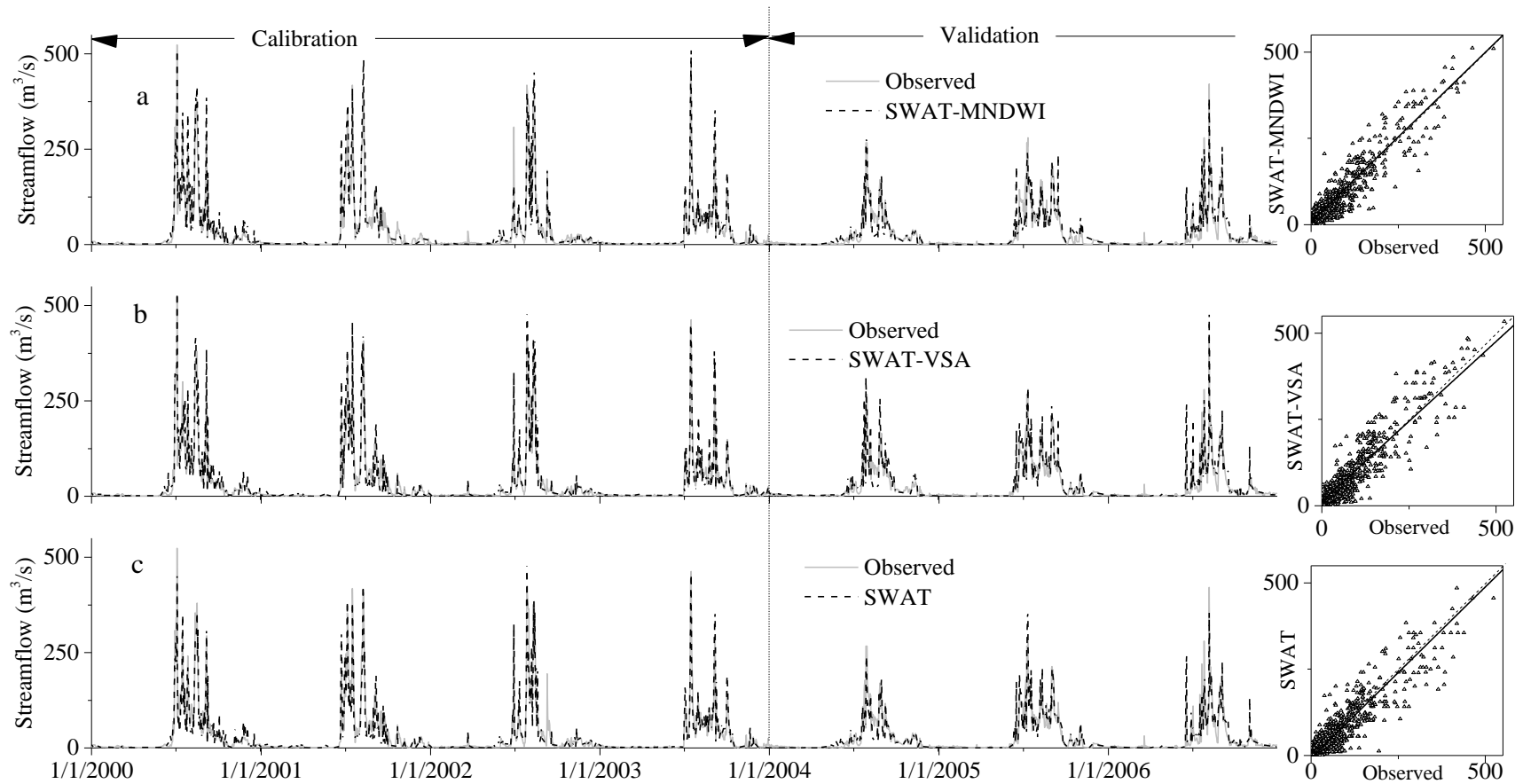


Fig. 5.11 Time series and scatter plots of observed and simulated daily stream flow inflow in the Harangi watershed using SWAT-MNDWI (a), SWAT-VSA (b) and SWAT (c) at the Harangi dam gauge site.

Table 5.5 Performance evaluation criteria for the three models during calibration and validation for Hemavathi and Harangi Watersheds

Phase	Statistical Criteria	Hemavathi Watershed			Harangi Watershed		
		SWAT-MNDWI	SWAT-VSA	SWAT	SWAT-MNDWI	SWAT-VSA	SWAT
Calibration	E_{NS}	0.89	0.88	0.85	0.90	0.88	0.87
	R^2	0.90	0.88	0.87	0.92	0.90	0.87
	PBIAS (%)	5.21	2.13	-11.45	4.78	3.98	-7.75
	RMSE (m ³ /s)	57.09	59.75	68.59	20.96	23.29	23.95
Validation	E_{NS}	0.85	0.79	0.73	0.88	0.86	0.86
	R^2	0.88	0.84	0.78	0.88	0.87	0.86
	PBIAS (%)	13.20	17.09	-11.29	1.09	5.10	-3.56
	RMSE (m ³ /s)	37.48	45.05	51.01	16.67	17.90	17.92

5.5.4 Water Balance Components

Spatially averaged water balance components for the Hemavathi and Harangi watersheds were extracted from the outputs of the SWAT-MNDWI, SWAT-VSA and SWAT models. From this, annual averages of the following water balance components were computed: the total amount of rainfall (P), actual evapotranspiration (ET) and the water yield from the watershed (WY). WY includes contributions from surface runoff (SURQ), lateral flow (LATQ) and groundwater (GWQ) minus the transmission losses.

The distribution of annual water balance components obtained from the three models for the Hemavathi watershed is shown in Table 5.6 and for the Harangi watershed in Table 5.7. Results are shown separately for calibration (2000-2003) and validation (2004-2006) periods. Calculations revealed that in the Hemavathi watershed the evapotranspiration loss (ET) was 44% of rainfall (P) during the calibration period and 48% during the validation period, with the corresponding values in the Harangi watershed being 27% and 32%. While the % ET loss seems somewhat reasonable for the predominantly agricultural Hemavathi watershed, the values for the forested Harangi watershed are significantly low especially considering the fact that the average annual rainfall for this watershed is much higher than for the Hemavathi

watershed. A possible reason for this anomaly could be due to the fact that ET computation in the SWAT model framework is focused more on agricultural crops and therefore may not accurately simulate the process for deep-rooted forests and also since interception losses are not accounted for.

Annual water yields (WY) in the Hemavathi watershed were in the range of 765 mm to 1068 mm (46% to 58% of annual rainfall). Significantly higher water yields occurred in the wet forested Harangi watershed (64% to 74% of annual rainfall) since ET values were much lower. From the results shown in Tables 5.6 and 5.7, it can be seen that except for the calibration period for Harangi watershed, the SWAT model predicts higher surface runoff (SURQ) than the SWAT-MNDWI and SWAT-VSA models. This is compensated for by the SWAT model through lowest groundwater contributions to streamflow (GWQ) for all cases. Probably on account of incorporating VSA mechanism, the other two models yield higher GWQ than SURQ, with the SWAT-MNDWI yielding the highest values of GWQ in all cases. Accordingly, the SWAT-MNDWI model also predicts the highest annual water yield (WY). The lateral flow component (LATQ) is small (< 5% of WY) for the Hemavathi watershed in comparison to the forested Harangi watershed (8-10 % of WY).

For annual periods, P must be equal to the sum of ET and WY. However, due to errors arising from a number of sources, this equality may not be satisfied, thereby resulting in a residual error. Accordingly, the annual water balance equation may be re-written as $P = ET + WY + \text{Residual}$. Values of Residual error are shown in Tables 5.6 and 5.7 from which it can be seen that for all cases considered the Residual forms a relatively small percentage of the rainfall (< 5%). In terms of ability to close the water balance with minimum error, the SWAT-VSA model is best (lowest Residual) for all cases considered.

Table 5.6 Average annual water balance components for the Hemavathi watershed derived using SWAT-MNDWI, SWAT-VSA and SWAT models (all values are in mm of water)

Model	P	SURQ	LATQ	GWQ	WY	ET	PET	Residual
(a) Calibration period								
SWAT-MNDWI		449	18	601	1068			-47
SWAT-VSA	1834	386	40	587	1013	813	1888	8
SWAT		489	12	467	968			53
(b) Validation period								
SWAT-MNDWI		292	17	612	921			-68
SWAT-VSA	1652	254	39	551	844	799	1840	9
SWAT		346	12	407	765			88

Table 5.7 Average annual water balance components for the Harangi watershed derived using SWAT-MNDWI, SWAT-VSA and SWAT models (all values are in mm of water)

Model	P	SURQ	LATQ	GWQ	WY	ET	PET	Residual
(a) Calibration period								
SWAT-MNDWI		1109	217	1287	2613			-31
SWAT-VSA	3517	1081	225	1279	2585	935	2135	-3
SWAT		1108	197	1201	2506			76
(b) Validation period								
SWAT-MNDWI		772	168	908	1848			-38
SWAT-VSA	2655	765	171	894	1830	845	2135	-20
SWAT		795	148	744	1687			123

P, Rainfall; SURQ, Surface runoff contribution to streamflow; LATQ, Lateral flow contribution to streamflow; ET, Actual Evapotranspiration; PET, Potential Evapotranspiration; WY, Water Yield ($WY = SURQ + LATQ + GWQ$); Residual = $P - ET - WY$

5.5.5 Spatial Patterns of Surface Runoff

In order to emphasize the advantages of using a distributed modelling approach and also to highlight differences in runoff generation by the three models, spatial variations of surface runoff predicted by these models were mapped for two small sub-watersheds within the Hemavathi and Harangi watersheds (Fig. 5.1). The watersheds were selected so that rainfall recorded at a single rain gauge located within each one of them could be used. Accordingly, a rainfall event of 20 mm on July 30, 2002 for Hemavathi sub-watershed (75.39 km²) and a 34 mm rainfall on August 27, 2002 for the Harangi sub-watershed (44.11 km²) were selected. Spatially distributed surface runoff output from all the three models for these dates are shown in Fig. 5.12 separately for the two sub-watersheds. Although, temporal variations and total WY at the watershed outlet predicted by the three models is very similar for both the watersheds (Fig. 5.10 and 5.11), the spatial patterns of predicted surface runoff by all the models appear to be noticeably different for both sub-watersheds (Fig. 5.12).

Considering the Hemavathi watershed, since a wetness index based on topography is used, the SWAT-VSA yields high surface runoff producing areas which follow the drainage network (Fig. 5.12b). The spatial extent of runoff producing areas is very small with a predominant portion of the watershed contributing little or no runoff. The pattern predicted by SWAT-MNDWI (Fig. 5.12a) is also very similar, but the runoff magnitudes are not as high as SWAT-VSA. Also, since a satellite-based wetness index was used, these source areas are not confined to only topographic lows. On the other hand, the SWAT model due to use of infiltration-excess mechanism, yields surface runoff from all parts of the watershed, the magnitude varying from extremely small values (0.16 to 0.36 mm) to reasonably high values (4.5 to 5.3 mm) (Fig. 5.12c).

Spatial patterns of surface runoff for the rainfall event over the Harangi watershed exhibit larger differences between the three models (Fig. 5.12). While the SWAT-MNDWI model indicates runoff producing areas interspersed throughout the watershed, the SWAT-VSA produces medium to high runoff from areas adjoining the drainage network. Since this sub-watershed is predominantly forested with low runoff potential, SWAT depicts variations in runoff as decided by HRUs with high runoff potential.

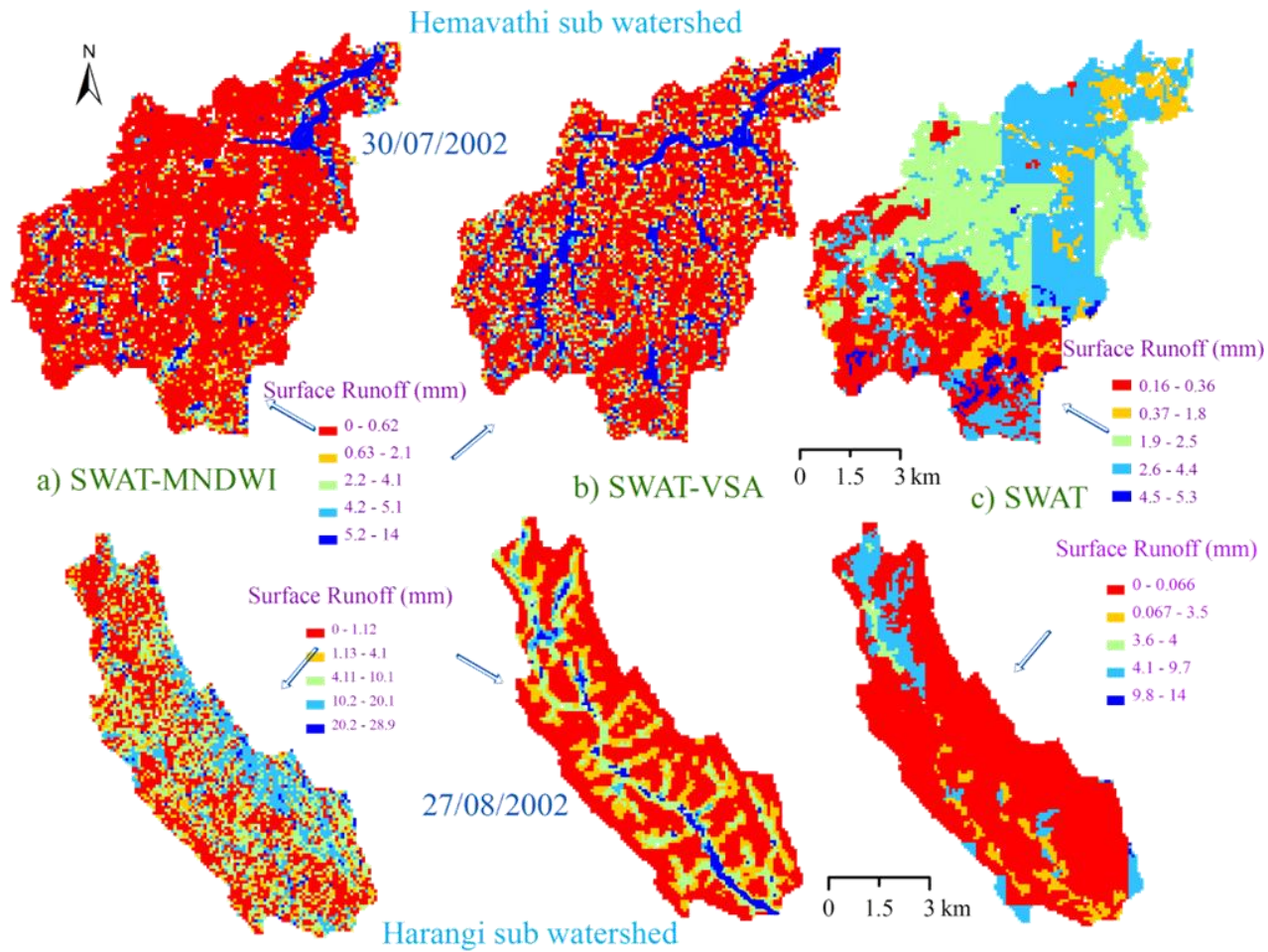


Fig. 5.12 Spatial distribution of surface runoff (mm) modeled by (a) SWAT-MNDWI, (b) SWAT-VSA and (c) SWAT for specific rainfall events over the sub watersheds of Hemavathi and Harangi watersheds

5.6 SUMMARY AND CONCLUSIONS

The performances of two hydrological models incorporating Variable Source Area (VSA) mechanism of runoff generation were compared with that of the SWAT model which computes surface runoff based the infiltration-excess mechanism. Performances were evaluated through application of the three models in two humid tropical watersheds located in Karnataka State, India. While the SWAT-VSA model proposed by Easton et al. (2008) uses a topographic wetness index to determine source areas of runoff, in this study a wetness index (MNDWI) derived from satellite imagery was used instead, leading to a new modelling approach called SWAT-MNDWI. The fact that one of the watersheds (Hemavathi – 2974 km²) possessed agriculture as the predominant land use and the other watershed (Harangi – 538.8 km²) was dominated by forest cover, permitted assessment of the effect of LU/LC on VSA hydrology. All three models were applied using a daily time step with relevant data inputs pertaining to rainfall, climate variables, satellite imagery-based LU/LC classification & DEM and soil types/properties. Observed daily streamflow records at the outlets of the watersheds were used to calibrate the models for the period 2000-2003 and validate them for the period 2004-2006.

The comparative assessment focused specifically on the following aspects for the six cases considered (3 models applied to 2 watersheds): 1) sensitivity of model parameters 2) accuracy of daily streamflow predictions at the watershed outlets 3) predictions of spatially and temporally averaged annual water balance components 4) differences in spatial patterns of source areas of surface runoff.

Sensitivity analysis indicated that for both the models based on VSA, the parameter representing the threshold depth of water in the shallow aquifer for return flow to occur (Gwqmn) proved to be a very important parameter in both watersheds. Not surprisingly, for the SWAT model, curve number for moisture condition II (CN₂) was the most important parameter. Overall, for both watersheds and all three models, parameters related to the unsaturated zone and shallow groundwater significantly effected streamflow responses. This result is typical of watersheds located in the

humid tropics where baseflow contributions to streamflow during both wet and dry seasons along with evapotranspiration losses largely determine runoff responses.

The ability of the three models to simulate daily streamflows at the watershed outlets was reasonably good both in calibration and validation phases. All models proved better at simulating low and medium flows than high flows. The performances of all the models were better for the forested Harangi watershed in comparison to the agricultural Hemavathi watershed, with the performances of the models based on VSA being slightly better than the SWAT model. Nash-Sutcliffe efficiency values (E_{NS}) during the validation phase in the Hemavathi watershed were 0.85, 0.79 and 0.73 for the SWAT-MNDWI, SWAT-VSA and SWAT models respectively with corresponding values in the Harangi watershed being 0.88, 0.86 and 0.86. The lowest value of coefficient of determination (R^2) in validation was 0.78 for SWAT in Hemavathi watershed and the highest value was 0.88 for the SWAT-MNDWI in both watersheds. Based on values of PBIAS, it was evident that the SWAT model underestimated flows in both watersheds, while the other two VSA models over-estimated flows. The highest values of RMSE were recorded by the SWAT model for all cases considered. Overall results indicated that the SWAT-MNDWI model performed best in simulating daily streamflows at the outlets of both watersheds probably on account of more accurate identification of source areas from satellite imagery.

Analysis of spatially and temporally averaged annual water balance components simulated by the three models for the two watersheds indicated that the evapotranspiration loss was between 44% to 48% of rainfall for the Hemavathi watershed. However, unreasonably low evapotranspiration losses (27% to 32% of rainfall) were obtained for the Harangi watershed probably because evapotranspiration computation in the SWAT framework may not be accurate enough for deep rooted forests. As a consequence, water yields (WY) as a percentage of rainfall were low in the Hemavathi watershed and high in the Harangi watershed. The conventional SWAT model yielded the highest values of surface runoff (SURQ) and lowest values of groundwater contributions to streamflow (GWQ), whereas the converse was true in the case of the other two models based on VSA.

Spatial patterns of surface runoff produced during a specific rainfall event by all three models were mapped separately for the two sub-watersheds within the Hemavathi and Harangi watersheds. Expectedly, the SWAT model owing to the use of infiltration-excess mechanism yielded surface runoff from all parts of the sub-watersheds. The models based on VSA theory, however, produced surface runoff mostly from areas located adjacent to the drainage network and little or no runoff from a major part of the sub-watersheds. Although, no field data was available to validate these findings, it still raises the important issue of different spatial patterns of runoff generation yielding almost the same water yield at the outlet. Since previous studies in similar watersheds in the Western Ghats region have identified VSA as a dominant mechanism of runoff generation, the spatial patterns obtained with the SWAT-VSA and SWAT-MNDWI models provide information which will prove to be extremely useful in soil and water conservation measures and in identifying source areas of non-point pollution.

The SWAT-MNDWI model proposed in this study is particularly attractive since it employs satellite imagery to accurately identify areas of different wetnesses within the watershed and integrates this information into a distributed hydrological model. As the results of this study have demonstrated, such a modelling approach using VSA hydrology provides an accurate and convenient tool for distributed hydrologic modelling and impact assessment of LU/LC changes in humid tropical watersheds.

CHAPTER 6

UNCERTAINTY ANALYSIS

6.1 GENERAL

The hydrological models used in the present study – SWAT, SWAT-VSA and SWAT-MNDWI models seek to simulate natural hydrological processes at basin or sub basin scale. As pointed out in Section (1.4), simulation modeling invariably leads to considerable uncertainty in model predictions due to a number of sources of error. All modeling studies must therefore quantify such uncertainties in predictions and provide the user, the information regarding the confidence with which model results may be used.

Hence, in the present chapter, uncertainty analysis of the SWAT, SWAT-VSA and SWAT-MNDWI models was carried out using two different techniques: i) Generalized Likelihood Uncertainty Estimation (GLUE) and ii) Sequential Uncertainty Fitting (SUFI-2) techniques. Details of the techniques and uncertainty results obtained for the Hemavathi and Harangi watersheds are presented in following sections.

6.2 SWAT-CUP TOOL

The SWAT-CUP (SWAT Calibration and Uncertainty Programs) tool has been used to integrate various calibration/uncertainty analysis procedures for SWAT model in a single user interface. It enables sensitivity analysis, calibration, validation, and uncertainty analysis of SWAT model. SWAT-CUP tool provides a rapid methodology for performing time consuming calibration operations and standardized calibration steps. The SWAT-CUP 2012 supports uncertainty analysis techniques of GLUE, SUFI-2, PSO, ParaSol, and MCMC. In this study GLUE and SUFI-2 uncertainty analysis techniques were used. GLUE and SUFI-2 uncertainty analysis techniques have been discussed previously by Beven and Binley (1992) and Abbaspour et al. (2004) respectively but are briefly described here for the sake of completeness

6.2.1 Generalized Likelihood Uncertainty Equation

GLUE is motivated by sampling and regional sensitivity analysis of hydrological modeling. GLUE assumes that, in the case of large over-parameterized models, there is no unique set of parameters, which optimizes goodness-of fit criteria. The sources of uncertainties associated with the input, model structure and its parameters are accounted through parameter uncertainty (Beven and Binley, 1992). Parameter uncertainty is described as a set of discrete behavioural parameter sets with corresponding likelihood weights. The following steps are used in the GLUE uncertainty analysis as described by (Yang et al., 2008):

- 1) After the detection of the generalized likelihood measure $L(\theta)$, a large number of parameter sets are randomly sampled from prior distribution and each parameter set is assessed as either behavioural or non-behavioural through a comparison of the likelihood measured with a selected threshold value.
- 2) Each behavioural parameter set is given a likelihood weight according to

$$W_i = \frac{L(\theta_i)}{\sum_{k=1}^N L(\theta_k)} \quad (6.1)$$

where N is the number of behavioural parameter sets.

- 3) The uncertainty is described by quantile of the cumulative distribution realized from the weighted behavioural parameter sets. In the literature, the most frequently used likelihood measure for GLUE is the Nash–Sutcliffe efficiency (E_{NS}), which is also used in the SWAT-CUP program

$$E_{NS} = 1 - \frac{\sum_{t_i=1}^n (y_{t_i}^m(\theta) - y_{t_i})^2}{\sum_{t_i=1}^n (y_{t_i} - \bar{y})^2} \quad (6.2)$$

where n is the number of the observed data points, y_{t_i} and $y_{t_i}^m(\theta)$ represents the observation and model simulation with parameters θ at time t_i respectively and \bar{y} is the average value of the observations.

6.2.2 Sequential Uncertainty Fitting algorithm

Similar to GLUE, SUFI-2 also accounts for all sources of uncertainties through parameter uncertainty in the hydrological modeling. The degree to which all uncertainties are accounted for is quantified by measuring P-factor, which is the percentage of observed data bracketed by the 95% prediction uncertainty (95PPU) (Abbaspour et al., 2007). Another measure quantifying the strength of an uncertainty analysis is the R-factor, which is the average thickness of the 95PPU band divided by the standard deviation of the measured data. The efficiency of the calibration uncertainty is evaluated on the basis of closeness of the P-factor to 100% and R-factor to 1. The following procedure is used in the SUFI-2 uncertainty analysis (Yang et al., 2008):

- 1) The objective function $g(\theta)$ and parameter ranges $[\theta_{\text{abs min}}, \theta_{\text{abs max}}]$ are defined.
- 2) A Latin Hypercube sampling is carried out in the hypercube $[\theta_{\text{min}}, \theta_{\text{max}}]$, the corresponding objective functions are evaluated, and the sensitivity matrix J and the parameter covariance matrix C are calculated employing equations

$$J_{ij} = \frac{\Delta g_i}{\Delta \theta_j}, \quad i = 1, \dots, C_2^m, j = 1, \dots, n, \quad (6.3)$$

$$C = S_g^2 (J^T J)^{-1} \quad (6.4)$$

- 3) A 95% predictive interval of parameter θ_j is computed as follows

$$\theta_{j,\text{lower}} = \theta_j^* - t_{v,0.975} \sqrt{C_{jj}}, \quad \theta_{j,\text{upper}} = \theta_j^* + t_{v,0.025} \sqrt{C_{jj}} \quad (6.5)$$

where θ_j^* is the parameter θ_j for the best estimates and v is the degrees of freedom ($m-n$).

- 4) The 95PPU is calculated and then P-factor and R-factor are calculated

$$R \cdot \text{factor} = \frac{\frac{1}{n} \sum_{t_i=1}^n (y_{t_i,97.5\%}^M - y_{t_i,2.5\%}^M)}{\sigma_{\text{obs}}} \quad (6.6)$$

where $y_{t_i,97.5\%}^M$ and $y_{t_i,2.5\%}^M$ represent the upper and lower boundary of 95PPU and σ_{obs} stands for the standard deviation of the observed data.

The goodness of calibration and prediction uncertainty is judged on the basis of the closeness of the p-factor to 100% (i.e., all observations bracketed by the prediction uncertainty) and the r-factor to 1 (i.e., achievement of a rather small uncertainty band). As all uncertainties in the model and inputs are reflected in the measurements, bracketing most of the measured data in the prediction 95PPU ensures that all uncertainties are depicted by the parameter uncertainties. If the P-factor and R-factor have satisfactory values, then a uniform distribution in the parameter hypercube $[\theta_{\min}, \theta_{\max}]$ is interpreted as the posterior parameter distribution. Otherwise, $[\theta_{\min}, \theta_{\max}]$ is updated according to (Yang et al., 2008):

$$\begin{aligned}\theta_{j,\min,\text{new}} &= \theta_{j,\text{lower}} - \max\left(\frac{\theta_{j,\text{lower}} - \theta_{j,\min}}{2}, \frac{\theta_{j,\max} - \theta_{j,\text{upper}}}{2}\right) \\ \theta_{j,\max,\text{new}} &= \theta_{j,\text{upper}} - \max\left(\frac{\theta_{j,\text{lower}} - \theta_{j,\min}}{2}, \frac{\theta_{j,\max} - \theta_{j,\text{upper}}}{2}\right)\end{aligned}\quad (6.7)$$

and another iteration is performed. SUFI-2 allows its users several choices of the objective function. In this study, E_{NS} efficiency is selected for the sake of comparison with GLUE technique.

6.3 RESULTS AND DISCUSSION

6.3.1 Sensitivity Analysis Using GLUE and SUFI-2

Sensitive analysis results discussed in Section 5.5.1, indicated that five parameters of the SWAT-MNDWI, SWAT-VSA and SWAT models were found to be sensitive with regard to simulating streamflow of the Hemavathi and Harangi watersheds. The five sensitive parameters are Alpha_Bf, CN₂, Gwqmn, Sol_Awc and Esco. These five parameters were considered for performing uncertainty analysis of the three models using GLUE and SUFI-2 techniques. By choosing optimal sensitive parameters, time consuming calibration operations can be speeded up.

For the Hemavathi watershed, the relative sensitivity values of the parameters are shown in Table 6.1 in terms of t-stat and P-value for both techniques. It can be seen that in both techniques, with P-value equal to zero, CN_2 and Sol_Awc are more sensitive in comparison with other parameters for all models. Similarly for the Harangi watershed, differences in parameter relative sensitivity of the three models for both the techniques are shown in Table 6.2. As in the previous case, CN_2 and Sol_Awc are important parameters. Alpha_Bf also proved to be an important parameter with P-value equal to zero for all models.

The scatter plots shown in Fig. 6.1 to 6.4 demonstrate that for each parameter, solutions with equally good values of the E_{NS} efficiency can be found within the complete prior range of the GLUE and SUFI-2 for all models. Moderate levels of good simulation can be found for both the techniques with E_{NS} efficiency above 0.70. Also, these plots clearly show that there is no single optimum parameter, but many parameter sets can provide similar E_{NS} efficiency values.

Table 6.1 Parameter sensitivities for Hemavathi Watershed

Parameter	SWAT -MNDWI				SWAT -VSA				SWAT			
	GLUE		SUFI-2		GLUE		SUFI-2		GLUE		SUFI-2	
	t-stat	P-value	t-stat	P-value	t-stat	P-value	t-stat	P-value	t-stat	P-value	t-stat	P-value
CN ₂	-42.64	0	-42.03	0	-25.268	0	-24.9	0	-55.312	0	-56.2	0
Esco	-2.8	0.005	-3.111	0.002	-2.155	0.031	-2.632	0.009	-1.126	0.261	-1.172	0.241
Gwqmn	-0.182	0.855	-0.638	0.527	-0.611	0.5415	-0.764	0.445	-0.153	0.878	-1.371	0.241
Alpha_Bf	-0.005	0.996	0.798	0.425	1.382	0.167	2.282	0.23	-0.716	0.474	0.658	0.51
Sol_Awc	10.29	0	12.06	0	10.528	0	11.464	0	6.452	0	7.923	0

Table 6.2 Parameter sensitivities for Harangi Watershed

Parameter	SWAT -MNDWI				SWAT -VSA				SWAT			
	GLUE		SUFI-2		GLUE		SUFI-2		GLUE		SUFI-2	
	t-stat	P-value	t-stat	P-value	t-stat	P-value	t-stat	P-value	t-stat	P-value	t-stat	P-value
CN ₂	-25.99	0	-22.94	0	11.89	0	11.34	0	-47.619	0	-42.142	0
Esco	-2.07	0.038	-2.77	0.005	-1.868	0.062	-1.893	0.589	-1.753	0.08	-2.483	0.013
Gwqmn	-1.21	0.223	-0.468	0.639	-1.14	0.254	-0.147	0.886	-0.914	0.36	-0.773	0.439
Alpha_Bf	7.42	0	7.3	0	16.36	0	14.867	0	6.62	0	6.452	0
Sol_Awc	9.61	0	10.14	0	1.632	0	0.1748	0	6.73	0	7.365	0

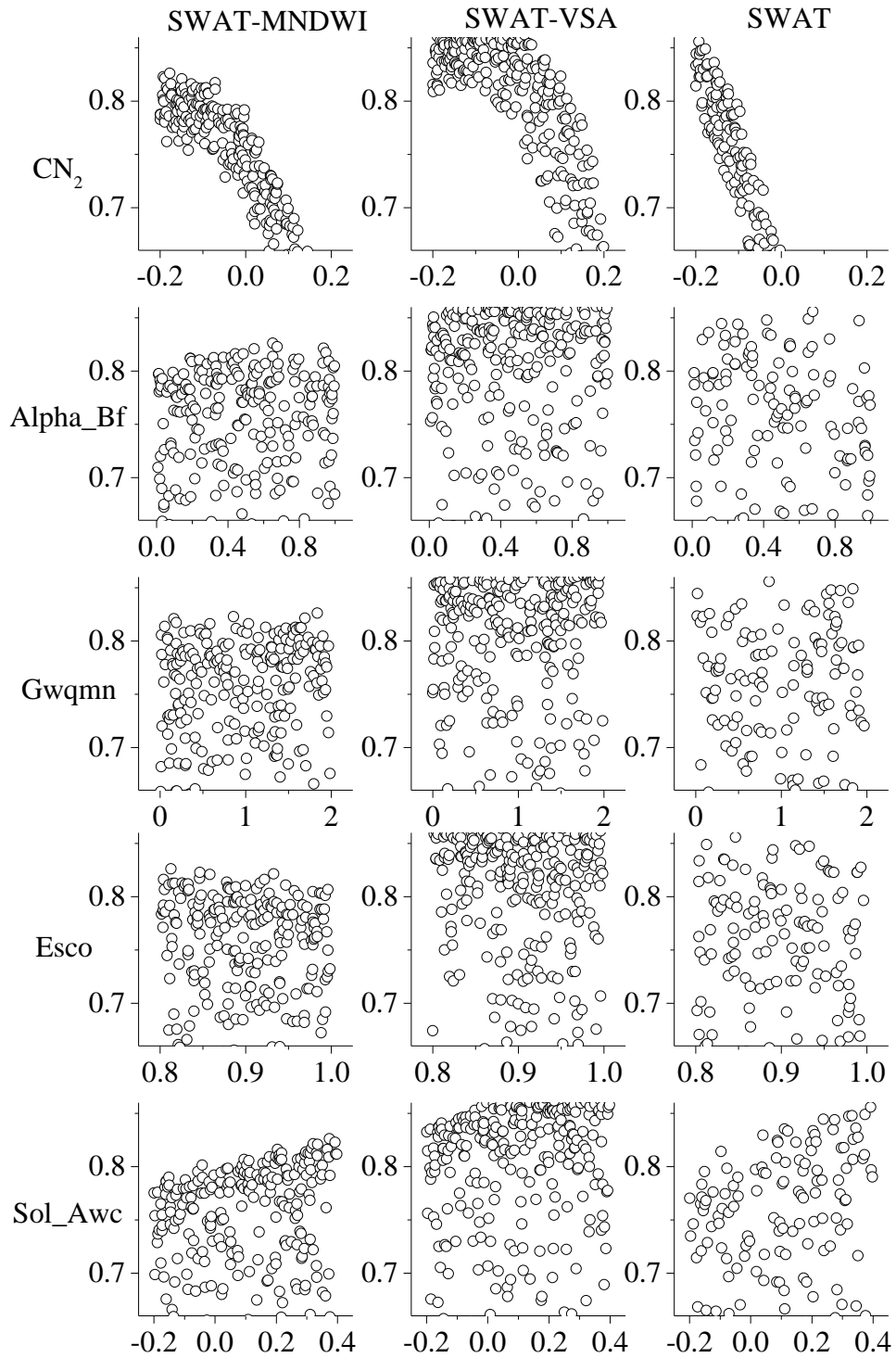


Fig. 6.1 Scatter plots of E_{NS} efficiency (y-axis) against each aggregate SWAT parameter (x-axis) conditioning with GLUE for Hemavathi watershed

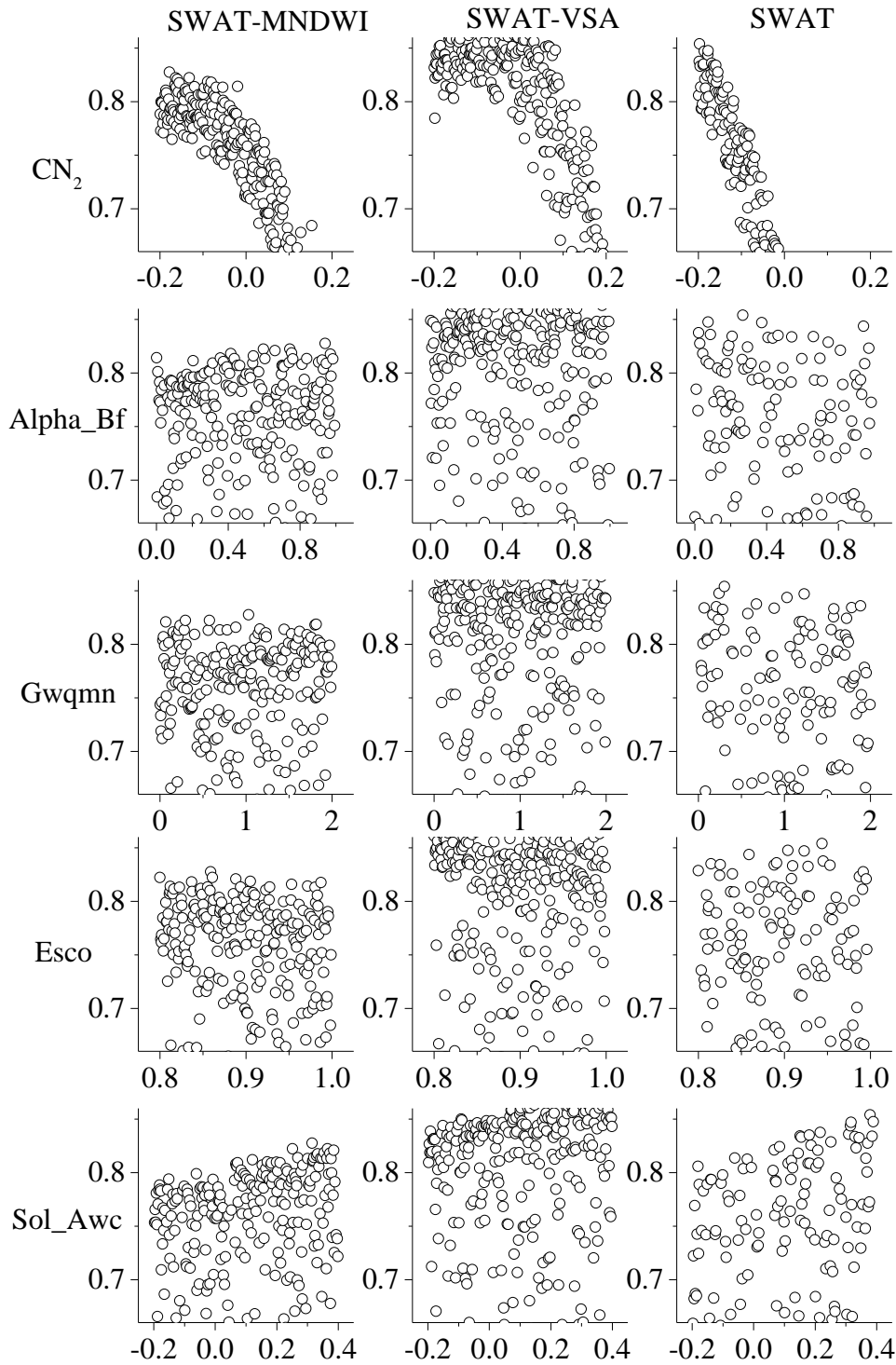


Fig. 6.2 Scatter plots of E_{NS} efficiency (y-axis) against each aggregate SWAT parameter (x-axis) conditioning with SUFI-2 for Hemavathi watershed

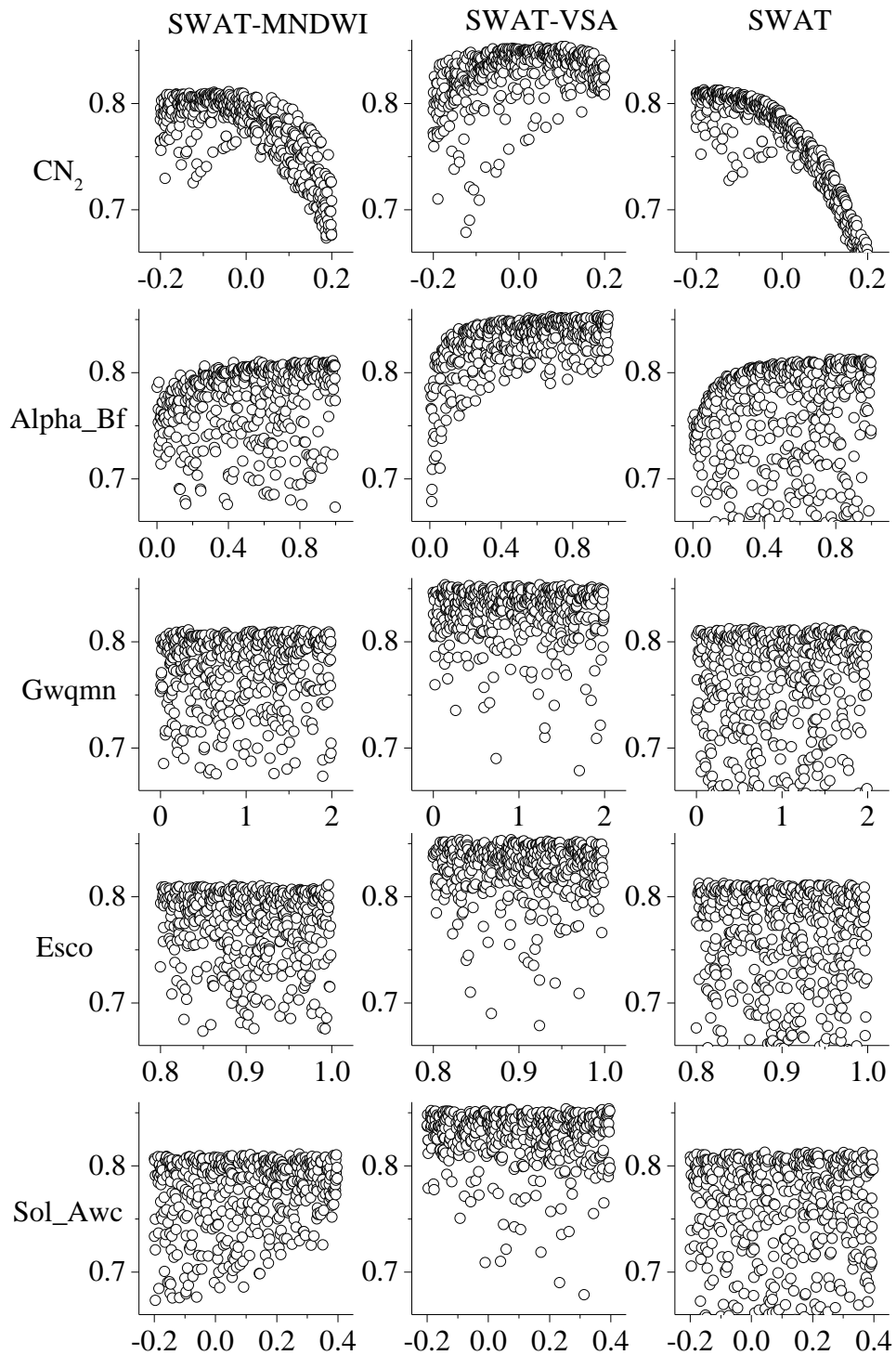


Fig. 6.3 Scatter plots of E_{NS} efficiency (y-axis) against each aggregate SWAT parameter (x-axis) conditioning with GLUE for Harangi watershed

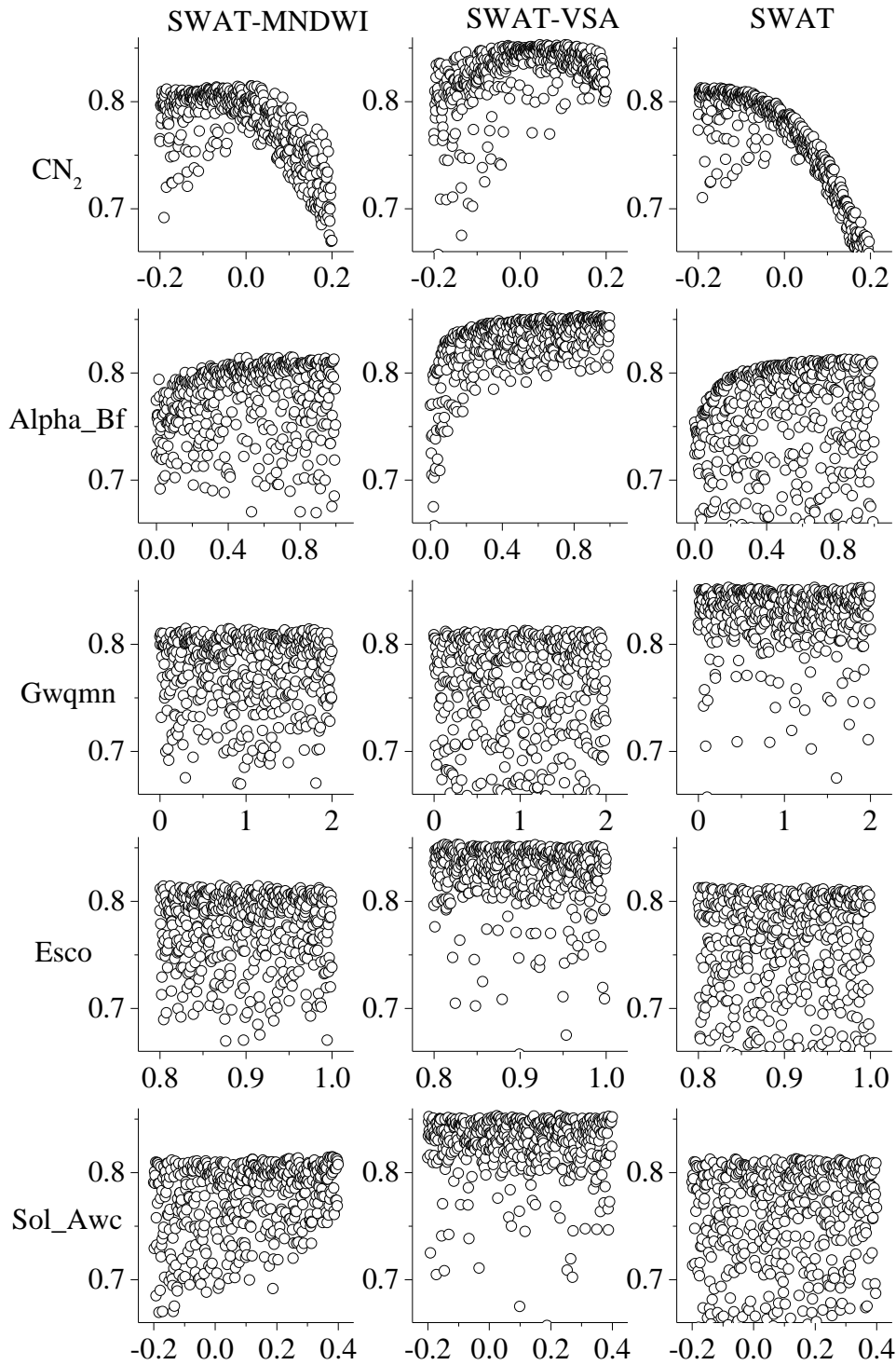


Fig. 6.4 Scatter plots of E_{NS} efficiency (y-axis) against each aggregate SWAT parameter (x-axis) conditioning with SUFI-2 for Harangi watershed

6.3.2 Uncertainty Analysis Using GLUE and SUFI-2

GLUE and SUFI-2 techniques were used for calibration and uncertainty analysis of the SWAT, SWAT-VSA and SWAT-MNDWI models using daily observed inflow data of Hemavathi dam for Hemavathi watershed and Harangi dam for Harangi watershed for the period January 01, 2000 to December 31, 2003. Daily observed inflow data from January 01, 2004 to December 31, 2006 was used to validate the models. Model performances evaluated using four statistical measures: P-factor, R-factor, E_{NS} and R^2 are shown both for calibration and validation phases in Table 6.3 and 6.4. The comparison between the observed and simulated streamflow indicated that there is a good agreement between the observed and simulated streamflow which was verified by higher values of R^2 and E_{NS} . Figs. 6.5 to 6.8 show the time series graphs for observed and simulated streamflow (m^3/s) with the 95% prediction uncertainty (95PPU) band for the GLUE and SUFI-2. From these figures it is noticed that during the calibration and validation phase, observed streamflow is simulated reasonably well by all three model versions for both Hemavathi and Harangi watersheds. From the values of P-factor and R-factor shown in Table 6.3 and 6.4, it should be noted that both GLUE and SUFI-2 cannot accurately quantify the uncertainty of prediction by SWAT-MNDWI, SWAT-VSA and SWAT models. Overall results indicated that the GLUE technique applied on the SWAT-MNDWI model performed best in quantifying the prediction uncertainty of streamflow at the outlets of both watersheds.

In the case of Hemavathi watershed, GLUE results indicated that the P-factor which is the percentage of observations bracketed by the 95% prediction uncertainty (95PPU), brackets 52% and 48% of the observation and R-factor value of 0.38 and 0.35 during calibration and validation periods respectively for SWAT-MNDWI model. For the Harangi watershed, GLUE results indicated that the P-factor brackets 56% and 52% of the observation and R-factor value of 0.42 and 0.41 during calibration and validation periods respectively for SWAT-MNDWI model.

Table 6.3 Performance evaluation criteria for the three models during calibration and validation for Hemavathi Watershed

Phase	Statistical Criteria	GLUE			SUFI-2		
		SWAT-MNDWI	SWAT-VSA	SWAT	SWAT-MNDWI	SWAT-VSA	SWAT
Calibration	P-factor (%)	52	54	59	56	59	60
	R-factor	0.38	0.40	0.39	0.36	0.38	0.35
	R ²	0.85	0.83	0.82	0.85	0.82	0.81
	E _{NS}	0.84	0.81	0.81	0.83	0.80	0.80
Validation	P-factor (%)	48	48	53	62	57	65
	R-factor	0.35	0.38	0.34	0.35	0.40	0.36
	R ²	0.86	0.82	0.78	0.85	0.81	0.78
	E _{NS}	0.85	0.81	0.77	0.84	0.81	0.78

Table 6.4 Performance evaluation criteria for the three models during calibration and validation for Harangi Watershed

Phase	Statistical Criteria	GLUE			SUFI-2		
		SWAT-MNDWI	SWAT-VSA	SWAT	SWAT-MNDWI	SWAT-VSA	SWAT
Calibration	P-factor (%)	56	43	51	55	47	48
	R-factor	0.42	0.35	0.32	0.32	0.33	0.30
	R ²	0.86	0.84	0.81	0.85	0.84	0.81
	E _{NS}	0.85	0.83	0.80	0.83	0.82	0.80
Validation	P-factor (%)	52	48	51	52	45	53
	R-factor	0.41	0.39	0.40	0.39	0.32	0.38
	R ²	0.84	0.84	0.82	0.84	0.85	0.82
	E _{NS}	0.83	0.83	0.81	0.82	0.84	0.81

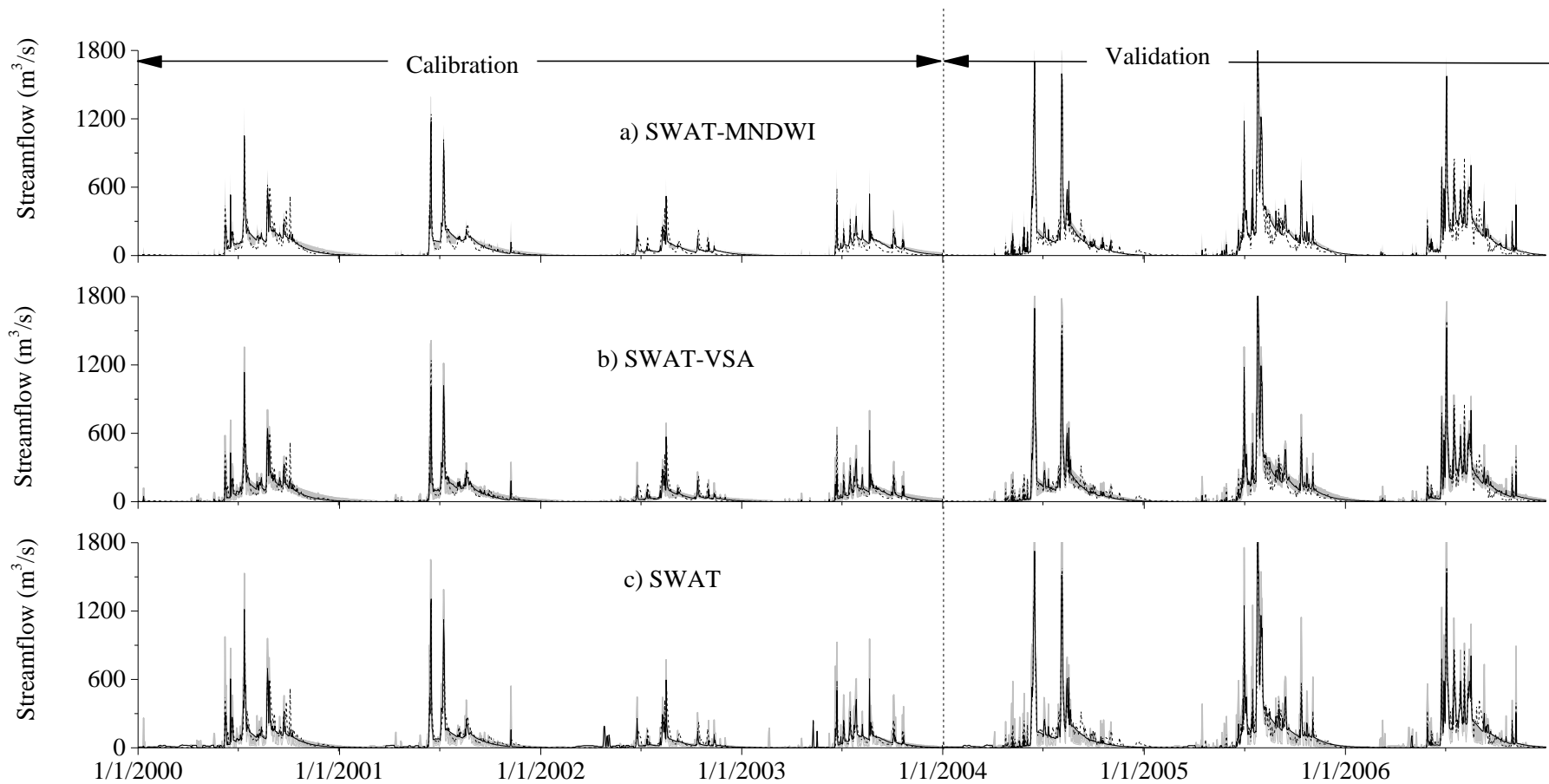


Fig. 6.5 95PPU (shaded area) derived by GLUE during calibration and validation period. The black dash line corresponds to the observed discharge at the outlet, while the black solid line represents the best simulation obtained for Hemavathi watershed

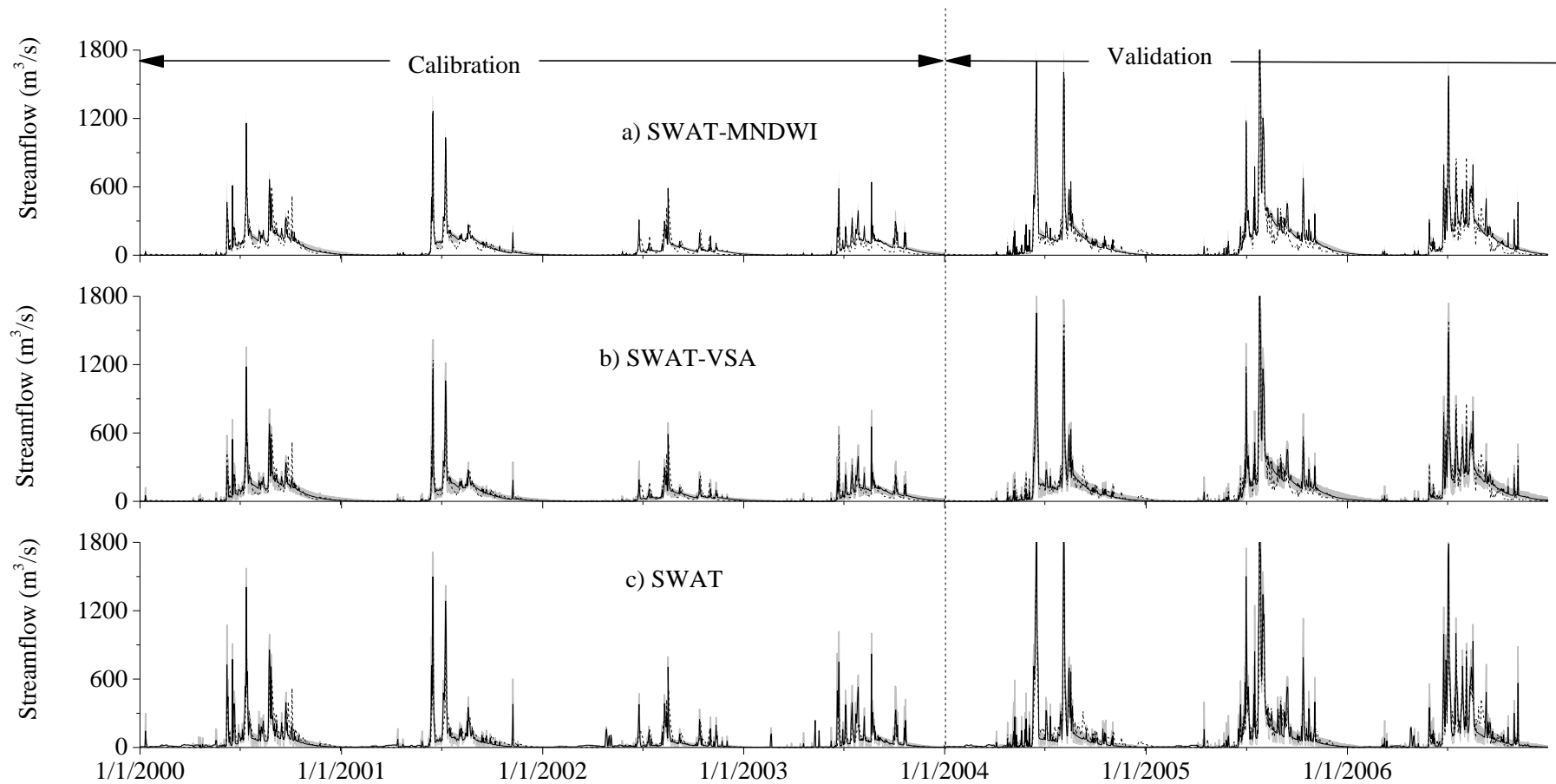


Fig. 6.6 95PPU (shaded area) derived by SUFI-2 during calibration and validation period. The black dash line corresponds to the observed discharge at the outlet, while the black solid line represents the best simulation obtained for Hemavathi watershed

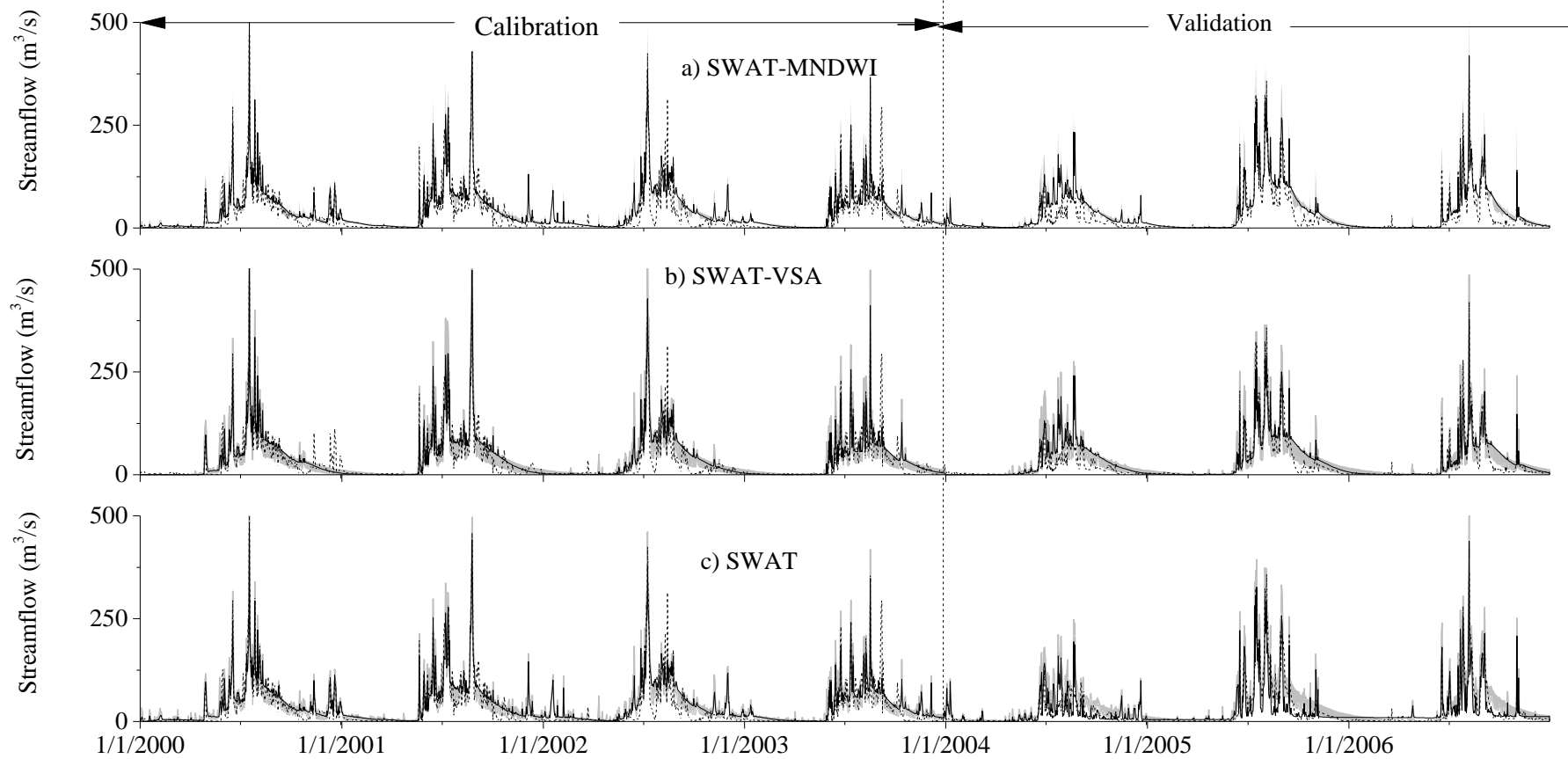


Fig. 6.7 95PPU (shaded area) derived by GLUE during calibration and validation period. The black dash line corresponds to the observed discharge at the outlet, while the black solid line represents the best simulation obtained for Harangi watershed

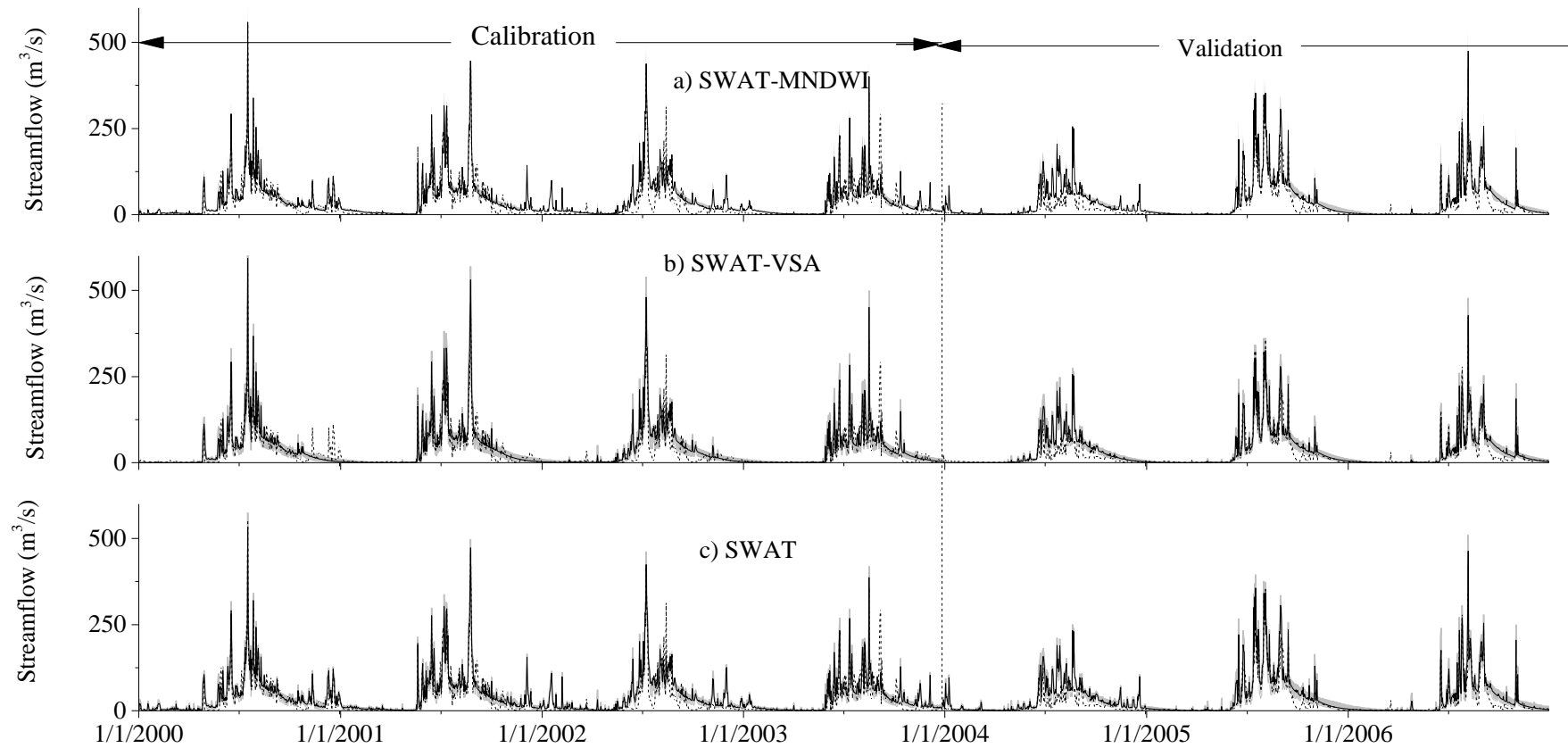


Fig. 6.8 95PPU (shaded area) derived by SUFI-2 during calibration and validation period. The black dash line corresponds to the observed discharge at the outlet, while the black solid line represents the best simulation obtained for Harangi watershed

6.4 SUMMARY AND CONCLUSIONS

Uncertainty analysis of SWAT-MNDWI, SWAT-VSA and SWAT models was performed for the Hemavathi and Harangi watersheds. Among the many uncertainty analysis methods that have been introduced in hydrologic modeling, GLUE and SUFI-2 technique were applied to infer the uncertainty of parameters of SWAT-MNDWI, SWAT-VSA and SWAT models, and to estimate the uncertainty interval of the simulated daily streamflow at the Hemavathi and Harangi watershed outlets. The comparative assessment focused specifically on sensitivity of model parameters and accuracy of daily streamflow predictions at the watershed outlets.

Sensitivity analysis indicated that for both the techniques, CN_2 and Sol_Awc are more sensitive in comparison with other parameters for all models for the Hemavathi watershed. For the Harangi watershed CN_2 and Sol_Awc were the important parameters while $Alpha_Bf$ also proved to be an important parameter with P-value equal to zero for all models.

The results show that GLUE performance was slightly better than SUFI-2 technique for all models for both the watersheds during calibration and validation periods. The 95PPU estimated by the GLUE and SUFI-2 techniques are very close to each other and larger than 45% (P-factor) for all models for both the watersheds during calibration and validation periods. For GLUE, R-factor during the validation phase in the Hemavathi watershed were 0.35, 0.38 and 0.34 for the SWAT-MNDWI, SWAT-VSA and SWAT models respectively with corresponding values in the Harangi watershed being 0.41, 0.39 and 0.40. The Nash-Sutcliffe efficiency values (E_{NS}) estimated by GLUE and SUFI-2 are more than 0.77 and coefficient of determination (R^2) are more than 0.77. It should be noted that that both GLUE and SUFI-2 cannot accurately quantify the prediction uncertainty of SWAT-MNDWI, SWAT-VSA and SWAT models. Overall results indicated that the GLUE technique applied on the SWAT-MNDWI model performed best in quantifying the prediction uncertainty of streamflow at the outlets of both watersheds.

CHAPTER 7

HYDROLOGIC RESPONSES TO LAND COVER CHANGES

7.1 GENERAL

Hydrologic responses to actual LU/LC were examined in Chapter 5 by applying SWAT-MNDWI, SWAT-VSA and SWAT models to Hemavathi and Harangi watersheds. However, as pointed out in Section (1.6), anthropogenic activities can result in LU/LC changes which in turn can affect the hydrologic components like surface runoff, lateral flow and ground water contributions to stream and also soil water content and actual evapotranspiration. In this regard, it is necessary to assess the spatial variations of hydrologic components resulting from LU/LC changes. Hence, this chapter concentrates on quantifying the changes in hydrologic components under two hypothetical LU/LC change scenarios using SWAT-MNDWI, SWAT-VSA and SWAT models for Hemavathi and Harangi watersheds.

7.2 LU/LC CHANGE SCENARIOS

The dominant land use type in the Hemavathi watershed is agriculture (72.50%) in the Harangi watershed it is forest (53.52%) (Tables 5.1 and 5.2). Keeping the existing land cover distribution in mind, two different hypothetical scenarios were formulated for the purpose of simulating the impact of LU/LC changes on hydrologic responses. In both the scenarios, the area of one of the land cover types was assumed to remain unchanged from the existing value, whereas the other land cover types were assumed to increase by adding pasture and grass land. Table 7.1 summaries the two scenarios for impact assessment of LU/LC changes on hydrologic responses using the three models for both Hemavathi and Harangi watersheds. Fig. 7.1 and 7.2 show maps of hypothetical LU/LC scenarios I and II for Hemavathi and Harangi watersheds respectively. All three models were applied to the two watersheds with these LU/LC distributions using procedures described in Chapter 5.

Table 7.1 Hypothetical scenarios for impact assessment of LU/LC changes on hydrologic responses for Hemavathi and Harangi watersheds

Scenarios	LU/LC Change	Hemavathi Watershed		Harangi Watershed	
		Unchanged area (km ²)	Changed area (km ²)	Unchanged area (km ²)	Changed area (km ²)
	Forest cover				
	unchanged while		2156.65		177.08
Scenario I	pasture and grass	439.11	+138.67	288.38	+47.36
	land replaced by agricultural land		=2295.32		=224.44
	Agricultural land				
	unchanged while		439.11		288.38
Scenario II	pasture and grass	2156.65	+138.67	177.08	+47.36
	land replaced by forest cover		=577.78		=335.74

7.3 FLOW DURATION CURVES

The impact on streamflow regime due to changes in LU/LC can be conveniently depicted using Flow Duration Curves (FDC). It is an important signature of the hydrologic response of the catchment and can also be used in a variety of hydrologic analyses related to design and operation of water use/ control structures. The FDC for a catchment provides a graphical and statistical summary of the stream flow variability at a given location, with the shape being determined by rainfall pattern, catchment size and the physiographic characteristics of the catchment. A FDC is a plot of discharge against the percent of time the flow is equalled or exceeded. The construction of a FDC using the streamflow observations can be performed through non-parametric plotting position formulae method. The method consists of following steps:

- a) The observed streamflows are ranked to produce a set of ordered streamflows from the largest to the smallest observations, respectively;

- b) Each ordered streamflow is then plotted against its corresponding duration.
- c) The percentage probability of the flow magnitude being equalled or exceeded is calculated using the formula,

$$P_e = \left(\frac{m}{(N+1)} \right) * 100 \quad (7.1)$$

where, m = rank given to the ordered streamflows

N = sample length or total number of streamflows

P_e = percentage probability of the flow magnitude being equalled or exceeded.

- d) The plot of discharge (Q) and P_e is the Flow Duration Curve.

Streamflows were then subject to frequency analysis to obtain flow quantiles at 10% duration intervals in the range 10% - 90%. Derived flow quantiles were used to fit an equation of the following form to obtain the FDC.

$$Q = ae^{-bP_e} \quad (7.2)$$

where, Q is the streamflow rate m^3/s , P_e is the percentage time Q is equalled or exceeded. a , b are shape parameters of FDC which are related to the catchment characteristics

Also, two commonly adopted indices which may be derived from the flow quantiles are:

High flow index (HFI) = (Q_{10}/Q_{50})

Low flow index (LFI) = (Q_{90}/Q_{50})

While the HFI is used to characterize the relative magnitudes of peak flow (Q_{10}) with reference to the median flow (Q_{50}), the LFI characterizes relative magnitudes of low flow (Q_{90}) and the median flow.

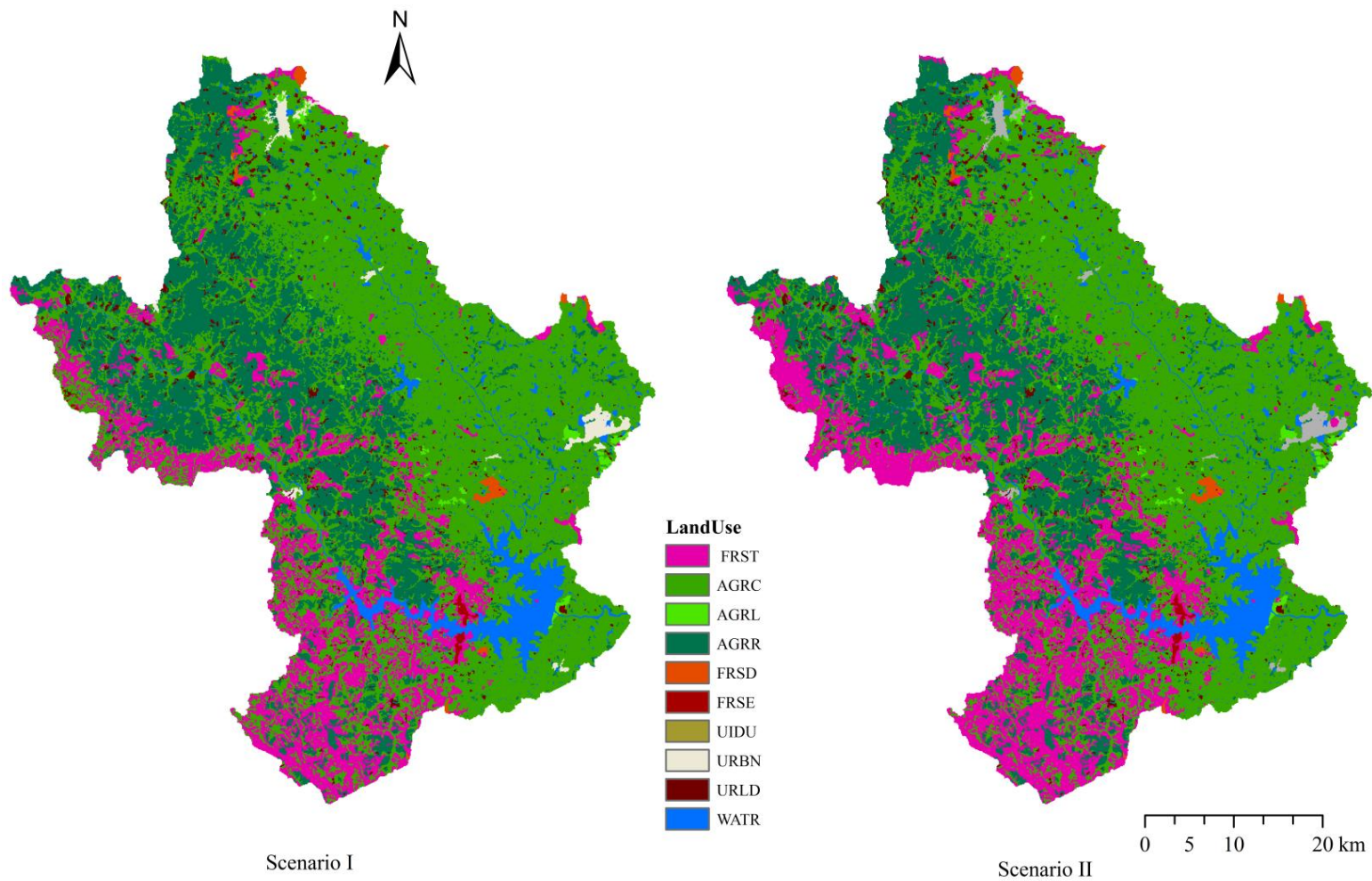


Fig. 7.1 Hypothetical LU/LC change scenario I and II for Hemavathi watershed

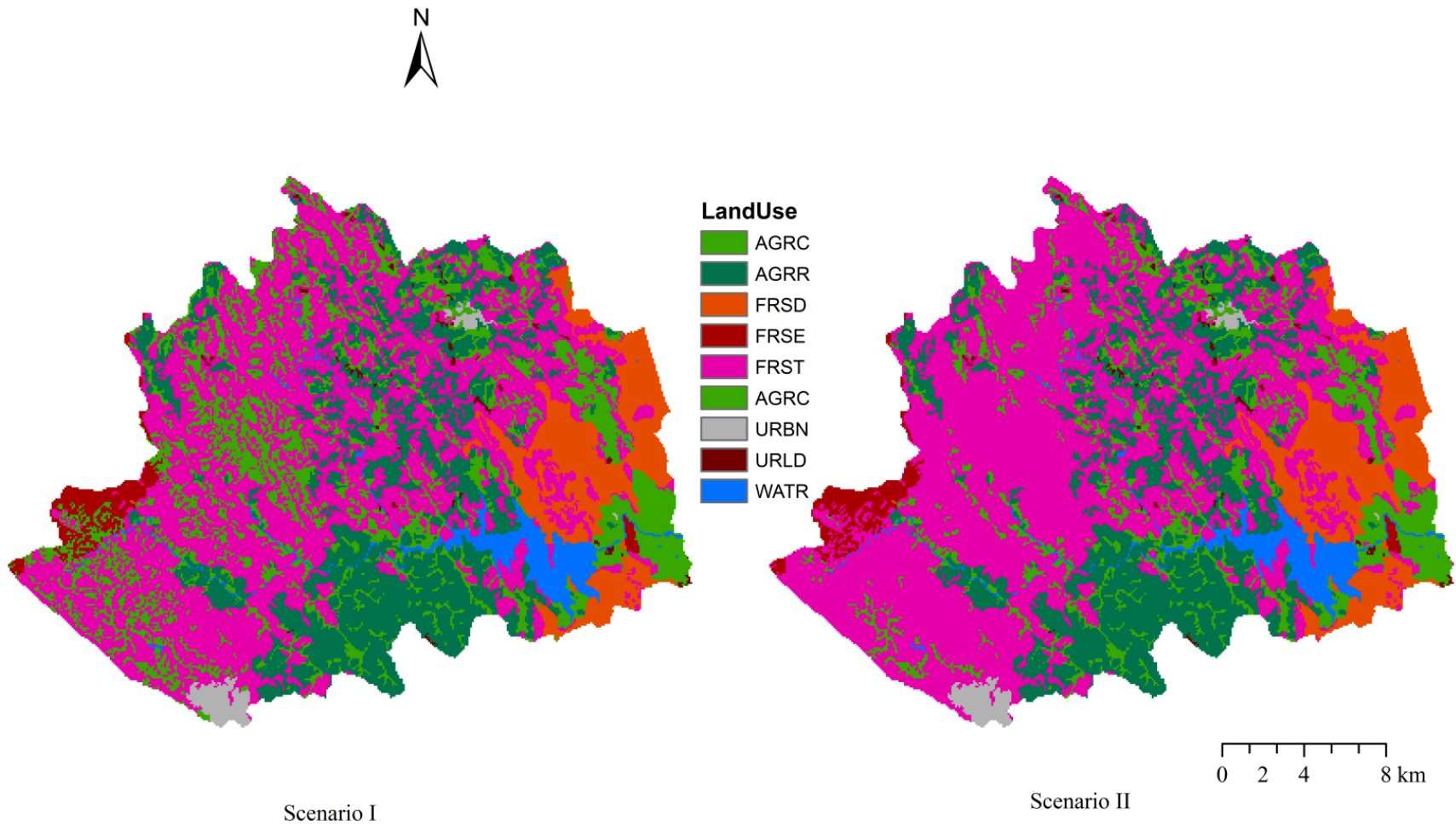


Fig. 7.2 Hypothetical LU/LC change scenario I and II for Harangi watershed

7.4 RESULTS AND DISCUSSION

7.4.1 Effects of LU/LC Change on Hydrologic Responses

Tables 7.2 to 7.5 show the distribution of water balance components simulated by SWAT, SWAT-VSA and SWAT-MNDWI models under the two different hypothetical scenarios as presented in Table 7.1 for Hemavathi and Harangi watersheds. The simulation results obtained from existing LU/LC types (Tables 5.6 and 5.7) were used as reference to compute changes in hydrological variables for the assumed hypothetical LU/LC scenarios.

For the Hemavathi watershed, average (2000-2003) annual water yield increased by 8.24% for scenario I and by 3% for scenario II in comparison to reference results obtained from the SWAT-MNDWI model. Annual water yield from SWAT-VSA for scenario I increased by 3.95% and for scenario II it decreased by 0.79%. Water yield from SWAT scenario I was increased by 3.87% and scenario II decreased by 0.70% respectively. Similarly Table 7.2 and 7.3 summarizes average annual values of other water balance components and their percentage change with respect to reference results obtained the three models for Hemavathi watershed.

For the Harangi watershed, average annual water yield, compared with reference results obtained from the SWAT-MNDWI, for scenarios I and II decreased by 2.03% and 2.76% respectively. For the SWAT-VSA model scenario I resulted in an increase of water yield by 1.12% and for scenario II it decreased by 4.02%. The SWAT model resulted in decreases of water yield by 11.91% and 12.41% for scenarios I and II respectively. Magnitudes of other water balance components and corresponding percentage changes with respect to reference results for the models are summarised in Table 7.4 and 7.5.

Calculations revealed that in the Hemavathi watershed the evapotranspiration loss (ET) was increased by 9.84% of rainfall (P) for scenario I and 10.95% for scenario II, with the corresponding values in the Harangi watershed being increased by 3.21% and 9.95%. The % ET loss of Hemavathi watershed remained somewhat unchanged for both the scenarios I and II, but for the Harangi watershed, % ET loss was significantly higher for scenario II compared to scenario I. Similar scenarios for water balance

components for Indian basins by the SWAT model has been reported in earlier studies (Wagner et al. 2013; Hari Krishna et al. 2014a).

Table 7.2 Distribution of water balance components over the period of 2000-2003 for the Hemavathi watershed using SWAT-MNDWI, SWAT-VSA and SWAT for scenario I

Model		SURQ	LATQ	GWQ	WY	ET	PET
SWAT-MNDWI	(mm)	480	25	477	980	733	1873
Change	(mm)	-31	-7	124	88	80	15
Percent	(%)	-6.90	-38.89	20.63	8.24	9.84	0.79
SWAT-VSA	(mm)	466	27	480	973	733	1873
Change	(mm)	-80	13	107	40	80	15
Percent	(%)	-20.73	32.50	18.23	3.95	9.84	0.79
SWAT	(mm)	560	13	395	968	733	1873
Change	(mm)	-71	-1	72	39	80	15
Percent	(%)	-14.52	-8.33	15.42	3.87	9.84	0.79

Table 7.3 Distribution of water balance components over the period of 2000-2003 for the Hemavathi watershed using SWAT-MNDWI, SWAT-VSA and SWAT for scenario II

Model		SURQ	LATQ	GWQ	WY	ET	PET
SWAT-MNDWI	(mm)	515	26	495	1036	724	1873
Change	(mm)	-66	-8	106	32	89	15
Percent	(%)	-14.70	-44.44	17.64	3.00	10.95	0.79
SWAT-VSA	(mm)	539	27	455	1021	724	1873
Change	(mm)	-153	13	132	-8	89	15
Percent	(%)	-39.64	32.50	22.49	-0.79	10.95	0.79
SWAT	(mm)	591	13	410	1014	724	1873
Change	(mm)	-102	-1	57	-7	89	15
Percent	(%)	-20.86	-8.33	12.21	-0.70	10.95	0.79

Table 7.4 Distribution of water balance components over the period of 2000-2003 for the Harangi watershed using SWAT-MNDWI, SWAT-VSA and SWAT for scenario I

Model		SURQ	LATQ	GWQ	WY	ET	PET
SWAT-MNDWI	(mm)	1072	305	1289	2666	905	2045
Change	(mm)	37	-88	-2	-53	30	90
Percent	(%)	3.34	-40.55	-0.16	-2.03	3.21	4.22
SWAT-VSA	(mm)	1042	289	1225	2556	905	2045
Change	(mm)	39	-64	54	29	30	90
Percent	(%)	3.61	-28.44	4.22	1.12	3.21	4.22
SWAT	(mm)	1015	204	1344	2563	905	2045
Change	(mm)	93	-7	-143	-57	30	90
Percent	(%)	8.39	-3.55	-11.91	-2.27	3.21	4.22

Table 7.5 Distribution of water balance components over the period of 2000-2003 for the Harangi watershed using SWAT-MNDWI, SWAT-VSA and SWAT for scenario II

Model		SURQ	LATQ	GWQ	WY	ET	PET
SWAT-MNDWI	(mm)	1155	285	1245	2685	842	2025
Change	(mm)	-46	-68	42	-72	93	110
Percent	(%)	-4.15	-31.34	3.26	-2.76	9.95	5.15
SWAT-VSA	(mm)	1178	255	1269	2689	842	2025
Change	(mm)	-97	-30	10	-104	93	110
Percent	(%)	-8.97	-13.33	0.78	-4.02	9.95	5.15
SWAT	(mm)	930	220	1350	2508	842	2025
Change	(mm)	178	-23	-149	-2	93	110
Percent	(%)	16.06	-11.68	-12.41	-0.08	9.95	5.15

7.4.2 Effects of LU/LC Change on Streamflow Regime

Results of the scenarios for the 6 cases considered – SWAT-MNDWI, SWAT-VSA and SWAT models applied separately to the Hemavathi and Harangi watersheds are presented in Table 7.6 and 7.7. These tables lists out the optimal values of parameters a & b of the fitted FDC, flow quantiles ranging from Q_{10} to Q_{90} , high flow index and low flow index. The results of scenario I are somewhat similar to the results obtained for scenario 2 for both the watersheds.

Accordingly, considering the Hemavathi watershed first, for all three models it can be seen from the results shown in Table 7.6, when agricultural land or forest cover is increased (scenarios I and II), smaller decrease in high flows takes place as is evident from the values of Q_{10} . This can also be seen from the decrease in HFI values while medium flow quantiles (Q_{40} and Q_{60}) show smaller increases. On the other hand, low flows (Q_{80} and Q_{90}) show increasing trends, a fact evident also from the increase in LFI values. Also, FDC model parameters a & b decrease as agricultural land or forest cover increases.

For the Harangi watershed, for all three models (Table 7.7), when agricultural land or forest cover is increased (scenarios I and II), smaller decrease in high flows takes place as is evident from the values of Q_{10} . This can also be seen from the large decrease in HFI values while medium flow quantiles (Q_{40} and Q_{60}) show significant increases. On the other hand, low flows (Q_{80} and Q_{90}) show smaller increases with LFI values with zeros. Also, FDC model parameters a & b were increases as the agricultural land or forest cover increases.

Overall, it appears that replacing pasture and grass land with agricultural land or forest cover there is a decrease in high flows & HFI and significant increases medium flows in both the watersheds. Similar kind prediction of flow for western Ghats watersheds by the FDC model has been reported in earlier study (Venkatesh 2011).

Table 7.6 Changes in streamflow regime of Hemavathi watershed for different scenarios using SWAT-MNDWI, SWAT-VSA and SWAT Models

Model	Scenarios	FDC Model Parameter		Flow Quantiles for various duration (m ³ /s)									Indices for various duration flows	
		a	b	Q ₁₀	Q ₂₀	Q ₃₀	Q ₄₀	Q ₅₀	Q ₆₀	Q ₇₀	Q ₈₀	Q ₉₀	HFI	LFI
SWAT-MNDWI	Actual	494.56	-0.41	287.90	192.00	148.00	108.10	74.59	53.31	31.56	17.50	9.95	3.86	0.13
	Scenario I	406.29	-0.34	274.20	162.20	135.30	116.30	95.79	67.38	43.41	26.46	13.18	2.86	0.14
	Scenario II	406.02	-0.33	271.30	166.60	139.50	120.30	98.11	70.10	44.81	27.90	14.12	2.77	0.14
SWAT-VSA	Actual	493.60	-0.40	278.20	189.50	150.00	116.80	81.02	52.30	30.75	18.30	10.16	3.43	0.13
	Scenario I	404.85	-0.34	271.20	161.70	135.60	116.70	95.35	67.41	42.84	26.77	13.03	2.84	0.14
	Scenario II	408.49	-0.34	271.70	165.70	139.90	120.40	98.18	69.20	44.35	27.79	13.77	2.77	0.14
SWAT	Actual	445.09	-0.50	272.00	137.30	90.75	65.75	44.49	27.72	15.67	8.74	4.60	6.11	0.10
	Scenario I	441.76	-0.36	268.20	135.30	85.30	68.56	87.62	65.54	42.12	26.18	13.22	3.06	0.15
	Scenario II	437.58	-0.35	266.30	136.50	88.30	72.56	90.08	67.50	43.20	27.88	13.97	3.84	0.16

Table 7.7 Changes in streamflow regime of Harangi watershed for different scenarios using SWAT-MNDWI, SWAT-VSA and SWAT Models

Model	Scenarios	FDC Model Parameter		Flow Quantiles for various duration (m ³ /s)									Indices for various duration flows	
		a	b	Q ₁₀	Q ₂₀	Q ₃₀	Q ₄₀	Q ₅₀	Q ₆₀	Q ₇₀	Q ₈₀	Q ₉₀	HFI	LFI
SWAT-MNDWI	Actual	479.16	-0.94	102.70	58.04	33.09	17.11	6.66	2.47	0.99	0.45	0.03	15.41	0.00
	Scenario I	611.39	-0.92	101.20	65.92	44.23	28.53	14.33	4.74	0.98	0.51	0.04	7.06	0.00
	Scenario II	615.03	-0.92	101.40	66.41	44.77	28.83	14.65	4.80	0.98	0.52	0.04	6.92	0.00
SWAT-VSA	Actual	541.95	-0.10	89.55	54.17	30.21	16.32	6.09	2.10	0.75	0.35	0.01	14.70	0.00
	Scenario I	665.14	-0.98	88.74	60.74	39.82	26.20	13.89	4.43	0.79	0.44	0.02	6.39	0.00
	Scenario II	713.03	-0.99	89.21	61.12	40.20	26.50	14.06	4.50	0.79	0.44	0.01	6.34	0.00
SWAT	Actual	886.15	-1.15	105.70	60.62	34.06	15.66	5.84	1.83	0.52	0.19	0.00	18.09	0.00
	Scenario I	1196.30	-1.13	103.40	67.96	44.67	28.00	14.97	5.16	0.70	0.26	0.00	6.91	0.00
	Scenario II	1201.20	-1.13	103.80	68.26	45.40	28.44	15.14	5.21	0.75	0.27	0.00	6.86	0.00

7.5 SUMMARY AND CONCLUSIONS

The impacts of hypothetical LU/LC changes in the Hemavathi and Harangi watersheds were assessed using SWAT-MNDWI, SWAT-VSA and SWAT models. In addition to calculating the SWAT-MNDWI, SWAT-VSA and SWAT models water balance components for above watersheds, an effort was also made to construct the FDCs using each scenario's streamflow regime. The streamflow regime was characterized by flow duration quantiles and high flow and low flow indices. For the Hemavathi watershed, with increase in agricultural land an increase in water yield is predicted all three models. With increase in forest cover, there is decrease in water yield as simulated by the SWAT-VSA and SWAT models while for SWAT-MNDWI an increase in water yield was predicted. For the Harangi watershed, with increase in agricultural land or forested area there is decrease in water yield for all three models except SWAT-VSA model in scenario I. Both the hypothetical LU/LC scenarios adopted in this study appeared to have the significant impacts on the runoff regime. The results obtained in this study are useful in understanding the impacts of LU/LC changes on water balance components which could promote proper planning and management of LU/LC to protect water resources of the Hemavathi and Harangi watersheds.

CHAPTER 8

CONCLUSIONS

8.1 GENERAL

The major focus of the present study was to evaluate the applicability and performance of the SWAT-MNDWI, SWAT-VSA and SWAT models in the Hemavathi and Harangi watersheds located in the Upper Cauvery Basin, Karnataka, India. The study also analyzed historical records of observed hydroclimatic variables in the region for temporal variability and trends. Also, the uncertainties associated with the predictions from the three hydrological models were quantified and hydrologic responses to hypothetical LU/LC change scenarios were simulated.

Major point-wise conclusions drawn from results obtained are presented herein. For convenience, chapter-wise conclusions are presented. Also, limitations of the study and scope for further studies are enumerated.

8.2 HYDRO METEOROLOGICAL DATA ANALYSIS

The present study examined the significance and magnitude of trends in the rainfall, maximum and minimum temperature and streamflow of the Upper Cauvery Basin. Daily rainfall data was obtained from 33 rain gauge stations for a 30 year historical period. Statistical analysis and trend analysis was performed separately for each rain gauge station and also for areal rainfall for each of the identified sub basins of the Upper Cauvery Basin. Daily maximum and daily minimum air temperature observations made at 6 climate stations and daily streamflow records from 4 gauging stations were also used.

1. As expected, the coefficient of variation (CV) for rainfall in each sub basin indicated large variabilities in the months December to March, while the percentage departure also varied during these months for different decades. But there is no significant trend found in rainfall over the sub basins except for the

Arkavathi sub basin where an increasing trend (0.06 mm/year) was found. For the Upper Cauvery basin as a whole no statistically significant trend in either monthly or annual rainfall was found.

2. Not much variation was observed in daily maximum temperature except in the months of May and June for the Hassan climate station. Statistically significant trend was observed in maximum temperature for Chikmagalur and Hassan stations.
3. The CV of minimum temperature showed a large variability from November to March for all climate stations and also a significant increasing trend for Hassan and Bangalore station, while for Madikeri a decreasing trend was observed with a variation of $-1.92\text{ }^{\circ}\text{C}/\text{year}$.
4. Not much variation was found in streamflow except for K M Vadi gauge site and T.Narasipur gauge site showed a significant decreasing trend with $-9.34\text{ m}^3/\text{s}/\text{year}$.
5. From long range dependence analysis a weak persistence was found for both rainfall and streamflow of the Upper Cauvery basin.

8.3 HYDROLOGICAL MODELING

The following conclusions can be drawn for hydrological modeling of the Hemavathi and Harangi watersheds. In addition to evaluating the performances of the SWAT, SWAT-VSA and SWAT-MNDWI models with respect to estimating temporal variations in streamflow, an effort was also made in the present study to evaluate the spatial variations of runoff generating areas with respect to land use types for Hemavathi and Harangi watersheds.

1. Based on the good performance statistics of the SWAT-MNDWI and SWAT-VSA model, it can be said that wetness indices obtained from remote sensing and DEM were accurate enough to delineate runoff contributing areas. Use of these data sources is recommended for future hydrological modeling in the semi-humid and humid regions.

2. The ability of the three models to simulate daily streamflows at the watershed outlets was reasonably good both in calibration and validation phases. All models proved better at simulating low and medium flows than high flows.
3. The performances of all the models were better for the forested Harangi watershed in comparison to the agricultural Hemavathi watershed, with the performances of the models based on VSA being slightly better than the SWAT model.
4. Nash-Sutcliffe efficiency values (E_{NS}) during the validation phase in the Hemavathi watershed were 0.85, 0.79 and 0.73 for the SWAT-MNDWI, SWAT-VSA and SWAT models respectively with corresponding values in the Harangi watershed being 0.88, 0.86 and 0.86.
5. Overall results indicated that the SWAT-MNDWI model performed best in simulating daily streamflows at the outlets of both watersheds probably on account of more accurate identification of source areas from satellite imagery.
6. Analysis of spatially and temporally averaged annual water balance components simulated by the three models for the two watersheds indicated that the evapotranspiration loss was between 44% to 48% of rainfall for the Hemavathi watershed. However, unreasonably low evapotranspiration losses (27% to 32% of rainfall) were obtained for the Harangi watershed probably because evapotranspiration computation in the SWAT framework may not be accurate enough for deep rooted forests.
7. Water yields (WY) as a percentage of rainfall were low in the Hemavathi watershed and high in the Harangi watershed. The conventional SWAT model yielded the highest values of surface runoff (SURQ) and lowest values of groundwater contributions to streamflow (GWQ), whereas the converse was true in the case of the other two models based on VSA.
8. The spatial patterns of surface runoff generation were somewhat similar for the SWAT-VSA and SWAT-MNDWI models, but completely different for the SWAT model.

9. Overall results of this study have demonstrated that models incorporating VSA hydrology, and in particular the proposed SWAT-MNDWI model, provide accurate and convenient tools for distributed hydrologic modelling in humid tropical watersheds.

8.4 UNCERTAINTY ANALYSIS

The SWAT-CUP tool was used for automatic calibration and uncertainty analysis of developed hydrological models. The following conclusions can be drawn.

1. GLUE and SUFI-2 techniques were implemented to SWAT-MNDWI, SWAT-VSA and SWAT models and applied to Hemavathi and Harangi watersheds. The performance of the above techniques were weak at bracketing uncertainty in the models using 95PPU band.
2. The results show that GLUE performance was slightly better compared to SUFI-2 technique for all models for both the watersheds during calibration and validation periods. The 95PPU estimated by the GLUE and SUFI-2 techniques are very close to each other and larger than 45% (P-factor) for all models for both the watersheds during calibration and validation periods.
3. Overall results indicated that the GLUE technique applied on the SWAT-MNDWI model performed best to quantify the prediction uncertainty of streamflows at the outlets of both watersheds.

8.5 HYDROLOGIC RESPONSES TO LAND COVER CHANGES

The hydrological impacts of hypothetical LU/LC changes in the Hemavathi and Harangi watersheds were assessed using the SWAT-MNDWI, SWAT-VSA and SWAT models. The following conclusions can be drawn for hydrologic responses to land cover changes of the hydrology of the watersheds. In addition to calculating the SWAT-MNDWI, SWAT-VSA and SWAT models average annual water balance components for the watersheds, an effort was also made to construct the FDCs using each change scenario's streamflow regime.

1. For Hemavathi watershed, with increase in agricultural land there is increase in

water yield predicted by all three models. Increase in forest cover leads to decrease in water yield for SWAT-VSA and SWAT models while for SWAT-MNDWI an increase in water yield was found.

2. For Harangi watershed, with increase in agricultural land or forested area there is decrease in water yield for all three models except SWAT-VSA model in scenario I (increase in agricultural land).
3. Both hypothetical LU/LC change scenarios resulted in significant changes in the flow quantiles for both watersheds.
4. Overall, it appears that replacing pasture and grass land with agricultural land or forest cover results in a decrease in high flows and HFI and significant increases in medium flows in both the watersheds.

8.6 LIMITATIONS OF THE STUDY

1. The developed SWAT-MNDWI model was tested only in two watersheds of the Upper Cauvery Basin. Availability of a larger database could have permitted more watersheds to be included in the testing.
2. A major limitation of the study has been with regard to validation of location and extent of Variable Source Areas predicted by the SWAT-VSA and SWAT-MNDWI models. Non-availability of field observations of source areas prevented such a validation from being carried out.
3. Absence of measured vegetation characteristics, soil characteristics and soil moisture content at internal points in the basin and non-availability of direct measurements of other water balance components except streamflow prevented a complete validation of the model predictions from being made.
4. Also in application of the hydrological models, LU/LC distribution has been assumed to be constant over the entire modeling period.
5. For a large basin like Upper Cauvery Basin, rainfall data from only 33 rain gauges and 6 climate stations were used in the trend analysis.

8.7 SCOPE FOR FUTURE STUDIES

1. Detailed field experiments and research can be taken up to map and characterize the VSAs.
2. Water quality, sediment yield, soil nutrient dynamics and non-point source pollution are effected by the nature of variable source areas. Experimental and modeling studies to characterize these issues need to be taken up.
3. Systematic procedures for implementing strategies for controlling non-point source pollution and best management practices need to be established. This may involve identifying the locations where runoff is generated.
4. Replacing wetness index such as STI and MNDWI with any microwave remote sensing derived wetness index in the VSA based hydrological models may be attempted.
5. It is possible to consider predicted changes in the climate conditions and jointly consider land use and climate changes impacts on the hydrologic responses of the watersheds.

REFERENCES

- Abbaspour, K. C., Johnson, C. A., and Van Genuchten, M. T. (2004). "Estimating uncertain flow and transport parameters using a sequential uncertainty fitting procedure." *Vadose Zone J.*, 3, 1340-1352.
- Abbaspour, K. C., Yang, J., Maximov, I., Siber, R., Bogner, K., Mieleitner, J., Zobrist, J., and Srinivasan, R. (2007). "Modelling hydrology and water quality in the pre-alpine/alpine Thur watershed using SWAT." *J. of Hydrol.*, 333, 413-430.
- Adeogun, A. G., Sule, B. F., Salami, A. W., and Daramola, M. O. (2014). "Validation of SWAT model for prediction of water yield and water balance: Case study of Upstream Catchment of Jebba Dam in Nigeria." *Int. J. of Mat, Comp, Phy. and Quantum Eng.*, 86, 264 - 270.
- Ahmadi, M., Arabi, M., Ascough II, J. C., Fontane, D. G., and Engel, B. A. (2014). "Toward improved calibration of watershed models: Multisite multiobjective measures of information." *Environ. Modelling & Software*, 59, 135-145.
- Ajami, N. K., Duan, Q., and Sorooshian, S. (2007). "An integrated hydrologic Bayesian multimodel combination framework: Confronting input, parameter, and model structural uncertainty in hydrologic prediction." *Water Resour. Res.*, 43, W01403.
- Akiner, M. E., and Akkoyunlu, A. (2012). "Modeling and forecasting river flow rate from the Melen Watershed, Turkey." *J. of Hydrol.*, 456–457, 121-129.
- Arabi, M., Govindaraju, R. S., and Hantush, M. M. (2007). "A probabilistic approach for analysis of uncertainty in the evaluation of watershed management practices." *J. of Hydrol.*, 333, 459-471.

- Archer, D. (2003). "Contrasting hydrological regimes in the upper Indus Basin." *J. of Hydrol.*, 274, 198-210.
- Arnold, J. G., Srinivasan, R., Muttiah, R. S., and Williams, J. R. (1998). "Large area hydrologic modeling and assessment part i: model development." *J. Am. Water Resour. Assoc.*, 34, 73-89.
- Athira, P., and Sudheer, K. P. (2014). "A method to reduce the computational requirement while assessing uncertainty of complex hydrological models." *Stoch. Environ. Res. Ris. Assess.*, 1-13.
- Bannwarth, M. A., Huggenschmidt, C., Sangchan, W., Lamers, M., Ingwersen, J., Ziegler, A. D., and Streck, T. (2014). "Simulation of stream flow components in a mountainous catchment in northern Thailand with SWAT, using the ANSELM calibration approach." *Hydrol. Proces.*
- Bartzokas, A., Lolis, C. J., and Metaxas, D. A. (2003). "A study on the intra-annual variation and the spatial distribution of precipitation amount and duration over Greece on a 10 day basis." *Int J. of Climato.*, 23, 207-222.
- Bekele, E. G., and Nicklow, J. W. (2007). "Multi-objective automatic calibration of SWAT using NSGA-II." *J. of Hydrol.*, 341, 165-176.
- Beven, K., and Binley, A. (1992). "The future of distributed models: Model calibration and uncertainty prediction." *Hydrol. Proces.*, 6, 279-298.
- Beven, K., and Freer, J. (2001). "Equifinality, data assimilation, and uncertainty estimation in mechanistic modelling of complex environmental systems using the GLUE methodology." *J. of Hydrol.*, 249, 11-29.
- Beven, K. J. (2001). *Rainfall-runoff modelling: the primer*, John Wiley & Sons.

- Bieger, K., Hörmann, G., and Fohrer, N. (2014). "Detailed spatial analysis of SWAT-simulated surface runoff and sediment yield in a mountainous watershed in China." *Hydrol. Sci. J.*
- Bingner, R. L., Garbrecht, J., Arnold, J. G., and Srinivasan, R. (1997). "Effect of watershed subdivision on simulated runoff and fine sediment yield." *Transactions of the ASAE*, 40, 1329-1335.
- Bitew, M. M., and Gebremichael, M. (2011). "Assessment of satellite rainfall products for streamflow simulation in medium watersheds of the Ethiopian highlands." *Hydrol. and Ear. Sys. Sci.*, 15, 1147-1155.
- Bormann, H., Breuer, L., Gräff, T., Huisman, J. A., and Croke, B. (2009). "Assessing the impact of land use change on hydrology by ensemble modelling (LUCHEM) IV: Model sensitivity to data aggregation and spatial (re-)distribution." *Adv. Water Resour.*, 32, 171-192.
- Bossa, A., Diekkrüger, B., and Agbossou, E. (2014). "Scenario-based impacts of land use and climate change on land and water degradation from the meso to regional scale." *Water*, 6, 3152-3181.
- Boyer, C., Chaumont, D., Chartier, I., and Roy, A. G. (2010). "Impact of climate change on the hydrology of St. Lawrence tributaries." *J. of Hydrol.*, 384, 65-83.
- Brabets, T. P., and Walvoord, M. A. (2009). "Trends in streamflow in the Yukon River Basin from 1944 to 2005 and the influence of the Pacific Decadal Oscillation." *J. of Hydrol.*, 371, 108-119.
- Breuer, L., Huisman, J. A., and Frede, H. G. (2006). "Monte Carlo assessment of uncertainty in the simulated hydrological response to land use change." *Environ Model Assess*, 11, 209-218.

- Burn, D. H., and Hag Elnur, M. A. (2002). "Detection of hydrologic trends and variability." *J. of Hydrol.*, 255, 107-122.
- Calder, I. R., Hall, R. L., and Adlard, P. G. (1992). *Growth and Water Use of Forest Plantations*, John Wiley and Sons, New York (United States).
- Chaubey, I., Cotter, A. S., Costello, T. A., and Soerens, T. S. (2005). "Effect of DEM data resolution on SWAT output uncertainty." *Hydrol. Proces.*, 19, 621-628.
- Chen, F., Crow, W. T., Starks, P. J., and Moriasi, D. N. (2011). "Improving hydrologic predictions of a catchment model via assimilation of surface soil moisture." *Adv. Water Resour.*, 34, 526-536.
- Chen, H., Guo, S., Xu, C.-y., and Singh, V. P. (2007). "Historical temporal trends of hydro-climatic variables and runoff response to climate variability and their relevance in water resource management in the Hanjiang basin." *J. of Hydrol.*, 344, 171-184.
- Chen, J., and Wu, Y. (2012). "Advancing representation of hydrologic processes in the Soil and Water Assessment Tool (SWAT) through integration of the TOPographic MODEL (TOPMODEL) features." *J. of Hydrol.*, 420-421, 319-328.
- Cheng, Q.-B., Chen, X., Xu, C.-Y., Reinhardt-Imjela, C., and Schulte, A. (2014). "Improvement and comparison of likelihood functions for model calibration and parameter uncertainty analysis within a Markov chain Monte Carlo scheme." *J. of Hydrol.*, 519, 2202-2214.
- Confesor, R. B., and Whittaker, G. W. (2007). "Automatic calibration of hydrologic models with multi-objective evolutionary algorithm and pareto optimization1." *J. Am. Water Resour. Assoc.*, 43, 981-989.

- Dahlke, H., Easton, Z. M., Walter, M., and Steenhuis, T. (2012). "Field Test of the Variable Source Area Interpretation of the Curve Number Rainfall-Runoff Equation." *J. of Irrig. and Drain. Eng.*, 138, 235-244.
- Datta, A., and Bolisetti, T. (2013). "Second-order autoregressive model-based likelihood function for calibration and uncertainty analysis of SWAT Model." *J. Hydrol. Eng.*, 04, 40-45.
- De Alwis, D. A., Easton, Z. M., Dahlke, H. E., Philpot, W. D., and Steenhuis, T. S. (2007). "Unsupervised classification of saturated areas using a time series of remotely sensed images." *Hydrol. and Ear. Sys. Sci.*, 11, 1609-1620.
- DeFries, R., and Eshleman, K. N. (2004). "Land-use change and hydrologic processes: a major focus for the future." *Hydrol. Proces.*, 18, 2183-2186.
- Deng, Z., Zhang, X., Li, D., and Pan, G. (2014). "Simulation of land use/land cover change and its effects on the hydrological characteristics of the upper reaches of the Hanjiang Basin." *Environ Earth Sci*, 1-14.
- Du, J., Rui, H., Zuo, T., Li, Q., Zheng, D., Chen, A., Xu, Y., and Xu, C. Y. (2013). "Hydrological simulation by SWAT model with fixed and varied parameterization approaches under land use change." *Water Resour. Manage.*, 27, 2823-2838.
- Duan, Q., Ajami, N. K., Gao, X., and Sorooshian, S. (2007). "Multi-model ensemble hydrologic prediction using Bayesian model averaging." *Adv. Water Resour.*, 30, 1371-1386.
- Dunne, T. (1978). "Field studies of hillslope flow processes". In *Hillslope hydrol.*, pp. 227-293. John Willey and Sons.
- Dunne, T., and Black, R. D. (1970). "Partial area contributions to storm runoff in a small New England watershed." *Water Resour. Res.*, 6, 1296-1311.

- Dunne, T., Moore, T., and Taylor, C. (1975). "Recognition and prediction of runoff-producing zones in humid regions." *Hydrol. Sci. Bull.*, 20, 305-327.
- Easton, Z. M., Fuka, D. R., Walter, M. T., Cowan, D. M., Schneiderman, E. M., and Steenhuis, T. S. (2008). "Re-conceptualizing the soil and water assessment tool (SWAT) model to predict runoff from variable source areas." *J. of Hydrol.*, 348, 279-291.
- Edwards, K. A., and Blackie, J. R. (1981). "Results of the East African catchment experiments 1958-1974." *Tropical Agri. Hydro.*, 163-188.
- Elfert, S., and Bormann, H. (2010). "Simulated impact of past and possible future land use changes on the hydrological response of the Northern German lowland 'Hunte' catchment." *J. of Hydrol.*, 383, 245-255.
- Ewen, J., O'Donnell, G., Burton, A., and O'Connell, E. (2006). "Errors and uncertainty in physically-based rainfall-runoff modelling of catchment change effects." *J. of Hydrol.*, 330, 641-650.
- Francis, P., and Gadgil, S. (2009). "The aberrant behaviour of the Indian monsoon in June 2009." *Cur. sci.*, 97, 1291-1295.
- Gadgil, S., Srinivasan, J., Nanjundiah, R. S., Kumar, K. K., Munot, A. A., and Kumar, K. R. (2002). "On forecasting the Indian summer monsoon: the intriguing season of 2002." *Cur. sci.*, 83, 394-403.
- Gao, B. C. (1996). "NDWI - A normalized difference water index for remote sensing of vegetation liquid water from space." *Remo. Sens. of Enviro.*, 58, 257-266.
- Gebriye, S. (2007) "Calibration and Validation of SWAT in Anjeni Gauged Watershed", 4th *International SWAT conference*, Delft The Netherlands, pp 375-384.

- George, S. (2007). "Streamflow in the Winnipeg River basin, Canada: Trends, extremes and climate linkages." *J. of Hydrol.*, 332, 396-411.
- Githui, F., Mutua, F., and Bauwens, W. (2009). "Estimating the impacts of land-cover change on runoff using the soil and water assessment tool (SWAT): case study of Nzoia catchment, Kenya " *Hydrol. Sci. J.*, 54, 899-908.
- Golding, D. L. (1980) "Calibration methods for detecting changes in streamflow quantity and regime", *Proceedings of Symposium on the Influence of Man on the Hydrological Regime with Special Reference to Representative and Experimental Basins*, Helsinki, pp 3-7.
- Gosain, A. K., Rao, S., and Basuray, D. (2006). "Climate change impact assessment on hydrology of Indian river basins." *Cur. sci.*, 90, 346-353.
- Guerrero, J. L., Westerberg, I. K., Halldin, S., Xu, C. Y., and Lundin, L. C. (2012). "Temporal variability in stage–discharge relationships." *J. of Hydrol.*, 446–447, 90-102.
- Gupta, H., Sorooshian, S., and Yapo, P. (1999). "Status of automatic calibration for hydrologic models: comparison with multilevel expert calibration." *J. Hydrol. Eng.*, 4, 135-143.
- Hamed, K. H. (2008). "Trend detection in hydrologic data: The Mann–Kendall trend test under the scaling hypothesis." *J. of Hydrol.*, 349, 350-363.
- Hamed, K. H. (2009). "Exact distribution of the Mann–Kendall trend test statistic for persistent data." *J. of Hydrol.*, 365, 86-94.
- Hari Krishna, B., Mani, A., Devi, M. U., and Ramulu, V. (2014a). "Simulation of impact of change in landuse on water yield of Upper Manair catchment." *Int. J. of Innovative Research & Development*, 3, 592-600.

- Hari Krishna, B., Mani, A., Devi, M. U., and Ramulu, V. (2014b). "Water productivity of agricultural crops in Upper Manair Catchment." *Int. J. of Innovative Research & Development*, 3, 377-382.
- Hewlett, J. D., and Hibbert, A. R. (1967). "Factors affecting the response of small watersheds to precipitation in humid areas." *Forest hydro.*, 275-290.
- Hewlett, J. D., and Nutter, W. L. (1970) "The varying source area of streamflow from upland basins", *Interdisciplinary Aspects of Watershed Management*, Montana, pp 65-83.
- Hirsch, R. M., Slack, J. R., and Smith, R. A. (1982). "Techniques of trend analysis for monthly water quality data." *Water Resour. Res.*, 18, 107-121.
- Hopkins, B. (1960). "Rainfall interception by a tropical forest in Uganda." *East African Agri. J.*, 25, 254-8.
- Horton, R. E. (1933). "The role of infiltration in the hydrologic cycle." *Transactions, AGU*, 14, 446-460.
- Huang, S., Krysanova, V., Österle, H., and Hattermann, F. F. (2010). "Simulation of spatiotemporal dynamics of water fluxes in Germany under climate change." *Hydrol. Proces.*, 24, 3289-3306.
- Im, S., Kim, H., Kim, C., and Jang, C. (2009). "Assessing the impacts of land use changes on watershed hydrology using MIKE SHE." *Environ Geol*, 57, 231-239.
- Jain, S. K., Kumar, V., and Saharia, M. (2013). "Analysis of rainfall and temperature trends in northeast India." *Int J. of Climato.*, 33, 968-978.
- Jain, S. K., P. K. Agarwal, and Singh, V. P. (2007). *Hydrology and water resources of India*, Water Science and Technology Library.

- Jayakrishnan, R., Srinivasan, R., Santhi, C., and Arnold, J. G. (2005). "Advances in the application of the SWAT model for water resources management." *Hydrol. Proces.*, 19, 749-762.
- Jha, C. S., Dutt, C. B. S., and Bawa, K. S. (2000). "Deforestation and Land Use Changes in Western Ghats, India." *Cur. sci.*, 79, 231-238.
- Jones, A. (1971). "Soil Piping and Stream Channel Initiation." *Water Resour. Res.*, 7, 602-610.
- Jones, A. (1979). "Extending the Hewlett model of stream runoff generation." *Inst. Of British Geographers*, 11, 110-114.
- Kannan, N., White, S. M., Worrall, F., and Whelan, M. J. (2007). "Sensitivity analysis and identification of the best evapotranspiration and runoff options for hydrological modelling in SWAT-2000." *J. of Hydrol.*, 332, 456-466.
- Kantelhardt, J. W., Koscielny-Bunde, E., Rego, H. H. A., Havlin, S., and Bunde, A. (2001). "Detecting long-range correlations with detrended fluctuation analysis." *Physica A: Stat. Mech. and its Appl.*, 295, 441-454.
- Karcher, S., VanBriesen, J., and Nietch, C. (2013). "Alternative land-use method for spatially informed watershed management decision making using SWAT." *J. of Environ. Eng.*, 139, 1413-1423.
- Kirchner, J. W. (2006). "Getting the right answers for the right reasons: Linking measurements, analyses, and models to advance the science of hydrology." *Water Resour. Res.*, 42.
- Kirkby, M. J. (1978). *Hillslope hydrology*, Wiley Chichester.

- Kuczera, G., and Parent, E. (1998). "Monte Carlo assessment of parameter uncertainty in conceptual catchment models: the Metropolis algorithm." *J. of Hydrol.*, 211, 69-85.
- Kumar, S., Merwade, V., Kam, J., and Thurner, K. (2009). "Streamflow trends in Indiana: Effects of long term persistence, precipitation and subsurface drains." *J. of Hydrol.*, 374, 171-183.
- Kumar, V., Jain, S. K., and Singh, Y. (2010). "Analysis of long-term rainfall trends in India." *Hydrol. Sci. J.*, 55, 484-496.
- Kushwaha, A., and Jain, M. (2013). "Hydrological simulation in a forest dominated watershed in himalayan region using SWAT Model." *Water Resour. Manage.*, 27, 3005-3023.
- Li, Q., Cai, T., Yu, M., Lu, G., Xie, W., and Bai, X. (2013). "Investigation into the impacts of land-use change on runoff generation characteristics in the Upper Huaihe River Basin, China." *J. Hydrol. Eng.*, 18, 1464-1470.
- Lyon, S. W., Walter, M. T., Gerard-Marchant, P., and Steenhuis, T. S. (2004). "Using a topographic index to distribute variable source area runoff predicted with the SCS curve-number equation." *Hydrol. Proces.*, 18, 2757-2771.
- Mamillapalli, S., Srinivasan, R., Arnold, J. G., and Engel, B. A. (1996) "Effect of spatial variability on basin scale modeling", *Third International NCGI Conference/Workshop on Integrating GIS and Environmental Modeling*, Santa Fe, New Mexico.
- Misgana, K. M., John, W. N., and Elias, G. B. (2007). "Sensitivity of a distributed watershed simulation model to spatial scale." *Hydrologic Eng.*, 12, 163-172.
- Mohan Kumar, S. (2011). Application of SWAT model to the Netravathi river basin, National Institute of Technology Karnataka, Surathkal.

- Mosbahi, M., Benabdallah, S., and Boussema, M. (2014). "Sensitivity analysis of a GIS-based model: A case study of a large semi-arid catchment." *Earth Sci Inform*, 1-13.
- Muleta, M. K., and Nicklow, J. W. (2005). "Sensitivity and uncertainty analysis coupled with automatic calibration for a distributed watershed model." *J. of Hydrol.*, 306, 127-145.
- Munot, A. A., and Kumar, K. K. (2007). "Long range prediction of Indian summer monsoon rainfall." *J. Earth. Sys. Sci.*, 116, 73-79.
- Murali Mohan, A. V. S. (2000). Application of a physically-based hydrologic model to a tropical river basin, National Institute of Technology Karnataka, Surathkal.
- Mythri, D. J. (2010). Climate change impact of assessment on hydrology of Netravathi river basin, National Institute of Technology Karnataka, Surathkal.
- Nash, J. E., and Sutcliffe, J. V. (1970). "River flow forecasting through conceptual models part I - A discussion of principles." *J. of Hydrol.*, 10, 282-290.
- Nina, O., Masoud, T., and Ahmad, A. (2007) "Modeling of a river basin using SWAT model and GIS", 2nd *International conference: Solutions towards sustainable river basins*.
- Pai, D. S., and Rajeevan, M. (2006). "Empirical prediction of Indian summer monsoon rainfall with different lead periods based on global SST anomalies." *Meteorol. Atmos. Phys.*, 92, 33-43.
- Parthasarathy, B., Kumar, K. R., and Munot, A. A. (1993). "Homogeneous Indian Monsoon rainfall: Variability and prediction." *Proc. Indian Acad. Sci. (Earth Planet Sci.)*, 102, 121-155.

- Pezet, F., Dorioz, J., Quetin, P., Lafforgue, M., and Trevisan, D. (2014). "Using SWAT-VSA to predict diffuse phosphorus pollution in an agricultural catchment with several aquifers." *J. Hydrol. Eng.*, 19, 1462-1470.
- Pikounis, M., Varanou, E., Baltas, E., Dassaklis, A., and Mimikou, M. (2003). "Application of the SWAT model in the Pinios river basin under different Land-use scenarios." *Global Nest: the Int.*, 5, 71-79.
- Prasena, A., and Pikha Shrestha, D. B. (2013). "Assessing the effects of land use change on runoff in Bedog sub watershed Yogyakarta." *Indo. J. of Geography*, 45.
- Putty, M. R. Y. (2009). "Curve-number-based watershed model incorporating quick subsurface runoff, with applications in the Western Ghats, South India." *J. Hydrol. Eng.*, 14, 876-881.
- Putty, M. R. Y., and Prasad, R. (2000). "Understanding runoff processes using a watershed model - a case study in the Western Ghats in South India." *J. of Hydrol.*, 228, 215-227.
- Refsgaard, J. C., and Knudsen, J. (1996). "Operational validation and intercomparison of different types of hydrological models." *Water Resour. Res.*, 32, 2189-2202.
- Ridwansyah, I., Pawitan, H., Sinukaban, N., and Hidayat, Y. (2014). "Watershed modeling with ArcSWAT and SUFI2 in Cisadane catchment area: calibration and validation of river flow prediction." *Int. J. of Sci. and Eng.*, 6.
- Sahoo, D., and Smith, P. K. (2009). "Hydroclimatic trend detection in a rapidly urbanizing semi-arid and coastal river basin." *J. of Hydrol.*, 367, 217-227.

- Santosh, G. T., Kolladi, Y. R., and Surya, T. V. (2010). "Influence of scale on SWAT model calibration for streamflow in a river basin in the humid tropics." *Water Resour. Manage.*
- Schaefli, B., Talamba, D. B., and Musy, A. (2007). "Quantifying hydrological modeling errors through a mixture of normal distributions." *J. of Hydrol.*, 332, 303-315.
- Schneiderman, E. M., Steenhuis, T. S., Thongs, D. J., Easton, Z. M., Zion, M. S., Neal, A. L., Mendoza, G. F., and Todd Walter, M. (2007). "Incorporating variable source area hydrology into a curve-number-based watershed model." *Hydrol. Proces.*, 21, 3420-3430.
- Sen, P. K. (1968). "Estimates of the regression coefficient based on Kendall's Tau." *J. of the American Stati. Asso.*, 63, 1379-1389.
- Shao, Q., and Li, M. (2011). "A new trend analysis for seasonal time series with consideration of data dependence." *J. of Hydrol.*, 396, 104-112.
- Shen, Z. Y., Chen, L., and Chen, T. (2012). "Analysis of parameter uncertainty in hydrological and sediment modeling using GLUE method: a case study of SWAT model applied to Three Gorges Reservoir Region, China." *Hydrol. and Ear. Sys. Sci.*, 16, 121-132.
- Shi, P., Hou, Y., Xie, Y., Chen, C., Chen, X., Li, Q., Qu, S., Fang, X., and Srinivasan, R. (2013). "Application of a SWAT Model for hydrological modeling in the Xixian watershed, China." *J. Hydrol. Eng.*, 18, 1522-1529.
- Shrivastava, P. K., Tripathi, M. P., and Das, S. N. (2004). "Hydrological modeling of a small watershed using satellite data and GIS technique." *J. of the Indian Society of Remo. Sens.*, 32.

- Singh, A. (2009). Characterizing runoff generation mechanism for modelling runoff and soil erosion, in small watershed of Himalayan region, International Institute for Geo-information Science and Earth Observation, The Netherlands.
- Singh, A., and Gosain, A. K. (2011). "Scenario generation using geographical information system (GIS) based hydrological modeling for a multijurisdictional Indian River basin." *J. of Ocean. and Mari. Sci.*, 2, 140-147.
- Somura, H., Hoffman, D., Arnold, J., and Takeda., M., Y (2008) "Application of the SWAT model to the Hii River Basin", *4TH International SWAT conference*.
- Sonali, P., and Nagesh Kumar, D. (2013). "Review of trend detection methods and their application to detect temperature changes in India." *J. of Hydrol.*, 476, 212-227.
- Steenhuis, T., Winchell, M., Rossing, J., Zollweg, J., and Walter, M. (1995). "SCS Runoff equation revisited for variable-source runoff areas." *J. of Irri. and Drain. Eng.*, 121, 234-238.
- Tabari, H., and Talaei, P. H. (2011). "Temporal variability of precipitation over Iran: 1966–2005." *J. of Hydrol.*, 396, 313-320.
- Thiemann, M., Trosset, M., Gupta, H. V., and Sorooshian, S. (2001). "Bayesian recursive parameter estimation for hydrologic models." *Water Resour. Res.*, 37, 2521-2535.
- Tolson, B. A., and Shoemaker, C. A. (2008). "Efficient prediction uncertainty approximation in the calibration of environmental simulation models." *Water Resour. Res.*, 44, W04411.

- Tripathi, M. P., Panda, R. K., and Raghuwanshi, N. S. (2003). "Identification and prioritisation of critical sub-watersheds for soil conservation management using the SWAT Model." *Biosystems Eng.*, 85, 365-379.
- Tripathi, M. P., Panda, R. K., Raghuwanshi, N. S., and Singh, R. (2004). "Hydrological modelling of a small watershed using generated rainfall in the soil and water assessment tool model." *Hydrol. Proces.*, 18, 1811-1821.
- USDA-SCS (1972). *National Engineering Handbook*, Soil Conservation Service, USDA, Washington, DC.
- Van Griensven, A., Meixner, T., Grunwald, S., Bishop, T., Diluzio, M., and Srinivasan, R. (2006). "A global sensitivity analysis tool for the parameters of multi-variable catchment models." *J. of Hydrol.*, 324, 10-23.
- Vandana, S., and Bandyopadhyay (1983). "Eucalyptus – a disastrous tree for India." *Ecologist*, 13, 184–187.
- Venkatesh, B. (2011). *Measurement and Modeling of Hydrological Responses under different Land Covers in Sahayadri Mountains, India*, National Institute of Technology Karnataka, Surathkal, India, India.
- Venkatesh, B., Lakshman, N., Purandara, B. K., and Reddy, V. B. (2011). "Analysis of observed soil moisture patterns under different land covers in Western Ghats, India." *J. of Hydrol.*, 397, 281-294.
- Vrugt, J. A., Diks, C. G. H., Gupta, H. V., Bouten, W., and Verstraten, J. M. (2005). "Improved treatment of uncertainty in hydrologic modeling: Combining the strengths of global optimization and data assimilation." *Water Resour. Res.*, 41, W01017.

- Vrugt, J. A., Gupta, H. V., Bouten, W., and Sorooshian, S. (2003). "A Shuffled Complex Evolution Metropolis algorithm for optimization and uncertainty assessment of hydrologic model parameters." *Water Resour. Res.*, 39, 1201.
- Vrugt, J. A., and Robinson, B. A. (2007). "Treatment of uncertainty using ensemble methods: Comparison of sequential data assimilation and Bayesian model averaging." *Water Resour. Res.*, 43, W01411.
- Wagner, T., and Gupta, H. V. (2005). "Model identification for hydrological forecasting under uncertainty." *Stoch. Environ. Res. Ris. Assess.*, 19, 378-387.
- Wagner, P. D., Kumar, S., and Schneider, K. (2013). "An assessment of land use change impacts on the water resources of the Mula and Mutha Rivers catchment upstream of Pune, India." *Nat. Hazards and Earth Sys. Sci.*, 17, 2233-2246.
- Wenzhi, C., William, B., Bowden, and Davie, T. (2009). "Modelling impacts of land cover change on critical water resources in the Motueka river catchment, New Zealand." *Water Resour. Manage.*, 23, 137-151.
- White, E. D., Easton, Z. M., Fuka, D. R., Collick, A. S., Adgo, E., McCartney, M., Awulachew, S. B., Selassie, Y. G., and Steenhuis, T. S. (2011). "Development and application of a physically based landscape water balance in the SWAT model." *Hydrol. Proces.*, 25, 915-925.
- White, K. L., and Chaubey, I. (2005). "Sensitivity analysis, calibration, and validations for a multisite and multivariable swat model." *J. Am. Water Resour. Assoc.*, 41, 1077-1089.
- Woodbury, J. D., Shoemaker, C. A., Easton, Z. M., and Cowan, D. M. (2014). "Application of SWAT with and without variable source area hydrology to a large watershed." *J. Am. Water Resour. Assoc.*, 50, 42-56.

- WRDO (1976). "Master plan for an equitable use of the waters of the Cauvery basin in Karnataka – an outline." WRDO, Karnataka, India.
- Xiang, P. U. (2010). "Runoff simulation and analysis in upstream Dagu River Watershed using a distributed hydrological model." Key Laboratory of Marine Environment and Ecology (Ocean University of China), China.
- Xu, H. (2006). "Modification of normalised difference water index (NDWI) to enhance open water features in remotely sensed imagery." *Int. J. of Remo. Sens.*, 27, 3025-3033.
- Xue, C., Chen, B., and Wu, H. (2014). "Parameter uncertainty analysis of surface flow and sediment yield in the Huolin basin, China." *J. Hydrol. Eng.*, 19, 1224-1236.
- Yan, H., and Edwards, F. (2013). "Effects of land use change on hydrologic response at a watershed scale, Arkansas." *J. Hydrol. Eng.*, 18, 1779-1785.
- Yang, J., Reichert, P., Abbaspour, K. C., Xia, J., and Yang, H. (2008). "Comparing uncertainty analysis techniques for a SWAT application to the Chaohe Basin in China." *J. of Hydrol.*, 358, 1-23.
- Yapo, P. O., Gupta, H. V., and Sorooshian, S. (1996). "Automatic calibration of conceptual rainfall-runoff models: sensitivity to calibration data." *J. of Hydrol.*, 181, 23-48.
- Yen, H., Jeong, J., Feng, Q., and Deb, D. (2014). "Assessment of input uncertainty in SWAT using latent variables." *Water Resour. Manage.*, 1-17.
- Yue, S., Pilon, P., and Cavadias, G. (2002). "Power of the Mann–Kendall and Spearman's rho tests for detecting monotonic trends in hydrological series." *J. of Hydrol.*, 259, 254-271.

Zhang, J., Li, Q., and Guo, B. (2014). "The comparative study of multi-site uncertainty evaluation method based on SWAT model." *Hydrol. Proces.*

Zhang, X. C., Liu, W. Z., Li, Z., and Chen, J. (2011). "Trend and uncertainty analysis of simulated climate change impacts with multiple GCMs and emission scenarios." *Agri. Forest Meteo.*, 151, 1297-1304.

Zhou, F., Xu, Y., Chen, Y., Xu, C. Y., Gao, Y., and Du, J. (2013). "Hydrological response to urbanization at different spatio-temporal scales simulated by coupling of CLUE-S and the SWAT model in the Yangtze River Delta region." *J. of Hydrol.*, 485, 113-125.

APPENDIX 1

Soil description of the Upper Cauvery Basin

Soil Class	Soil Name
1	Very deep, somewhat excessively drained clayey soils with surface crusting on very gently sloping coliuval plains, with moderate erosion:
3	Deep, somewhat excessively drained, gravelly clay soils on rolling lands, with moderate erosion
4	Deep, somewhat excessively drained, gravelly clay soils on gently sloping interfluves, with moderate erosion,
6	Deep well drained, gravelly clay soils on gently sloping interfluves, with slight erosion
8	Moderately deep, well drained, clayey soils in undulating interfluves, with slight erosion
9	Very deep, well drained, clayey soils on undulating inverfluves, with slight erosion
11	Moderately shallow, well drained, gravelly clay soils with very low AWC on undulating interfluves with moderate erosion
13	Moderately shallow, well drained, gravelly clay soils on gently sloping interfluves, with slight erosion
15	Shallow, somewhat excessively drained loamy soils with very low AWC on undulating inverfluves, with moderate erosion
16	Moderately deep, well drained, clayey soils with medium AWC on undulating interfluves with moderate erosion
27	Moderately deep, well drained, gravelly clay soils with low AWC on undulating interfluves, with moderate erosion
30	Shallow, well drained, gravelly clay soils with very low AWC, strongly gravelly in the subsoil on undulating interfluves
31	Deep, well drained, clayey soils on undulating intergluves, with moderate erosion

32	Very deep, moderately well drained, clayey soils of valleys, with problems of drainage and slight salinity in patches
33	Deep, moderately well drained, clayey soils of valleys, with problems of drainage and slight salinity in patches
34	Very deep, excessively drained, clayey soils on ridges with steep slopes, high runoff and moderate erosion
37	Moderately deep, well drained, clayey soils on gently sloping interfluves, with moderate erosion
38	Shallow, somewhat excessively drained, gravelly clay soils with very low AWC on rolling lands, with moderate erosion
40	Very deep, well drained, clayey soils on undulating interfluves, with slight erosion
43	Deep, well drained, calcareous, cracking clay soils on undulating interfluves, with moderate erosion
53	Very deep, moderately well drained, calcareous, cracking clay soils on gently sloping interfluves, with slight erosion
54	Very deep, moderately well drained, cracking clay soils of nearly level valleys, with moderate erosion
55	Deep, moderately well drained, cracking clay soils on gently sloping intergluves, with moderate erosion
58	Very deep, well drained, gravelly loam soils, strongly gravelly in the subsoil on rolling lands, with moderate erosion.
59	Shallow, somewhat excessively drained, gravelly loam soils with very low AWC on undulating interfluves, with severe erosion
62	Very shallow, excessively drained, gravelly loamy soils on ridges, with severe erosion
67	Very shallow, well drained, loamy soils with stoniness on ridges, with severe erosion
77	Rock outcrops
78	Very deep, well drained, gravelly clay soils, strongly gravelly in the subsoil on steeply sloping high hill ranges, with moderate erosion

79	Deep, well drained, clayey soils on dissected hills and valleys, with moderate erosion
80	Moderately deep, well drained, gravelly clay soils with low AWC, strongly gravelly in the subsoil on rolling lands, with slight erosion
82	Deep, well drained, gravelly clay soils on slopes of steeply sloping high hill ranges with moderate erosion
83	Very deep, well drained, clayey soils with medium AWC on laterite plateaus, with moderate erosion.
84	Deep, well drained, clayey soils with medium AWC on laterite plateaus, with moderate erosion
85	Deep well drained, clayey soils with medium AWC on foothill slopes, with severe erosion
87	Deep, well drained, gravelly clay soils with low AWC on rolling lands, with moderate erosion
89	Moderately deep, well drained, clayey soils on escarpment slopes, with severe erosion
91	Deep, well drained, gravelly clay soils with low AWC on undulating uplands, with moderate erosion
92	Moderately deep, well drained, clayey soils with low AWC on undulating uplands and valleys
94	Moderately shallow, well drained, gravelly clay soils on hills and ridges, with moderate erosion
95	Moderately shallow, somewhat excessively drained, clayey soils on hills and ridges, with severe erosion
100	Very deep, moderately well drained, loamy over sandy soils of valleys, with shallow water table
101	Shallow, somewhat excessively drained, gravelly clay soils on steep ridges, with severe erosion
102	Very shallow, somewhat excessively drained, loamy soils on ridges, with severe erosion
105	Very deep, well drained, gravelly clay soils with low AWC on laterite

	plateau, with severe erosion
108	Very deep, well drained, clayey soils with medium AWC on isolated hills with moderate erosion
109	Very deep, well drained, gravelly clay soils with low AWC on low hill ranges, with moderate erosion
111	Deep, well drained, clayey soils on undulating uplands, with moderate erosion
200	Water Body
201	Bangalore and Mysore

International Journal Papers

- **Kumar Raju B. C.** and L. Nandagiri (2015) “Identification of Hydrologically Active Areas in a Watershed using Satellite Data”, *International Conference On Water Resources, Coastal And Ocean Engineering – ICWRCOE’2015*, National Institute of Technology Karnataka, Surathkal. *Published in Aquatic Procedia (Elsevier)*, 4, 1339-1344 DOI:[10.1016/j.aqpro.2015.02.174](https://doi.org/10.1016/j.aqpro.2015.02.174)
- **Kumar Raju B. C.** and L. Nandagiri (2015) “Evaluating Uncertainty of the Soil and Water Assessment Tool (SWAT) Model in the Upper Cauvery Basin, Karnataka, India”, *International Journal of Earth Sciences and Engineering*.
- **Kumar Raju B. C.** and L. Nandagiri (2016) “Application of Variable Source Area Hydrological Models in Humid Tropical Watersheds Located in the Upper Cauvery River Basin, India”, *Journal of Hydrologic Engineering (ASCE)*, (Under Review).
- **Kumar Raju B. C.** and L. Nandagiri (2016) “Analysis of Historical Trends in Hydrometeorological Variables in the Upper Cauvery Basin, Karnataka, India”, *Current Science*, (Under Review).

International Conference papers

- **Kumar Raju B. C.** and L. Nandagiri (2015) “Application and Test of the SWAT Model in the Upper Cauvery River Basin, Karnataka, India”, 4th *International Engineering Symposium – IES 2015, Kumamoto University, Japan*.

RESUME

Name : Kumar Raju B. C.

Date of Birth : 08-02-1987

Address : S/o Chikka Venkategowda,
Marigudi Street,
Bahrathi Nagar (K. M. Doddi),
Maddur Tq, Mandya Dist,
Karnataka, India-571422

Mobile : (+91) 9742501982

Email(s) : kumarrajubc@gmail.com

Qualification : B.E. (Civil), M.Tech. (RS&GIS)

Journal Publications : 2

No. of Conference Publications : 2

